Analysis and Parametric Study of Tangent Pile Wall as Deep Excavation Support System Using Finite Element Based Software

By

Zerihun Lemesa Tolossa

A Thesis Submitted to

Civil Engineering Department

School of Civil Engineering and Architecture

Presented in Partial Fulfillment of the Requirement for the award of Degree of Masters in Civil Engineering (Geotechnical Engineering).

Office of Graduate Studies

Adama Science and Technology University

June, 2019

Adama, Ethiopia

Analysis and Parametric Study of Tangent Pile Wall as Deep excavation Support System Using Finite Element Based Software.

By

Zerihun Lemesa Tolossa

Major Advisor: Dr.-Ing. Henok Fikre

Co-Advisor: Hiyaw Hatiya (MSc)

A Thesis Submitted to

Civil Engineering Department

School of Civil Engineering and Architecture

Presented in Partial Fulfillment of the Requirement for the award of Degree of Masters in Civil Engineering (Geotechnical Engineering).

Office of Graduate Studies

Adama Science and Technology University

June, 2019

Adama, Ethiopia

Approval sheet of the board of Examiners

We, the undersigned, members of the Board of Examiners of the final open defense by Zerihun Lemesa Tolossa have read and evaluated his thesis entitled "Analysis and Parametric Study of Tangent Pile Wall as Deep excavation Support System Using Finite Element Based Software, Ethiopia." and examined the candidate. This is, therefore, to certify that the thesis has been accepted in partial fulfillment of the requirement of the Degree of Masters in Civil Engineering (Geotechnical Engineering).

______________________	________________	______________
Advisor	Signature	Date
______________________	________________	______________
Co-Advisor	Signature	Date
______________________	________________	______________
Internal Examiner	Signature	Date
______________________	________________	______________
External Examiner	Signature	Date
______________________	________________	______________
Chairperson	Signature	Date
______________________	________________	______________
Department head of Civil Engineering and Architecture	Signature	Date
______________________	________________	______________
School Dean (SoCEA)	Signature	Date
______________________	________________	______________
Post Graduate Dean	Signature	Date

Declaration

I hereby declare that this MSc Thesis is my original work and has not been presented for a degree in any other University, and all sources of material used for this thesis have been duly acknowledged.

Name: Zerihun Lemesa Tolossa

Signature: _____________

This MSc has been submitted for examination with my approval as thesis advisor.

Name: Dr.-Ing. Henok Fikre

Signature: ______________

Name: Hiyaw Hatiya (MSc)

Signature: _____________

Date of submission: ______

Acknowledgement

Before all, I would like to thank God for helping me in every aspect of my work. Secondly, I would like to forward my deepest gratitude to my advisor Dr.-Ing Henok Fikre for his critical observations, suggestions, comments and endless support at various stage of this thesis work.

I also express my sincere thanks to my co-advisor Mr. Hiyaw Hatiya for his continues comments, encouragements and many useful contributions in my study. I really appreciate your support for every helpful assistance you have made for me on a day to day during the period of my study.

I would like to forward my heartfelt thanks to ADDIS GEOSYSTEMS P.L.C, who gave me soil data for my thesis.

I thank all staffs of the Civil Engineering Department for their encouragements during my thesis work.

Abstract

The need for deep excavations become increasing in urban areas to have underground spaces. Addis Ababa is a fast growing city in number and types of construction activities. The excavations for multi-story buildings and, new and maintenance of old roads are currently in the city. As most of these excavations are very deep as involved by current constructions, a support system is necessary for protecting soil movement and adjacent structures. Hence, accurate predictions of lateral wall deflections and ground surface settlement are important design criteria in the analysis and design of excavation support systems. The purpose of this study is to analyze tangent pile wall as deep excavation support system on silty-clay soil. A parametric study was conducted by varying the adjacent surface load, equivalent thickness (diameter) of pile wall and strut horizontal spacing for different excavation heights. PLAXIS 3D was used as a tool to carry out all the analysis of parameters. The analysis resulted in the horizontal displacements of the wall, ground surface settlement behind the wall and bending moments induced in the pile wall. The change in the adjacent surface load and equivalent wall thickness showed the greatest effect on the result. The normalized allowable deformation values from literatures have been compared with the cases with normalized deformation values. The comparison indicated that the vertical deformation fall in between 0.5 to 1.0 times the maximum horizontal displacement. This study definitely answers the questions about the analysis and parametric study of tangent pile wall as deep excavation support system and the effect of change in adjacent surface load, equivalent thickness and strut horizontal spacing.

Key words: deep excavation, tangent pile wall, plaxis 3D foundation and Hardening soil model.

Table of Contents

Contents pages

Lists of Tables

Table of Figures

Lists of Symbols and Abbreviations

C- Soil cohesion value

d-Pile diameter

de- Equivalent thickness of the tangent pile wall

E^{ref}_{50}- Reference secant modulus of elasticity

E^{ref}_{oed} – Tangent stiffness for primary odometer loading

E^{ref}_{ur} –Unloading/ Reloading stiffness

EBCS-Ethiopian Building Code Standards

FEM- Finite Element Model

He- Height of excavation

HS-Hardening soil model

K^{c}_{oc} -Coefficient lateral earth pressure

MC- Mohr- Coulomb

M_{11} – Maximum bending moment in tangent pile wall in 1-1 direction

M_{22} – Maximum bending moment in tangent pile wall in 2-2 direction

(SHS) 1- Strut Horizontal Spacing 4m

(SHS) 2- Strut Horizontal Spacing 3m

(SHS) 3- Strut Horizontal Spacing 5m

SPT- Standard Penetration Test

Ux (max) - Maximum horizontal displacement of tangent pile wall

Uy (max) - Maximum vertical displacement in the ground in the y-direction

Uz (max) - Maximum horizontal displacement of tangent pile wall in the z-direction

Φ- Friction angle

Chapter 1: Introduction

1.1: General Introduction

The need for deep excavations become increasing in urban areas to have underground space, such as subway stations, basements for high-rise buildings, underground car parks, and shopping centers. Addis Ababa is a fast growing city in number and types of construction activities. The excavations for multi-story buildings and, new and maintenance of old roads are the majors currently in the city. A large number of these excavations are near adjacent structures. Excavation unloads the surrounding ground. Removing large amounts of soil during construction stages invariably results in the stress changes and additional deformations on the structures in addition to the deformation caused by their own weight. As most of these excavations are very deep as involved by current constructions, they may cause collapse of soil that pose potential hazards on life, structures and economy. One of the world's building disaster occurred in Shanghai in China, in June 2009, when a 13 floors building under construction at Lian Huanan Road in Min Hand district of Shanghai city collapsed. It was reported that one worker was killed. The collapse was caused by the deep excavation of 4.6m made for an underground car park alongside the building, being piled to depths of up to 10m on the other side of the structure. The weight of the pile created a pressure differential, which led to a shift in the structure, eventually weakening the foundations and causing them to fail. This situation may have been aggravated by several days of heavy rain leading up to the collapse. Improper construction methods are believed to the reason of building collapse, according to the investigation team report, (Chai et al., 2014). They stated that workers dug an underground garage on one side of the building while on the side earth was heaped up to 10m high, which was apparently an error in construction.

Thus, a support system is necessary for protecting the soil from movement and adjacent structures. However, supports are provided in all deep excavations, still there is a possibility of deformation and consequently for failure. This could be accounted to the sensitivity of the soil and the closeness to the excavation.

The type of the retaining wall used influenced by the sub-structure construction method and will vary geographically due to soil and groundwater conditions, proximity to the source of materials, and the skill of local contractors. Various types of retaining systems categorized according to the reasons. A comprehensive review of various types of retaining systems such as sheet walls, diaphragm walls, braced walls, contiguous pile walls, secant pile walls, tangent pile walls are provided in (Deep excavation manual, 1996).

Therefore, it is necessary to study and know the effects of excavations and come up with a situation that helps to take the necessary measure for upcoming construction undertakings.

1.2: Statement of the Problem

Addis Ababa is a fast growing city in number and construction activities, which aimed at providing accessible roads, transportation and construction of multi-story buildings for residence and business purposes. These increase the need for deep excavations which will result in lateral movement of soil that induce settlement in the adjacent ground which may result in damage to nearby infrastructure and making the study of these displacements vital.

Support system is necessary for protecting the soil movements and adjacent structures. The types of systems used are influenced by the construction method, soil and ground water conditions, proximity to source of materials and the skill of local contractors.

Tangent pile walls have been used as structural elements for supporting deep excavations in urban areas due to their low construction costs over secant pile and diaphragm walls, structural advantages and designed with respect to their lateral displacements, which can be reduced by adopting a stiffer wall, by reinforcing the anchor or strut system, or by pre-stressing these components. To see the factors that influence the support system, analysis and parametric study is important. All the above cases necessitates this study.

1.3: Objective of the Study

1.3.1: General Objective

The main objective of this thesis is to analyze tangent pile wall as deep excavation support system in silty-clay soil using PLAXIS finite element software.

1.3.2: Specific Objectives

The specific objectives of this work include:

- Analysis of vertical deformation, horizontal displacements and bending moments of the supporting.
- Provide predictions of lateral wall deflection and ground surface settlement.

1.4: Scope of the Study

The soil of Addis Ababa around Bole area was simulated based on silty-clay soil. In this study, adjacent surface load at 3.5m from the edge of excavation, recommended by Addis Ababa City Municipality, strut horizontal spacing and equivalent thickness of the tangent pile wall is varied. The staged excavation is used. The situations analyzed are regarding vertical settlement, horizontal displacements, and moments in the support. The support type used in the thesis is a tangent pile wall modeled as an equivalent wall to effectively use in the software and retain the actual behavior as much as possible. The retaining purpose is assumed for long period and soil is in drained condition. For all the cases, only the parametric study has been done, and the finite element modeling and measurement of deformations on site using inclinometers and such instrument is out of the scope of this study. The effect of water, the stress changes and the effect of heave are not in this scope.

1.5: Significance of the Study

The results of this study will have a great importance on ever-growing building infrastructures and high-rise buildings in Ethiopia, especially for those constructed in Addis Ababa.

This study presents the three-dimensional finite element analysis and provides a deformation-based design method for the analysis and design of excavation support systems. It has expected that the proposed deformation-based method would save costs typically expended in repairs and mitigation of excavation-induced damage to adjacent infrastructure.

1.6: Organization of Thesis

The thesis has five chapters. Chapter 1 provides a general introduction of deep excavation and support systems and statement of the problem. The research objectives together, scope and research output practical implications are discussed.

Chapter 2 presents the background, types of retaining structures and existing literatures on deep excavations. The empirical/semi-empirical methods are also discussed which, were developed to predict the behavior of deep excavations in terms of maximum lateral deflections and maximum ground surface settlements. Support systems and the use of numerical analysis are discussed.

Chapter 3 discusses the research materials and methods used to achieve the above stated objectives. Description of study area is also presented. The parameter used in the study is as well discussed.

The results and discussion of the parametric study carried out in PLAXIS 3D Foundation are presented in Chapter 4. The results of finite element analysis by varying adjacent surface load, equivalent pile-wall thickness and strut horizontal spacing for an existing deep excavation study are discussed. The findings of this study are also compared with the previous studies for generalized braced excavations.

Moreover, Chapter 5 summarizes the work of previous chapters and gives general conclusion and recommendation for possible future work.

Chapter 2: Literature Review

2.1: Introduction

Presently limiting movements and deformations that result from constructing deep excavations is becoming a significant design issue, especially in urban environments. Because failure to control deformations and movements can cause significant damage to adjacent structures and utilities. And this makes design more challenging due to increasing requirements for deeper excavations on poorer sites, tighter limits on allowable displacements for adjacent structures and new methods of construction that extend beyond the experience base used to develop historical design methods. Increasingly designs are controlled by the need to limit movements, which goes beyond the traditional approach of focusing on required support loads and avoiding collapse.

Designing to control movements became possible with the development of nonlinear finite element analysis in the early 1970's. However, it was not a practical design tool in its early versions. In recent years, finite element software has greatly improved. There are more realistic stress-strain models, more stable numerical methods, tools to ease the creation of the geometric model, and especially tools to provide powerful and useful graphical output for quick interpretation and presentation of results. Some products also compute a factor of safety against soil failure at any stage of the excavation.

Ground movements adjacent to deep excavations occur in response to lateral deflections of the excavation support system. These movements are influenced by wall installation, soil ground conditions, support system stiffness, and methods of support system installation and interaction between the soil and the support. Hence, parameters have to be identified accordingly.

2.2: Types of Retaining Structures

More than several types of in-situ walls support excavations. The criteria for the selection of type of wall are size of excavation, ground conditions, groundwater level, vertical and horizontal displacements of adjacent ground and limitations of various structures, availability of construction, cost, speed of work and others. One of the main decisions is the water-tightness of wall. The types of in-situ walls are common types (Ou, 2006) and (Ergun, 2008)**.**

1. Braced walls, Soldier pile and lagging walls.
2. Sheet pile walls.
3. Pile walls (Contiguous, Secant and Tangent).
4. Diaphragm walls or Slurry trench walls.

1. Braced walls

Excavation proceeds systematically after placement of soldier piles or so-called king posts around the excavation at about 2 to 3m intervals. These may be steel H, WF sections or I. Rail sections and timber are also used. At each level, horizontal waling beams and supporting elements (struts, anchors and nails) are constructed. Soldier piles are driven or commonly placed in bored holes in urban areas, and timber lagging is placed between soldier piles during the excavation. Soils with some cohesion and without water table are usually suitable for this type of construction or dewatering is accompanied if required and allowed. Strut support is commonly preferred in narrow excavations for pipe laying or similar works but also used in deep and large excavations as shown in Figure 2.1. Ground anchor support is increasingly used and preferred due to access for construction works and machinery. Waling beams or anchors may be placed directly on soldier piles without any beams (Ergun, 2008).

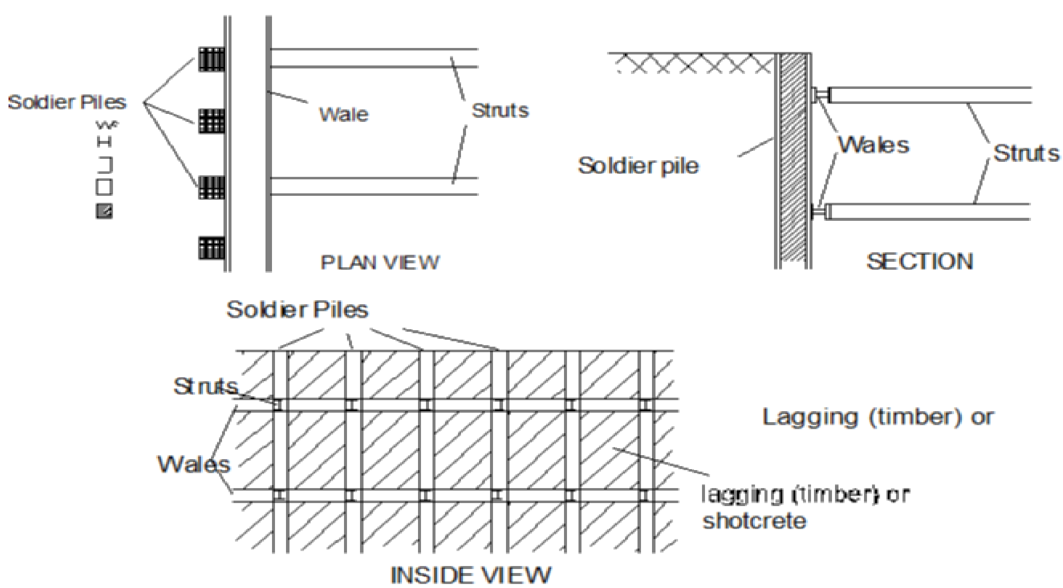

Figure 2.1: Braced Walls; Plan, Section and Inside Views (Ergun, 2008)

2. **Sheet pile walls.**

Sheet pile is a thin steel section (7-30mm thick) 400-500mm wide. It is manufactured in different lengths and shapes like U, Z and straight-line sections shown in Figure 2.2. There are interlocking watertight grooves at the sides, and they are driven into soil by hammering or vibrating. Their use is often restricted in urbanized areas due to environmental problems like noise and vibrations. New generation hammers generate minimum vibration and disturbance, and static pushing of sections have been recently possible. In soft ground, several sections may be driven using a template. The product is a watertight steel wall in soil. One side (inner) of wall is excavated systematically and struts or anchor gives support. Waling beams (walers) are frequently used. They are usually constructed in water bearing soils (Ou, 2006) and (Ergun, 2008).

Steel sheet piles are the most common but sometimes reinforced concrete precast sheet pile sections are preferred in soft soils if driving difficulties are not expected. Steel piles may also encounter driving difficulties in very dense, stiff soils or in soils with boulders. Jetting may be accompanied during the process to ease penetration. Steel sheet pile sections used in such difficult driving conditions are selected according to the driving resistance rather than the design moments in the project. Another frequently faced problem is the flaws in interlocking during driving which result in leakages under water table (Ou, 2006) and (Ergun, 2008).

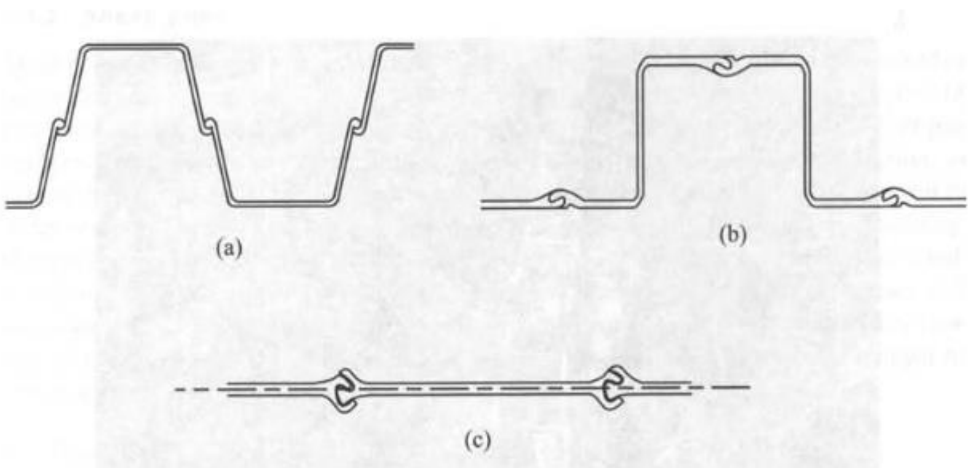

Figure 2.2: Sections sheet piles (a) U- pile, (b) Z-pile and (c) Straight line (Ou, 2006)

3. Pile walls.

In-situ pile retaining walls are very popular due to their availability and practicability. There are different types of pile walls as shown in Figure 2.3. In contiguous (intermittent) bored pile construction, spacing between the piles is greater than the diameter of piles. Spacing is decided based on type of soil and level of design moments but it should not be too large otherwise, pieces of lumps etc. drop and extra precautions are needed. Cohesive soils or soils having some cohesion are suitable. No water table should be present. Acceptable amount of water is collected at the base and pumped out. Common diameters are 0.60, 0.80, 1.00m. Waling beams (usually called “breasting beams”) are mostly reinforced concrete but sheet pile sections or steel beams are also used (Ergun, 2008) and (Venkata Ramasubbarao GODAVARTHI, 2011).

Secant bored pile walls are formed by keeping spacing of piles less than diameter (S<D). It is a watertight wall and may be more economical compared to diaphragm wall in small to medium scale excavations due to cost of site operations and bentonite plant. There is also need for place for the plant. It may be constructed “hard-hard” as well as “soft-hard”-“Soft” concrete pile contains low cement content and some bentonite. Primary unreinforced piles are constructed first and then reinforced secondary piles are formed by cutting the primary piles. Pile construction methods may vary in different countries for all types of pile walls like full casing support, bentonite support, and continuous flight auger (CFA).Tangent pile walls are constructed with no overlap and ideally, one pile touches the other. Compared secant pile walls, tangent pile walls offer increased construction alignment flexibility, easier and quicker construction and low construction cost. Tangent piles with grouting in between are used in cases where ground water exists (Ergun, 2008) and (Venkata Ramasubbarao GODAVARTHI, 2011).

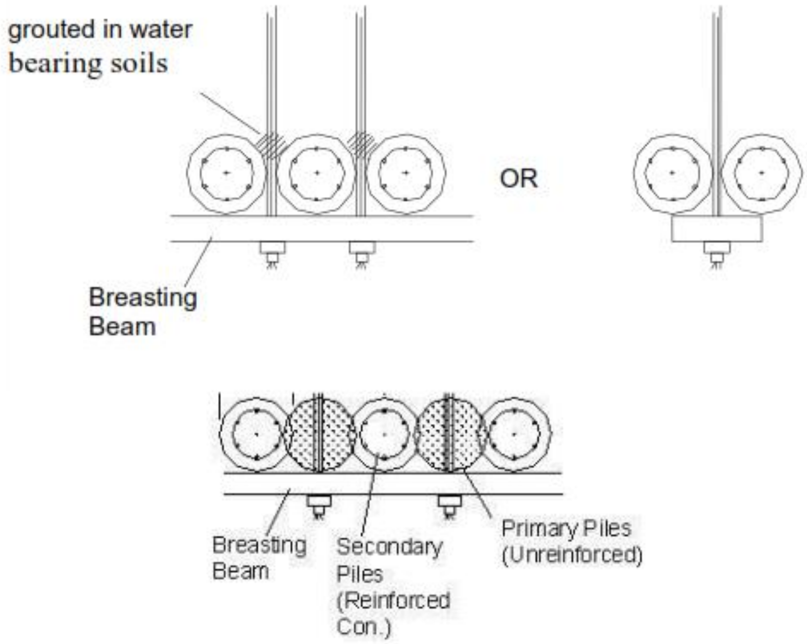

Figure 2.3: Types of Pile Wall (Ergun, 2008)

4. Diaphragm walls or Slurry trench walls.

Diaphragm walling is a technique of constructing a continuous underground wall from ground level. These reinforced concrete diaphragm walls are also called Slurry trench walls due to the reference given to the construction technique where excavation is made possible by filling and keeping the wall cavity full with bentonite-water mixture during excavation to prevent collapse of vertical excavated surfaces. Typical wall thickness varies between 0.6 to 1.1m. The wall is constructed panel by panel in full depth. Panel width varies from 2.5m to about 6m. Short widths of 2.5m are selected in less stable soils, under very high surcharge or for very deep walls. It must be remembered that Diaphragm walls are constructed as a series of alternating primary and secondary panels. Alternate primary panels are constructed first which are restrained on either side by stop-end pipes. Before the intermediate secondary panel excavation is taken up, the pipes are removed and the panel is cast against two primary panels on either side to maintain continuity. The major disadvantage of Diaphragm wall is it requires massive equipment, long construction period, and huge cost (Venkata Ramasubbarao GODAVARTHI, 2011).

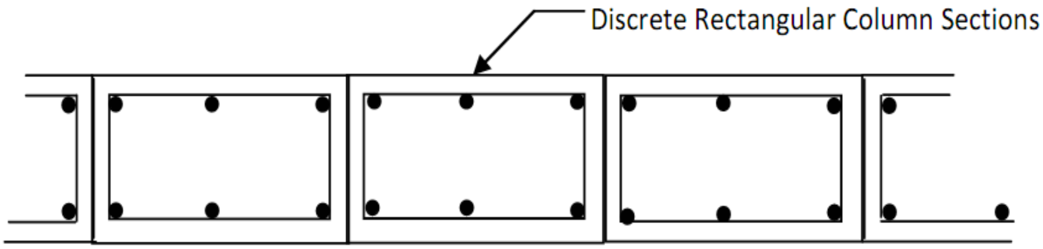

Figure 2.4: Diaphragm Wall (Venkata Ramasubbarao GODAVARTHI, 2011)

2.3: General Deflection Behavior of an Excavation Support System

Lateral wall deflections and ground surface settlements are important parameters to predict the performance of an excavation support system. These are a function of excavation support system stiffness, excavation geometry, the in-situ soil and groundwater conditions, stability against basal heave and the construction procedures and workmanship.

Excavation activities generally include these three stages: installation of retaining wall, excavation of soil mass and installation of lateral support elements at different levels, and removal of supports and backfill. However, the removal of temporary support system after the construction of permanent retaining wall is optional.

(Clough, G. W., and O’Rourke, T. D., 1990) associated ground settlement. The general deflection behaviors of lateral support systems during different phases of constructions are presented in Figure-2.5. At early excavation phase i.e. prior to installation of first level of lateral support is shown in Figure-2.5a. During this phase, the deflection of wall is approximated to be cantilever type while the associated settlements in adjacent ground may be represented by a triangular distribution having the maximum value very near to the wall. As the excavation continues, ground anchors or struts are installed at design locations that induce inward movement of wall Figure-2.5b similarly, due to inward movement of wall the ground settlement profile also changes.

The combinations of these two types of movements i.e. cantilever and deep inward movements results in the cumulative wall and ground surface displacement profiles shown in Figure-2.5c.

The authors stated that if deep inward movements are the predominant form of wall deformation, the settlements tend to be bounded by a trapezoidal displacement profile as in the case with deep excavations in soft to medium clay. If cantilever movements predominate, as can occur for excavations in sands and stiff to very hard clay, then settlements tend to follow a triangular pattern.

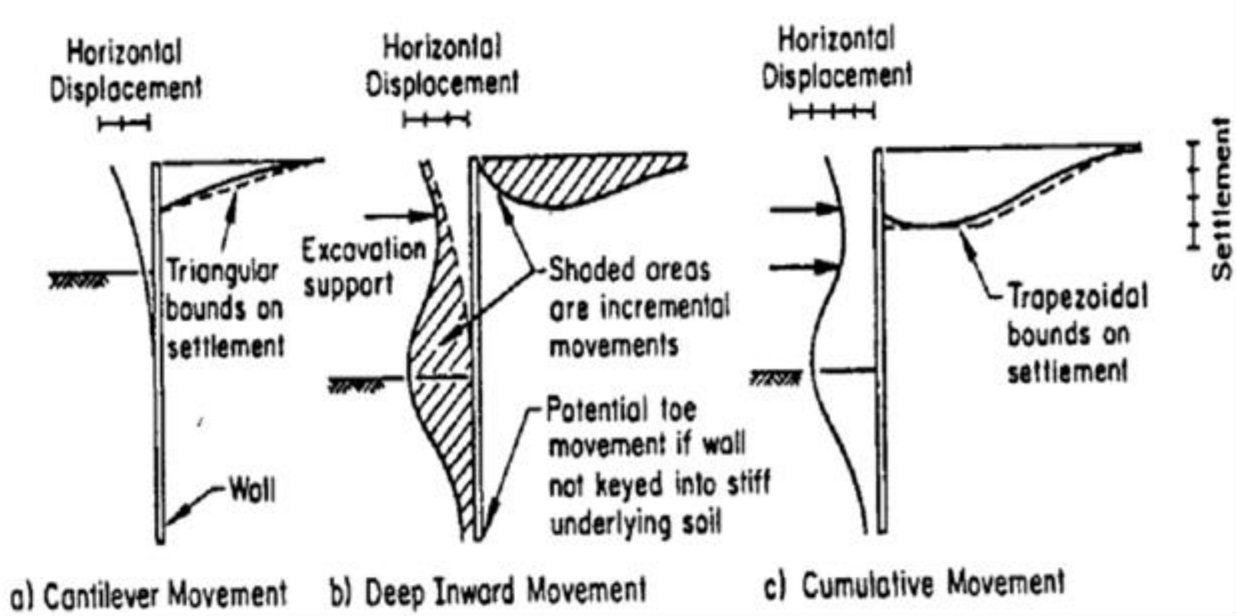

Figure 2.5: Typical Profiles of Movement for Braced and Tieback Walls (Clough, G. W., and O'Rourke, T. D., 1990)

It has to be noted that Figure 2.5 only describes the general wall deflection behavior in response to the excavation and neglects important factors such as soil conditions, wall installation methods, and excavation support system stiffness, which have been shown to influence the magnitude and shape of both lateral wall movements and ground settlements.

The authors also conducted a finite element parametric study on stiff clays. Their analyses showed that parameters such as wall stiffness and support spacing have only a small influence on the predicted movements in these soils because in most circumstances these soils are stiff enough to minimize the need for stiff support elements. They found soil modulus and coefficient of lateral earth pressure have a more significant impact on the ground movements. Their results suggested that in a stiff soil, variations in soil stiffness have a more profound effect on wall behavior than system stiffness.

2.4: Ground Movement Predictions Adjacent to Excavations

The stresses in the ground mass change during excavation activities. These changes are evidenced in the form of vertical and horizontal ground movements whose magnitude and distribution are closely related to factors such as (i) soil condition, (ii) excavation geometry, (iii) stability against basal heave, (iv) type and material of retaining wall, (v) stiffness and spacing of vertical and horizontal supports, (iv) construction procedures, and (vii) workmanship. A direct and quantitative analysis of excavation related ground movements is not an easy task. It requires an analysis of the complex interaction between the aforementioned parameter in the three-dimensional way.

(Ou et al., 1993) Proposed a procedure to estimate excavation-induced ground settlement profile normal to the excavation support wall. Their work was based on observation of 10 case histories in soft soils (Taipei, Taiwan). From these data, they developed a trilinear settlement profile (Figure 2.6) called spandrel-type settlement, which presents the maximum settlement very near to the wall. The spandrel type of settlement profile occurs if a large amount of wall deflection occurs at the first phase of excavation when cantilever conditions exist and the wall deflection is relatively small due to subsequent excavation. The data presented in Figure 2.6 is normalized settlement, $\delta v/\delta v$ (max), where δv (max) is the maximum ground surface settlement, versus the square root of the distance from the edge of the excavation, d , divided by the excavation depth, He .

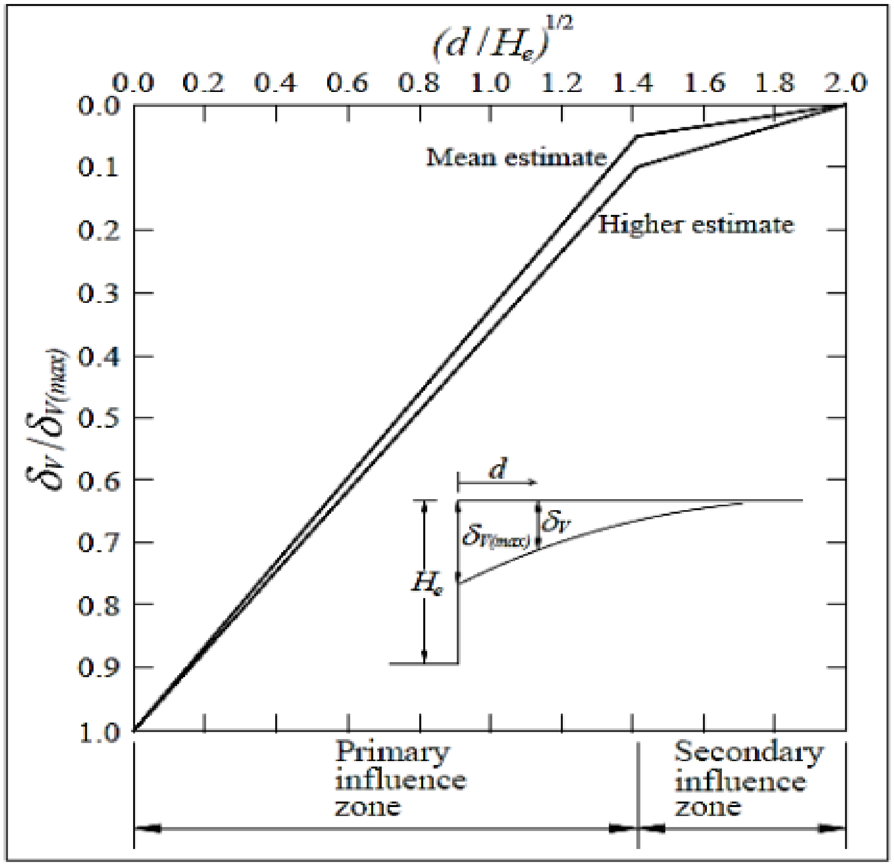

Figure 2.6: Shape of Spandrel Settlement Profile after (Ou et al., 1993).

(Hsieh, P. G., and Ou, C. Y., 1998) , extended the work of (Ou et al., 1993) and proposed a concave type settlement profile for vertical deflection induced by deep excavations This work was based on data from nine case histories worldwide. For the concave type, it was proposed that a tri-linear line, in which the maximum ground surface settlement occurred at a distance equal to half the depth where the maximum lateral wall deflection occurred, represented the profile. The estimated concave type settlement profile is shown in Figure 2.7. It can be seen that the maximum settlement occur at a distance of He/2 from the wall and the predicted settlement at the face of wall is equal to half the maximum settlement i.e. δv(max)/2.

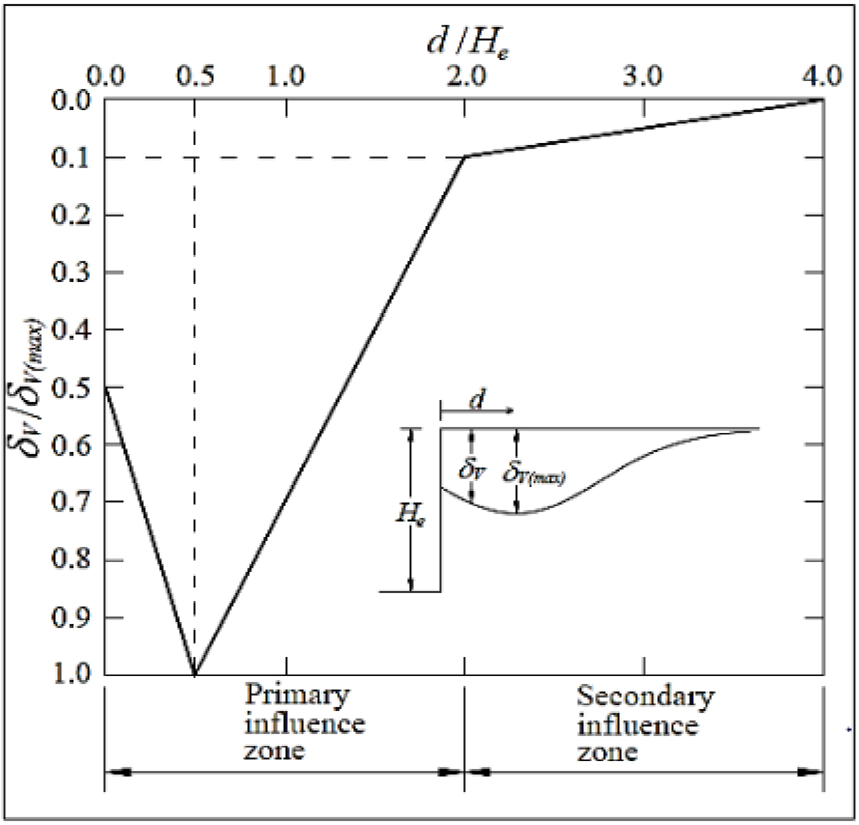

Figure 2.7: Proposed Method for Predicting Concave Settlement Profile after (Hsieh, P. G., and Ou, C. Y., 1998)

(Hsieh, P. G., and Ou, C. Y., 1998), also proposed a procedure to predict the settlement profile based on following simple steps;

i. Predict maximum lateral deformation based on finite element methods.
ii. The cantilever area and deep inward bulging area of the wall are calculated to determine the type of settlement profile. If $As \geq 1.6Ac$, concave type of settlement profile is adopted where, *As* and *Ac* refer to areas of deep inward movement and area of cantilever movement.
iii. The maximum ground surface settlement is estimated using empirical correlations $\delta v\ (max) \approx 0.5$ to $1.0\delta h\ (max)$.
iv. Plot the relevant settlement profile type using Figure 2.6 and Figure 2.7 for spandrel and concave type profiles, respectively.

(Moormann, 2004), had carried out extensive empirical studies by taking 530case histories of retaining wall and ground movement due to excavation in soft soil (Cu< 75kPa) . It was concluded that the ground conditions and excavation depth H are found to be the most influential parameters for deformation due to excavation. The location of maximum horizontal displacement is at 0.5H to 1.0H below the ground Figure 2.8 and Figure 2.9. The retaining wall and ground movements seem to be largely independent of the system stiffness of the retaining system.

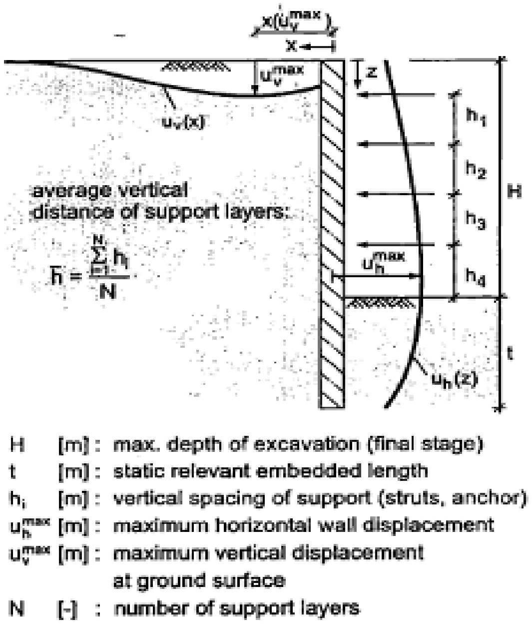

Figure 2.8: Definition of symbols used in analysis (Moormann, 2004).

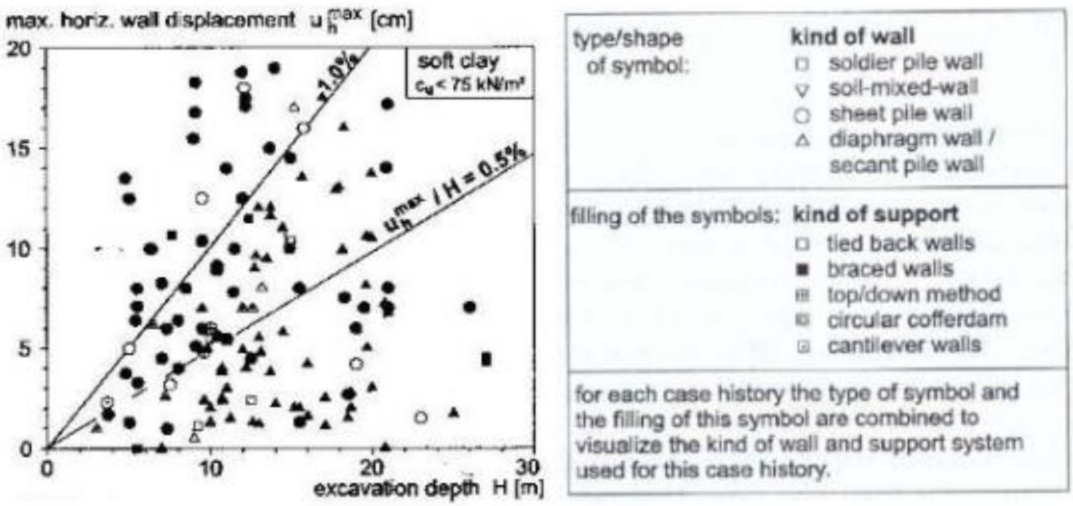

Figure 2.9: Variation of maximum horizontal displacement with excavation depth following (Moormann, 2004)

Figure 2.10 shows variation of normalized horizontal displacement with the system stiffness of the retaining structure. The large scatter was observed and calculated factor of safety of about one could lead to observed maximum wall displacement Uhma_x/H as low as 0.1% even when the value expected by (Clough et al., 1993) was about 1% even for the system stiffness support system.

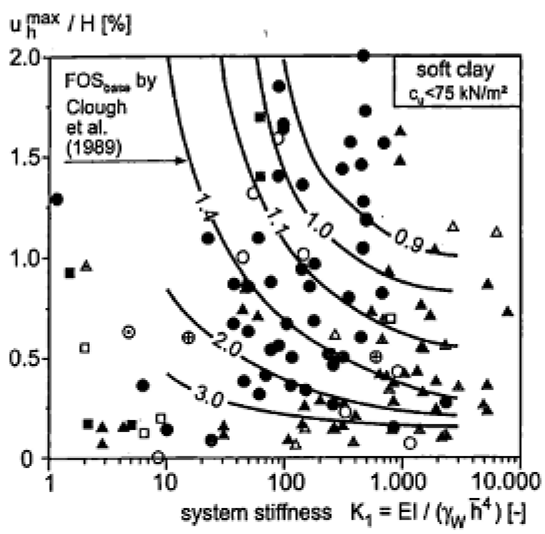

Figure 2.10: Variation of normalized maximum horizontal displacement with system stiffness following (Moormann, 2004).

2.4.1: Relation between δh (max) and δv (max)

The magnitude of maximum ground settlement is a function of maximum lateral movement of wall. Based on number of case histories of braced excavations reported.

The data presented in the Figure 2.11 was reported by (Ou et al., 1993), (Mana, A. I., and Clough, G. W., 1981) and (Hsieh, P. G., and Ou, C. Y., 1998) in clays from several case histories around the world. Both these deformation values were normalized with respect to height of excavation He. According to their study, the correlation between the maximum ground and maximum lateral deformation is given as:

$\delta v(max) \approx 0.5\delta h(max)\ to\ 1.0\delta h(max)$……………………………………….equation (2.1)

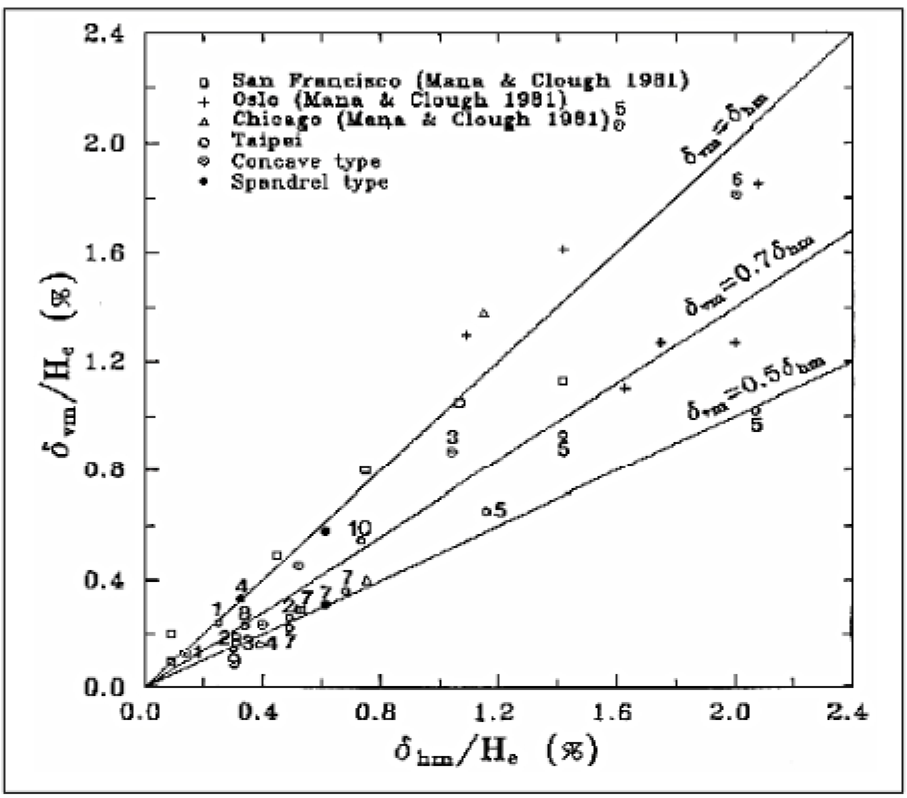

Figure 2.11: Relationship between Maximum Ground Settlement and Maximum Lateral Wall Deflection Adapted from (Ou et al., 1993) and (Hsieh, P. G., and Ou, C. Y., 1998).

2.5: Review of Earlier Works

(Peck, 1969) developed the first empirical method to predict maximum surface settlement δv(max) based on actual ground deformation data collected from temporary braced sheet pile and soldier pile walls with tie back support as shown in Figure 2.9.

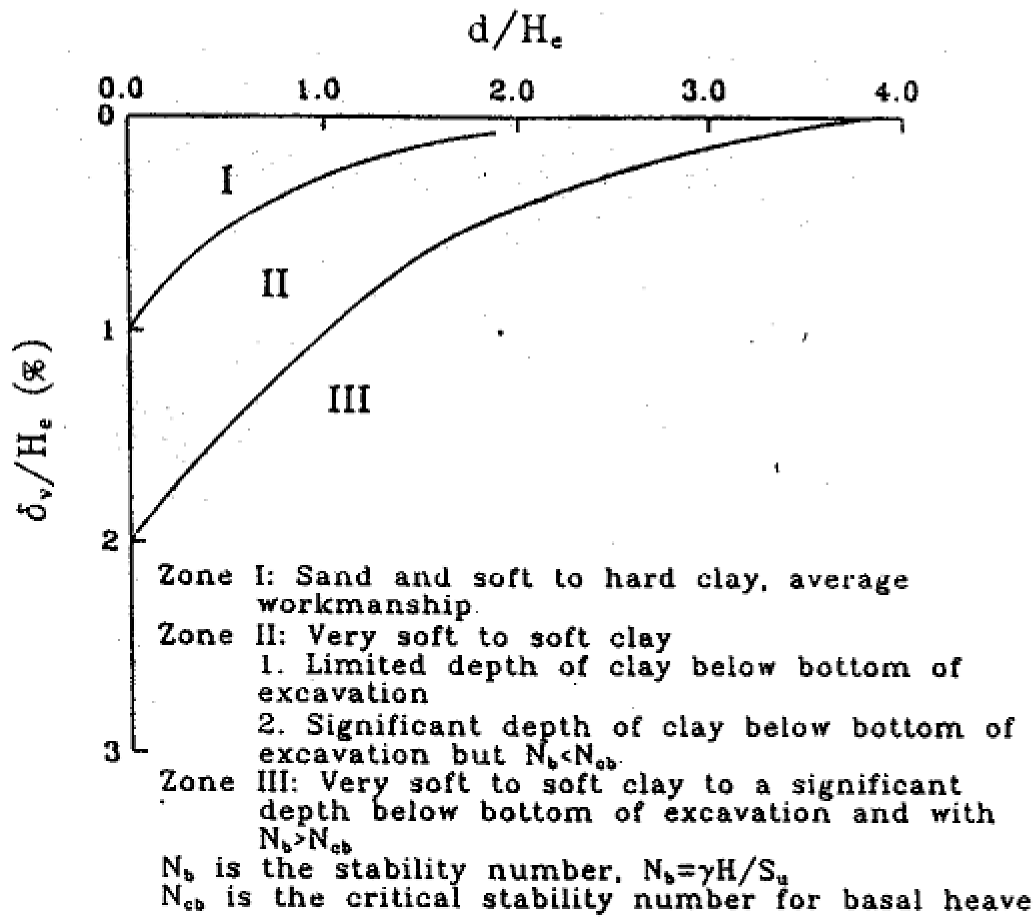

Figure 2.12: Summary of Settlements Adjacent to Open Cuts in Various Soils as a Function of Distance from edge of Excavation (Peck, 1969).

Figure 2.12 gives the settlements δv (max), divided by the maximum excavation depth (He), and plotted against the distance (d) from the walls also divided by the depth (He).

The author classified the soil based on undrained shear strength in three zones. Zone I for sands and hard clays and Zone III for very soft-to-soft clay with a low margin of safety against excavation basal heave. According to the findings, the maximum ratio of δv (max) normalized by depth of excavation (He) was 1.0% for Zone I and > 2.0% for Zone III soils.

(Clough, G. W., and O'Rourke, T. D., 1990) presented dimensionless settlement profile shown in Figure 2.13 as basis for estimating settlement patterns adjacent to excavations. Distinct profiles were developed for sands, stiff to very hard clays, and soft to medium clays. Based on the figures below, the settlement influence zone is 3He for excavations in stiff to very hard clays and 2He for excavations in sands and soft to medium clays. Nevertheless, other settlement-associated activities, such as dewatering, deep foundation removal or construction, and wall installation as practiced in modern day construction of diaphragm walls are not taken into consideration and it should be used as a conservative settlement prediction method.

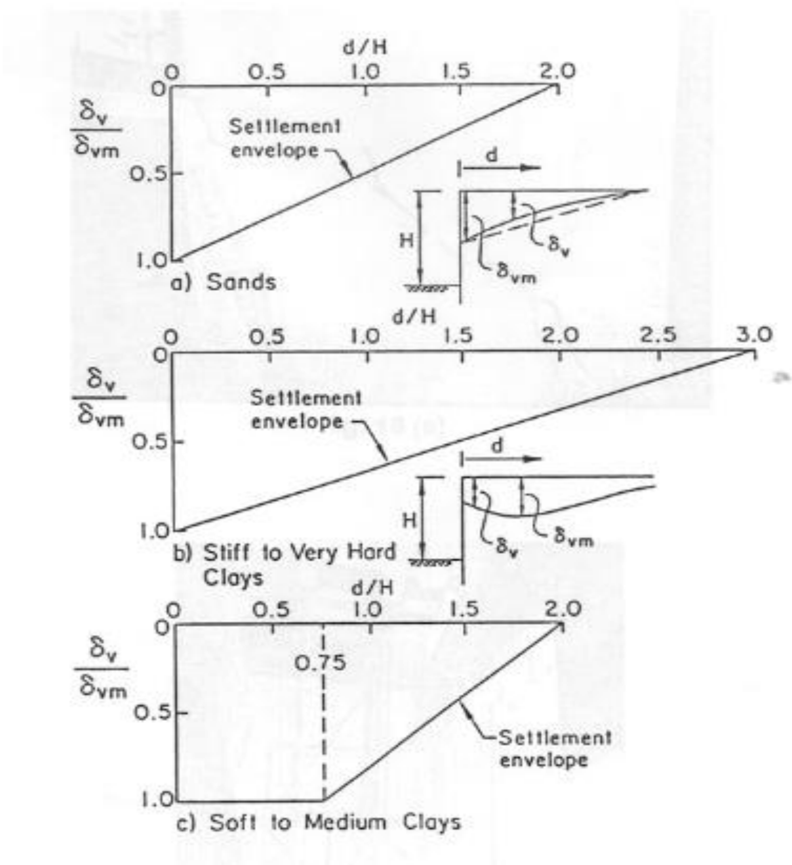

Figure 2.13: Settlement Profiles Recommended for Estimating the Settlement Distribution Adjacent to Excavation (Clough, G. W., and O'Rourke, T. D., 1990)

Figure 2.13 shows that a trapezoidal envelope bounds the settlement distribution in soft clays. Inside the envelope, two zones of movement could be identified. The zone in which the maximum settlement occurred was at 0 = d/He = 0.75 (d is the distance from the excavation and H is the final height of the excavation). At 0.75 < d/H = 2.0, there was a transition zone in which settlements decreased from maximum to negligible values. In using the diagrams presented above, it should be recognized that they pertain to settlements caused during the excavation and bracing stages of construction. Excavations in stiff to very hard clays showed variable behavior, with heave possible for some conditions. For stiff to very hard clays, the dimensionless diagram in Figure 2.13 should be used as a conservative estimate, if the wall is stable and not affected by poor construction techniques.

(Hsieh, P. G., and Ou, C. Y., 1998) found that the ground settlement profile induced by deep excavation could be categorized into the spandrel type and concave type. These two types are closely related to the wall deflection shape as shown in Figure 2.14. In the spandrel, the maximum settlement occurs very close to the wall, while in the concave type the maximum settlement occurs at a distance away from the support wall. The spandrel type of settlement profile occurs if a large amount of wall deflection occurs at the first stage of excavation when cantilever conditions exist and the wall deflection is relatively small due to subsequent excavation. After the initial stages of excavation, additional cantilever wall deflection is restrained by installation of support as the excavation proceeds to deeper elevations. The concave settlement profile reflects the ground settlement profile that develops when the movements are more deep-seated.

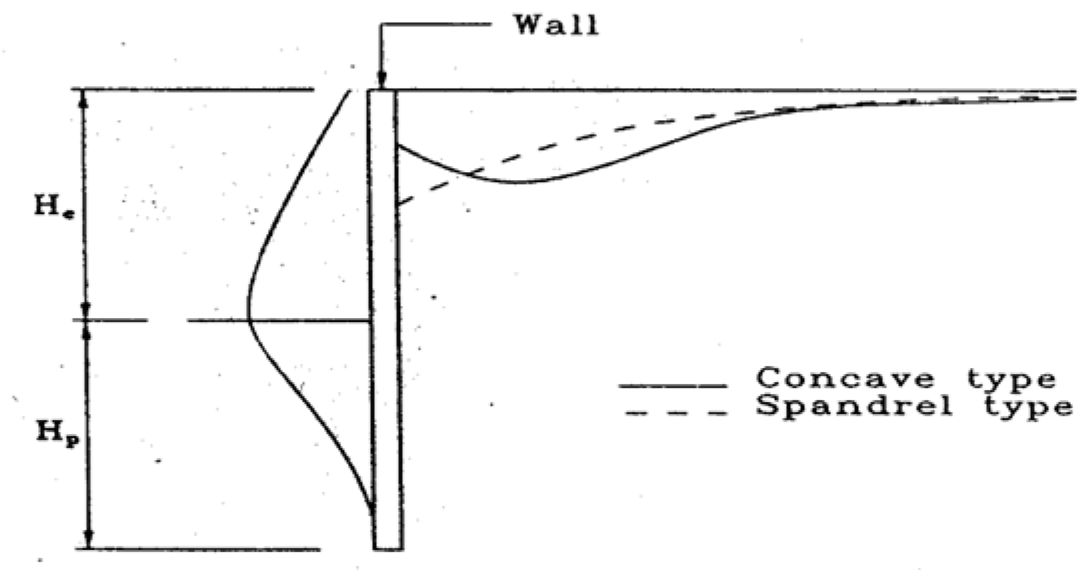

Figure 2.14: Type of Ground Surface Settlement (Hsieh, P. G., and Ou, C. Y., 1998)

Figure 2.15 show the settlement profile for a spandrel-type condition. The data are presented as normalized settlement v/v_m where v_m is the maximum ground settlement; versus the square root of the distance from the edge of the excavation divided by the excavation-depth, (d/He).The relationship was based on 10 case histories from Taipei, Taiwan. The "mean" estimate curve shown in the figure was derived based on the results of regression analysis.

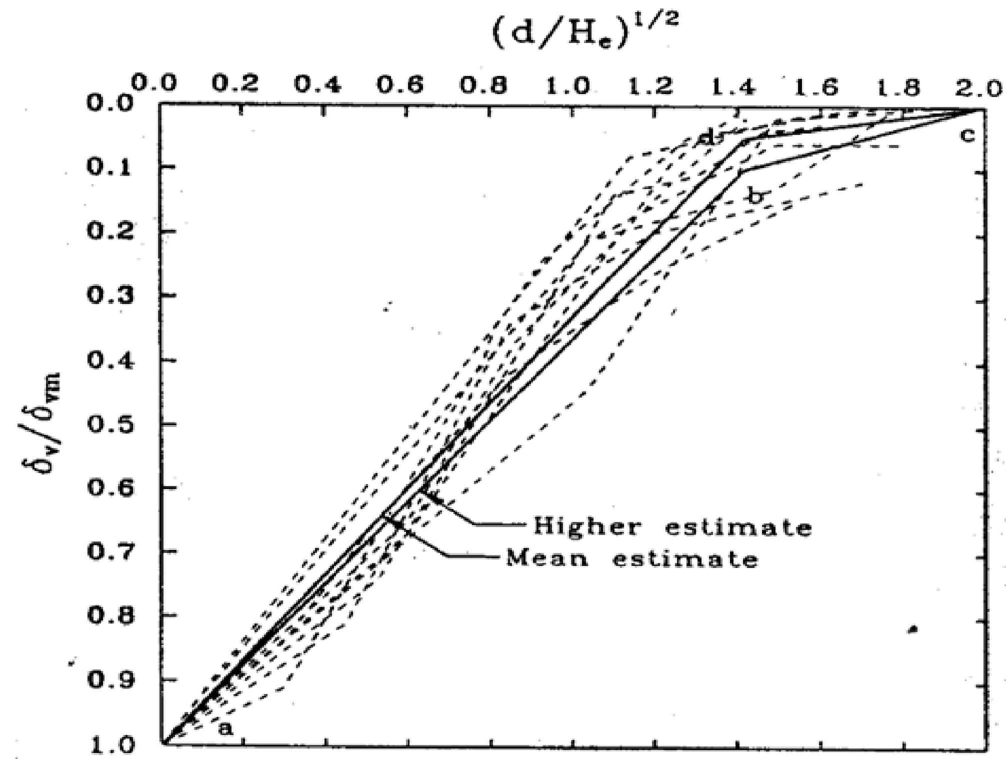

Figure 2.15: Proposed Method for Predicting Spandrel Settlement (Clough, G. W., and O'Rourke, T. D., 1990)

In figure 2.15, the broken lines show the 10 cases and the solid lines show the higher and the mean estimate. The curve in Figure 2.16 was developed for the concaved settlement profile from case histories and obtained from additional sites in Taipei. It was concluded that the distance from the wall to the point where the maximum ground surface settlement occurred was approximately equal to half the excavated depth. Assuming the maximum lateral wall deflection occurs near the excavation bottom, the distance where the maximum ground surface settlement occurs can be taken as half the final excavation depth (He/2). Using case histories, the settlement at the wall was established as 0.5Vvm. The point marked by d/He=2 corresponds to the extent of the primary influence zone. The case histories also showed that settlement was practically negligible at a distance from the wall equaled to four excavation depths (4He) and was thus used as the farthest most point on the curve. For simplicity, a linear relationship was assumed between each turning point.

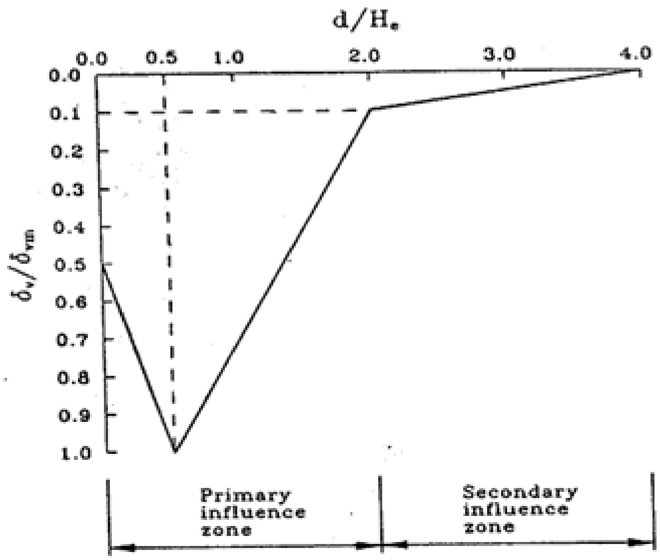

Figure 2.16: Proposed Method for Predicting Concave Settlement Profile (Clough, G. W., and O'Rourke, T. D., 1990)

The influence range behind an excavation has been also called as AIR (Apparent Influence Range). The AIR is found by:

$\mathrm{AIR} = (\mathrm{He} + \mathrm{Hp}) \tan\left(45 - \frac{\phi}{2}\right) \leq (\mathrm{He} + \mathrm{Hp})$ ……………………………………equation (2.2)

Where: *He* is the final excavation depth and H_p is the wall penetration depth

The primary influence zone ends at 2He and agrees with (Clough, G. W., and O'Rourke, T. D., 1990)'s analysis result. For economical purpose, wall depth is designated based on the concept of free earth support in which the toe of the wall is allowed to move freely. Therefore, the extent of the active zone behind the wall may be equal to the wall depth. It has also been suggested in the paper that the primary settlement influence zone might be the same as the extent of active zone behind the wall.

(L. Sebastian Bryson & and David G. Zapata-Medina, 2012) studied 30 case histories of excavation support system in soft clays, medium stiff and stiff clays (10 in each case). The author conducted a series of parametric studies to analyze the three dimensional ground movements using the system stiffness as a variable parameter. A total of 48 cases using full scale three dimensional finite element analysis was carried out to account for actual three dimensional ground movements using Hardening soil model to incorporate the elasto-plastic response of the soil in analysis. The grouping of data was based on soil conditions and different parameters like wall stiffness, system flexural rigidity and support spacing that were varied or kept constant during different simulations to study their effect on ground movement and finally compared with (Clough, G. W., and O'Rourke, T. D., 1990) design chart.

Based on the studies, the author concluded that the results for stiff clays agree well with (Clough, G. W., and O'Rourke, T. D., 1990) design chart. In soft to medium clays, the stiffening effects of excavation corners and the influence of wall embedment depth on the factor of safety induce a scatter in data when compared (Clough, G. W., and O'Rourke, T. D., 1990). The scatter in data is attributed to the fact that (Clough, G. W., and O'Rourke, T. D., 1990) does not incorporate the three dimensional effects of excavations. The author suggested that the stiffness parameter given by (Clough, G. W., and O'Rourke, T. D., 1990) does not represent the real nature of deep excavations.

(Ramadan E.H., 2013) presented analysis of piles supporting excavation adjacent to existing buildings. Contiguous pile wall was used and analyzed by PLAXIS 3D. Since the buildings around the excavation were old buildings, which suggested that there might be shallow foundations in which the new bottom level excavation would be below the existing foundation levels. Therefore, an estimation of ground movement as well as stability check of the adjacent buildings was necessary. This happened because the lateral loads from the soil movements induce bending moments and deflections in the piles supporting excavation, which may lead to structural distress or failure of both the existing building and the excavation supporting system. The excavation area was 10*10m.The foundation of the adjacent building was assumed to be three strip footings of 10m length and 2m width each and in between distance of 2m and modeled as plate of thickness of 0.5m at depth of 1.5m. Foundation was idealized with six nodes triangular plate element in the analysis. Interface element was used to represent the contact between plate elements and soil. The soil strata investigated was a deposit of clay with Mohr-Coulomb model adopted in PLAXIS. The diameters of the piles used were 0.3 and 0.4m (Ramadan E.H., 2013).

The excavation stages followed were as follows:

- Applying the stress of the adjacent building at the foundation level without the pile wall and the excavation which was 100kPa
- Activation of the pile wall in the soil
- Excavation of the soil

It was suggested by this study that excavation height (H) and cohesion of clay (Cu) are two main parameters in the design of the pile wall. Further, it was found that results should be related to a factor that has both the effect of excavation height (H) and the undrained soil shear strength (Cu). The stability factor (Nc) relates both H and Cu.

$N_c = \frac{\gamma.H}{C_u}$ …...equation (2.3)

Large soil movement was observed due to the stress of the adjacent building in the case of unsupported excavation. The lateral displacement increases rapidly as the excavation height increases. Maximum lateral displacement increased from about 0.06 to 0.2m when Nc increased from 1.9 to 3.2. However, the maximum lateral displacement increased to very large value of 1.2 m for Nc = 4.5. This means that the excavation was failed at Nc = 4.5. When the excavation is supported using contiguous pile wall, soil movement decreases in the zone above the excavation level. However, below the excavation level, there is no obvious decrease in soil movement. It should be noted that in all cases the pile wall is translated horizontally. Pile wall lateral deflection increased as excavation height (H) or the stability factor (Nc) increased. As Nc increased pile wall movement changed from translation (H =3m) to both translation and rotation (H = 5 and 7m) as shown in Figure 2.17. Maximum lateral deflection was observed at a depth of 0.6 to 0.8H with the lowest value for small Nc value (Ramadan E.H., 2013).

The results of the analysis are depicted on the graphs below (Ramadan E.H., 2013).

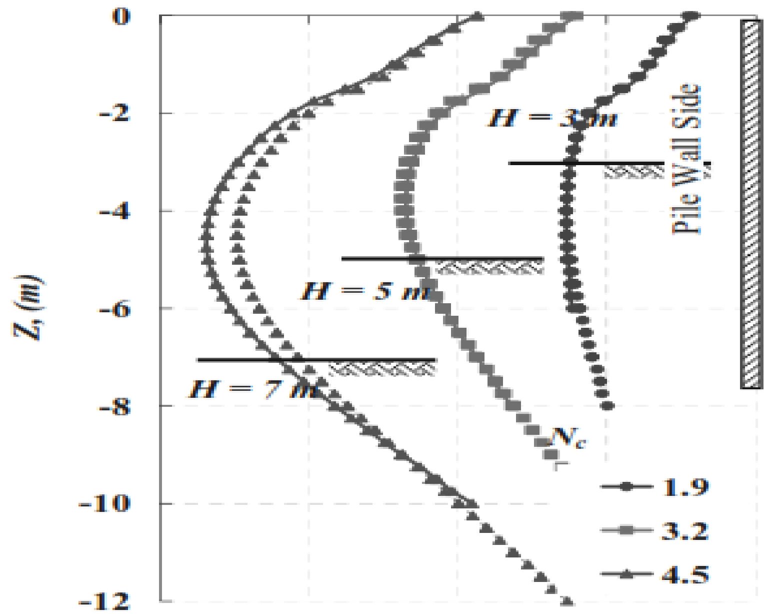

Figure 2.17: Lateral Displacement Profile of Contiguous Pile Wall for Different Nc Values (Ramadan E.H., 2013).

Where d is the distance from the edge of the supporting wall. The horizontal displacement is normalized by d. In addition, the different graphs are for Nc values of 4.5, 3.2 and 1.9 from left to the right of the graph respectively. For Nc value 4.5, the first line is for depth of embedment of 3m and the second line is for embedment depth 5m (Ramadan E.H., 2013).

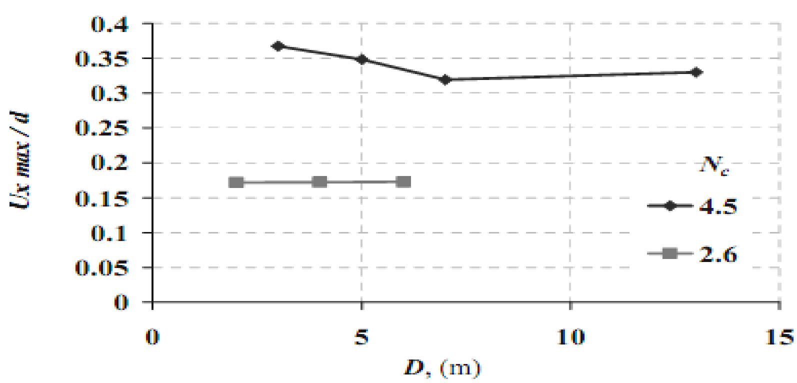

Figure 2.18: Normalized Maximum Lateral Pile Wall Displacement Versus The Stability Factor Nc (Ramadan E.H., 2013).

It can be seen from Figure 2.18, the depth of embedment (D) affects the horizontal displacement to some extent. After embedment depth of around 6m, the decrease of horizontal displacement is small.

(Chavda Jetish, 2014) presented numerical modeling of pile wall using PLAXIS -3D in order to carry out parametric studies, effect of stage wise excavation on the ground and pile wall deformation. The length of wall is taken as 16m, diameter of pile as 750mm, Capping beam of 750 x 375 mm considering same properties of pile, height of excavation is up to 8m with stage-wise excavation of every 2m, 3D model of 30m x 3m x 20m (X, Y & Z) having pile wall at distance of 20m. In order to discard the effect of pore water pressure, modeling (Mohr-Coulomb) is done considering no water table i.e. dry soil. The stage wise excavation is done in phases to stimulate actual site condition on field. The depth of excavation in each phase is of 2m with total 4 phase, excavation depth of 8m is done. The first parametric studies carried out varying the soil friction angle, the soil friction angle used in the previous section is 30˚. Therefore, the model of Φ=30˚ is used as the control model. The values of Φ used in this part are 20˚, 25˚, 30˚, 35˚ and 40˚. Second parametric study is carried out by varying the unit weight of soil. Similar to the first parametric study, PLAXIS model in pervious section with unit weight of 16KN/m^3 is used as control model. In the study, the unit weights used is 14, 15, 16, 17 and 18kN/m^3 .The third parametric study is height of wall. In control model from pervious section, the height of wall used is 16m.The values of height of wall used are 14, 15, 16, 17 and 18m for parametric study. The last parametric study conducted based on diameter of pile by increasing from 750 to 1500mm.

Based on the method used and output results (Chavda Jetish, 2014) concluded the following.

- With progress in excavations, the ground deformation increases and the settlement value becomes larger and larger as the excavation deepens. According to numerical analysis, a distance range of 0m to 10m from the foundation excavation is the main influence area, and the away from excavation, there is less influence on the surface settlement.
- In parametric studies, when soil friction angle increases, the deformation of Pile-wall decreases, this due to the increasing internal shear strength within the soil with increasing soil friction angle. Hence, active earth pressure developed on the wall is reduced.
- When the soil unit weight increases the deformation of Pile-wall increases.

- When soil unit weight increases, vertical stress acting on a soil mass increases, and eventually causes lateral active stress to increase.
- With increase in height of Pile- wall from14m to17m, there is decrease in deformation of pile wall. At a wall height of 18m there is increase in deformation of pile wall is observed, this is due to increases in slenderness ratio and it cannot take passive resistance from the bottom portion of pile wall when it rotates.
- With increase in diameter of pile reduces the deformation of pile wall. This is due to increase in structural stiffness.

(Zhou, 2015) discussed the use of 3D finite element method in deep excavations, especially the simulation of sequential excavation method in 3D finite element model. Spaarndammer tunnel project in Amsterdam was used as study area and the soil parameters used in the models were derived from in-situ soil investigation. Cone penetration tests and boreholes were carried out along the tunnel location. Parametric study has been done in order to investigate how the domain and mesh set-up influence the results in 3D finite element model. Comparison where done between 2D and 3D finite element by taking certain geometry of excavation section. Also after comparison, the sequential excavation method was implemented into 3D finite element model. Different excavation rates, excavation directions and lateral support design were tested in order to optimize the sequential excavation model. The response of sheet pile walls as well as surrounding soil were recorded and compared with the results from normal 3D excavation model.

Based on the parametric studies results the author concluded the following:

- When the excavation section is longer than 50m, the whole domain can be considered as plain strain, so that the results in 2D and 3D finite element models were almost the same.
- When the section lowered from 50 to 30m the bending of sheet pile wall reduced by 20% due to the corner effect in 3D scenario. The settlement and the heave at the bottom of excavation pit were also reduced significantly.
- On the other hand, the deflection of sheet pile wall and settlement from the normal staged excavation models were well within the range of acceptance, but the improvement was not as striking as expected. The excavation is almost 10 meter on one side, but the difference of deflection results is only1.5cm.The difference is almost negligible in practice.

2.6: Numerical and Analytical Studies of Deep Excavations

(Wong, I., Poh, T., & Chuah, H., 1996) Presented the performance of deep excavations for the Central Expressway (CTE) Phase-II project in Singapore. The authors examined lateral wall deflections, soil settlements, and prop loads for the different support systems used and soil conditions encountered. They found that maximum wall movements were typically less than 0.005He for excavations with a combined thickness of soft soil layers of 0.9He overlying stiff soils. The maximum wall movements were typically less than 0.0035He for excavations with a combined thickness of soft soil layers of 0.6He overlying stiff soils and concluded that placing the first layer of struts near the top of braced walls is effective in reducing movements for walls embedded in stiff soil

(Hoe N.H, 2007) **c**arried out a parametric study using finite element method to investigate the effects of soil stiffness, the initial coefficient of lateral earth pressure and rock socket length. They also investigated the suitability of constitutive models (Hardening Soil model and Mohr-Coulomb model) by comparison with field monitored measured data. They used PLAXIS V-8 employing plain strain assumption and wished-in-place diaphragm wall. From the study, they concluded that wall deflection was very sensitive to change in soil stiffness and coefficient of lateral earth pressure. Though comparison with measured field monitored data, it was observed that Hardening Soil model can predict ground deformation more precisely than Mohr-Coulomb model.

(H. Popa, A. Marcu & L. Batali, 2009) presented Numerical modeling and experimental measurements for a retaining wall of a deep excavation in Bucharest, Romania. They summarized a case history of a diaphragm wall for a deep basement of a new building in the center of Bucharest. The excavation affected a number of historic structures, leading to the use of “top-down” techniques to support the excavation. The numerical results obtained by plane strain FE simulation were compared with measurements recorded during construction. For the soil, a perfect elasto-plastic constitutive law has been used, with Mohr – Coulomb criteria, using the geotechnical parameters issued from laboratory and in situ tests. From the results obtained, they concluded that the computed lateral displacements were 15% and 75% of the observed values, depending on if the comparisons were made in an area with or without a grouted wall not explicitly modeled in the finite element simulations adjacent to the diaphragm wall. The main factors leading to these differences were the soil parameters.

(Schweiger, 2009) Studied the analysis of a deep excavation project in clayey silt in Salzburg. A diaphragm wall, a jet grout panel and three levels of struts supported the excavation. Hardening-Soil model was used as a constitutive model. Because of insufficient information available at the time of design on the material properties of the jet grout panel, the authors varied its stiffness in a parametric study. The effect of taking into account the stiffness of a cracked diaphragm wall on the deformations was also investigated. In some of the 3D calculations, a non-perfect contact between diaphragm wall and strut was simulated by means of a non-linear behavior of the strut. The evaluation of the results and comparison with in situ measurements showed that analyses, which took into account the reduced stiffness of the diaphragm wall due to cracking, achieved the best agreement with the measurements. Furthermore, the three-dimensional model could best reproduce settlements of buildings.

(Korff M. & Mair R.J., 2013) discussed ground displacements related to deep excavation in Amsterdam. The settlement measurements for the Amsterdam deep excavations have been compared to several empirical relationships to determine the green field surface displacements and displacements at depth. It is concluded that the surface displacement behind the wall was 0.3-1.0% of the excavation depth, if all construction works were included. Surface displacements behind the wall can be much larger than the wall deflections and become negligible at 2-3 times the excavated depth away from the wall. The shape of the displacement fits the profile of (Hsieh, P. G., and Ou, C. Y., 1998) best. In all three of the Amsterdam cases, the largest effect on the ground surface displacement can be attributed to the preliminary activities. The actual excavation stage caused only about 25 - 45% of the surface displacements, with 55 -75% attributed to the preliminary activities. At larger excavation depths, the influence zone was significantly smaller than 2 times the excavation depth

(Birhanu, 2016) investigated the of Effects of Excavations on Adjacent Foundations using Finite Element Modeling on red clay and silty clay soil of Addis Ababa. In the study, the author determined the effects of foundation loads at different levels on a red clay soil to see the effect on adjacent excavations because of vertical and horizontal displacements. Four foundation levels were used by differentiating between the numbers of their respective building basements: no basement, one basement, two basements and three basements foundation levels. For the same foundation level, the distance from the edge of excavation was also varied from 0m to 3.5m and to 7m. The variations of vertical and horizontal displacements were plotted against the distance from the face of excavation. The results showed that at 3.5m from the face of excavation and beyond that, the displacements decreased to a minimum value. Similar trends were shown in the decrease of the vertical and horizontal displacements for those cases with the same number of strut levels showing that the strut level will affect the value of the deformation in spite of the vertical excavation level.

In the second, the author determined the vertical and horizontal displacements of the ground and wall under different cases by changing soil, wall and excavation properties by means of parametric study. PLAXIS 3D Foundation V.1 was used as a tool to carry out all the analysis. The parameters are varied for three levels of 4.9, 10.35 and 15m Final excavation. The modulus of elasticity and the excavation depth showed prominent effect on the results.

Chapter 3: Materials and Methods

3.1: General Description of Study Area

3.1.1: Location

The study area is located in Addis Ababa, Bole sub-city in the west of Bole international airport around Africa Avenue area. In this area, there are high-rise buildings and crowded traffic.

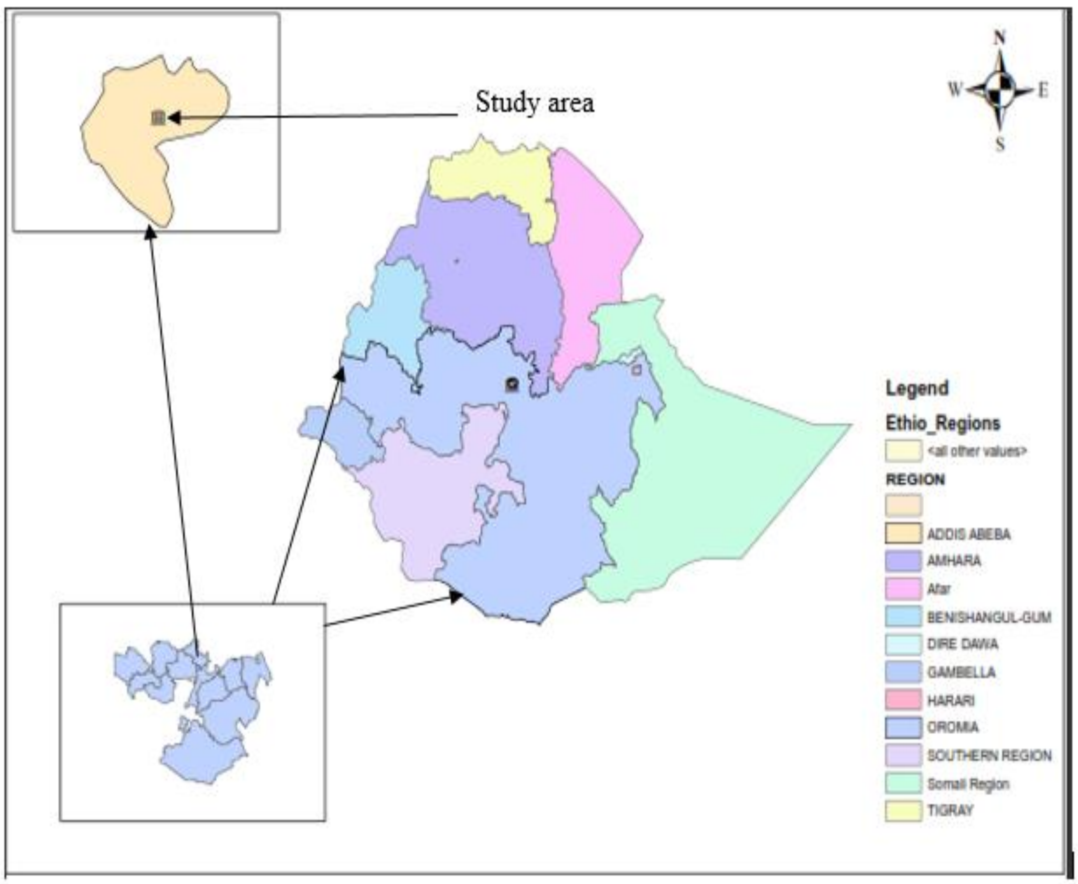

Figure 3.1: Location of Study Area

3.1.2: Geology and Subsurface Condition

Regional Geology

Four volcanic units represent the geology of Addis Ababa and its surrounding area. In the lower part it is dominated by basaltic lava flows (Addis Ababa basalt), followed by a pyroclastic sequence, mainly formed by ignimbrites (Addis Ababa Ignimbrite), followed by central composite volcanoes (Central Volcanoes unit), and finally small spatter cones and lava flows (Akaki unit) (Addis Geosystems Plc., 2016).

Addis Ababa basalt extensively crops out along Akaki, Kebena, and Dukem rivers at the east to southeastern part of Addis Ababa, and represents the oldest unit of the area. It consists of essentially sub-horizontal lava flows with thickness ranging from few meters up to 20m. Maximum thickness exposed found east of Addis Ababa, along the Kebena River. Addis Ababa basalt predominantly constituted by alkaline and olivine basalts with three main textural attributes, that is, porphyritic, aphyric, and sub-aphyric (Addis Geosystems Plc., 2016).

Addis Ababa ignimbrite is exposed close to Addis Ababa along the Akaki and Kebena rivers. It overlies the Addis Ababa basalt and locally covers the products of the composite central volcanoes of Wechecha and Furi. Different flow units, consisting of pale-green to pale-yellow welded and crystal rich ignimbrites, constitute the sequence (Addis Geosystems Plc., 2016).

Central volcanoes unit includes the Yerer volcano and the product of the two composite volcanoes Wechecha and Furi west and southeast of Addis Ababa, respectively. Wechecha and Furi volcanoes are two large edifices composed by predominant trachyte with minor pyroclastic. Yerer represents the largest volcanic edifice in the region, with a relief of 1000m from the plain and 14km wide along east-west direction. Products mainly consists of trachytes even if pyroclastics are widespread mainly in the central part eastern sector. The highest part of Yerer volcano was affected by a more recent volcanic activity that produces spatter cones and associated basalt (Addis Geosystems Plc., 2016).

Akaki unit crops out east of Addis Ababa and consists of scoria and spatter cones with associated tabular lava flows and phreato-magmatic deposits. Alluvial deposits covering these units consists of regolith, reddish brown soils, talus and alluvium with maximum thickness of about two meters (Addis Geosystems Plc., 2016).

Site Geology and Subsurface Condition

The selected site and its surroundings are covered with made ground at the top underlain by silt-CLAY and sandy silty-CLAY developed from complete weathering of underlying vesicular BASALT. Sub-surface investigation done by (Addis Geosystems Plc., 2016) for the construction 2B+SB+G+18 mixed-use building in Addis Ababa Bole area has confirmed the presence of made ground, silty CLAY, sandy silty CLAY and medium strong vesicular BASALT. The geological section showing lateral and vertical extent of these layers is shown in Appendix B.

Ground Water Observation

Measurement of ground water level was made on the borehole. Drilling operation recorded that there was no ground water boreholes within depth of 30m (Addis Geosystems Plc., 2016).

3.2: Methodologies

The existing literatures and theories in this study area were examined to establish the proper functioning of tangent pile wall. The soil data for the case of Addis Ababa Bole area was collected and correlated to use as an input during analysis using finite element software. A suitable finite element software was then used to determine the effect of strut horizontal spacing; adjacent surface load and equivalent thickness (diameter) of pile wall in the analysis of tangent pile wall and the results were discussed compared with published data of international case studies. Field measured ground deformation analysis carried out by (Clough, G. W., and O'Rourke, T. D., 1990), (Ou et. al., 1993), (Moormann, 2004), and (L. Sebastian Bryson & and David G. Zapata-Medina, 2012) were also used to compare results of FEA.

The results of FEA are verified using data of international case studies of braced excavations. A comprehensive data of 25 case studies have been gathered from published literature. Data gathered for excavation case histories, includes the excavation width, final depth of excavation, wall length, wall thickness, maximum lateral wall deflection (δh max) and maximum vertical settlement (δv max). The case studies are tabulated in Table C.13 to C.14 the appendix C. The whole process was documented in the final report together with the important conclusions and recommendations.

There were different activities that were applied for thesis work. These were classified into three main phases: preparing soil parameters, strut parameters and load parameters.

3.2.1: Parameter Identification

The performance of deep excavation support system and lateral wall movements are influenced by several factors including wall installation, soil conditions, support system stiffness, ground water conditions and methods of support system installation and interaction between the soil and the support, parameters have to be identified accordingly.

1. Soil Parameters

The basic elements for analysis of deep excavation support system are identifying parameters for base model, using in-situ test or correlations of parameters. Based on the investigations made by (Addis Geosystems Plc., 2016) a representative value of standard penetration test (SPT) data are chosen and required soil parameter correlations are done. The soil types considered for this study are the stratified silty-clay from Addis Ababa around Bole area. The engineering design parameters were extracted from SPT N values of representative borehole log sheet, shown in the appendix B, and considered to represent the soil in the study area. These parameters are used as input parameters for PLAXIS 3D.

Strength and Deformation Characteristics of the Soil

According to the SPT N values, undrained shear strength parameter of the soil is calculated by using the correlations recommended by (Hara et al., 1971) and (Kulhawy FH and Mayne Paw, 1990).

$Cu = 29N_{60}^{0.72}$ ……………………………………………………………Equation 3.1

For the effective cohesion value, the method recommended by (Sorensen KK and Okkels N, 2013) suggest that a

$C' = 0.1Cu$ ……………………………………………………………………Equation 3.2

In order to determine the long-term soil parameters, effective angle of internal friction (ϕ'), which is related to effective cohesion value, was used as recommended by (G.Look, 2007). Table B.1 in the appendix is used for correlation.

The unit values are determined with the help of Table B.2, which was prepared by (Michael Carter and Stephen P.Bentley, 1991).

Young's Modulus, E

The soil as identified at the borehole in appendix B when conducting the Standard Penetration Test was correlated. Long-term young's modulus is determined from Table B.3. Summary of ground conditions encountered in borehole is shown in Table 3.3.

Strut and Wales Parameters

Strut is a compression member. The load carried by a strut can be determined from pressure envelope. Strut is selected in the presence of neighboring building and boundary wall at the immediate vicinity, which denied the provision of anchors in any form of retaining system. In this study, there is adjacent building and that is why strut is selected.

The location and spacing of struts should be critiqued with respect to the allotted working space and proposed construction. Workers, supplies and equipment should consider access. Strut should have a minimum vertical spacing of about 2.5m. In the case braced cuts in clay soils, the depth of the first strut below the ground surface should be less than the tensile crack (Z_c), which is equal to,

$$Z_C = \left(\frac{2C}{\gamma\sqrt{ka}}\right) \quad \text{.......Equation (3.3)}$$

Wailing beam is used to distribute the loads induced by the excavation to the surrounding soil. It is attached to struts so that lateral force coming from struts can be distributed over the wall and into the retained soil.

The horizontal spacing of struts is related to construction activities and kept as large as possible 4 to 5m (Ergun, 2008). In this study, 4 and 5m is used and 3m is randomly taken to see the effect of decreasing spacing in the parametric study. The load carried by the strut is determined from pressure envelope in appendix B.

2. **Adjacent Surface Load Parameters**

In this paper, excavations are modeled with adjacent surface loads at 3.5m away from the excavation that is recommended by the Municipality of Addis Ababa (Birhanu, 2016).

The excavations and the surface loads are modelled on a silty-CLAY soil. The value of the presumptive bearing capacity for stiff soil in EBCS 7, 1995 is 100-200kPa. In order to account for safety and to show the effects with low bearing capacity for clay, which may be true for less stiff silty-CLAYS, a bearing capacity value of 150kPa is used. In addition, to study the effect of change in the load the maximum bearing capacity of 200kPa and the value of 250kPa was used randomly to see the effect.

3.2.2: Model Geometry

A characteristic base model geometry and general dimensions for the study is shown in Figure 3.2. For the 3-D finite element modelling, 15-node 'wedge' elements were used in this study for soil layers and other volume clusters. These comprise 6-node triangular faces in the horizontal direction and 8-node quadrilateral faces in the vertical direction. Beam elements consists of 3-node line elements with 6 degrees of freedom per node including three translational degrees of freedom and three rotational degrees of freedom. In PLAXIS 3-D Foundation, 'floors' are 6-node triangular plate elements, also with 6 degrees of freedom per node. In addition, the interfaces consist of 16-node interface elements, which comprise 8 pairs nodes in order to coincide with the vertical face of wedge elements.

In the software PLAXIS 3D, the hardening soil model (HS) is used because the HS model allows modeling soil hardening properties and stress dependent stiffness. Compared with the Mohr-Coulomb model, the unloading behavior of the soil is better taken into account in the HS model. The HS model may be used to calculate realistic pressure distribution below raft foundations and behind soil retaining structures. Details on the hardening soil model are given in Appendix A.

The relevant soil properties used for the base model, the drained material model is used for silty-clay soil. The tangent pile wall is modeled as plate elements in which the unloading of the ground during the installation of tangent pile wall is not considered. The Young's modulus, Es = 30,000Mpa, of the tangent pile wall is kept constant for all the analyses, a change in equivalent thickness of the tangent pile wall represents a change in both the bending stiffness and the axial stiffness of the tangent pile. In addition to that, PLAXIS adds interface elements into the model to take account the soil-structure behavior.

Struts and wailings were modeled with horizontal beam elements and the supporting walls were "wished into place," which means that the installation of the wall caused no stress changes or displacements in the surrounding soil.

The geometry of the excavation is 27.46x34.20m. However, in order to increase the feasible mesh fineness to obtain a satisfying mesh quality, the advantage of symmetry is used. Hence, only 1/3 of the excavation area is modelled. The horizontal dimensions of the excavation are l/b = 21/15m. This geometry is adopted from a design done for a building in Addis Ababa in Bole area for soil data. The geometry of the building simulated by the load is the same as excavation geometry, which is 21x15m. Tangent pile-wall diameter, adjacent surface load and strut horizontal spacing, are varied. For this purpose, modeling of pile-wall surface load and the soil is made using fine mesh with internal clusters very fine size. The geometry of the excavation and the area where the load is applied are kept constant throughout all the runs.

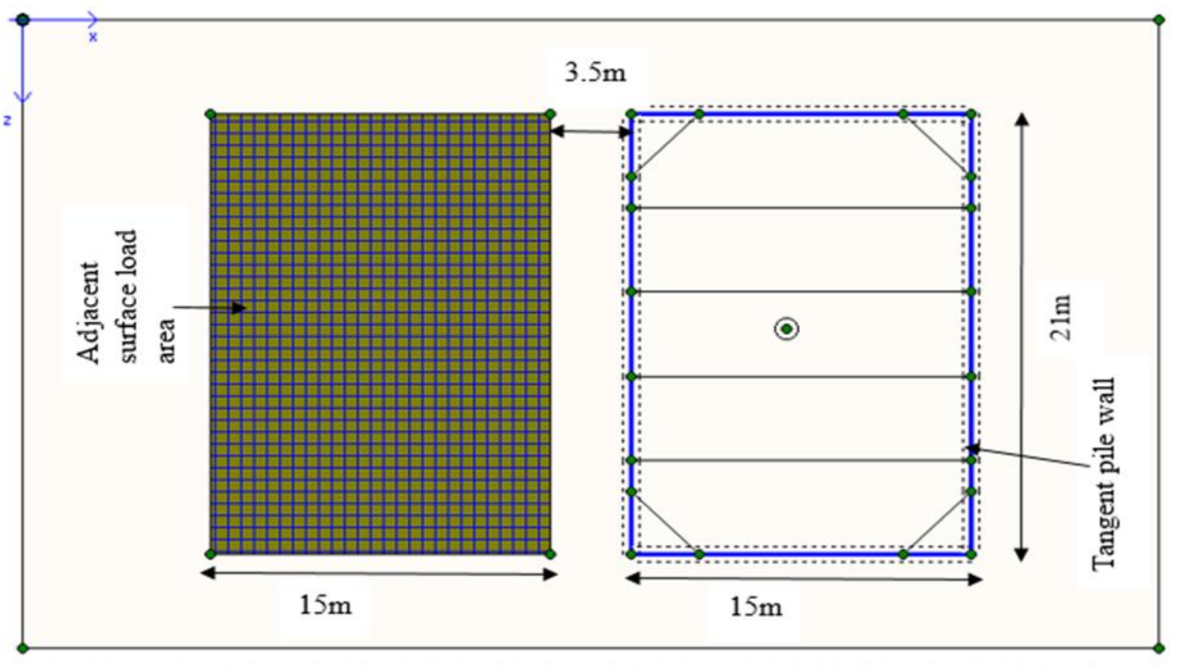

Figure 3.2: Geometry of the Excavation and Adjacent Surface Load

1. Work planes

The excavation is constructed in several phases. Work planes are horizontal planes (x-z planes) at a certain vertical level (y-level) in which geometry points and lines and, in particular, structures and loads can be identified. Hence used to model the separation between the phases. Every model in PLAXIS 3D, before the beginning of any calculation phase, starts with the initial Phase. The initial phase consists of the soil clusters only in which not all other structural parts are activated. Therefore, this stage calculates the stresses and deformations due to the soil clusters only by means of gravity loading. The undrained behavior is not considered for the initial phase because, in the this phase, the stresses from the self-weights are considered to have occurred for a long period of time making the development of excess pore water pressures irrelevant. Therefore in the initial phase, the option “ignore undrained behavior is selected”. For the other loading phases, this option is not selected, as it is needed to consider the excess pore water pressures during construction and at the end of all loading phases.

In any non-linear analysis where a finite number of calculation steps are used, there will be some drift from the exact solution. To limit this drift, tolerated error option is available in PLAXIS 3D. The tolerated error used in these runs for all phases except for few phases is 0.01. A tolerated error of 0.01 is suggested for most type of calculations. A tolerated error of 0.01 means the computed value differs from the exact solution by maximum of 1%. Therefore, this error is considered to be within safe and working limits.

The maximum iterations that this version of PLAXIS 3D allow is 100. The default value is 50 iterations. Therefore, this value has worked and has resulted in convergence of the results of all phases.

Table 3.1: Work Planes and Their Respective Structures and Phases for 8m Depth of Excavation

Work plane (y-level) in m	Structures and phases present in that work plane
0.00	Tangent pile wall and building surface load
-2.00	Tangent pile wall and first level of support
-3.00	Tangent pile wall and first level of excavation
-5.00	Tangent pile wall and second level of support
-6.00	Tangent pile wall and second level of excavation
-8.00	Tangent pile wall and final level of excavation
-13.00	Pile toe

Deformed mesh

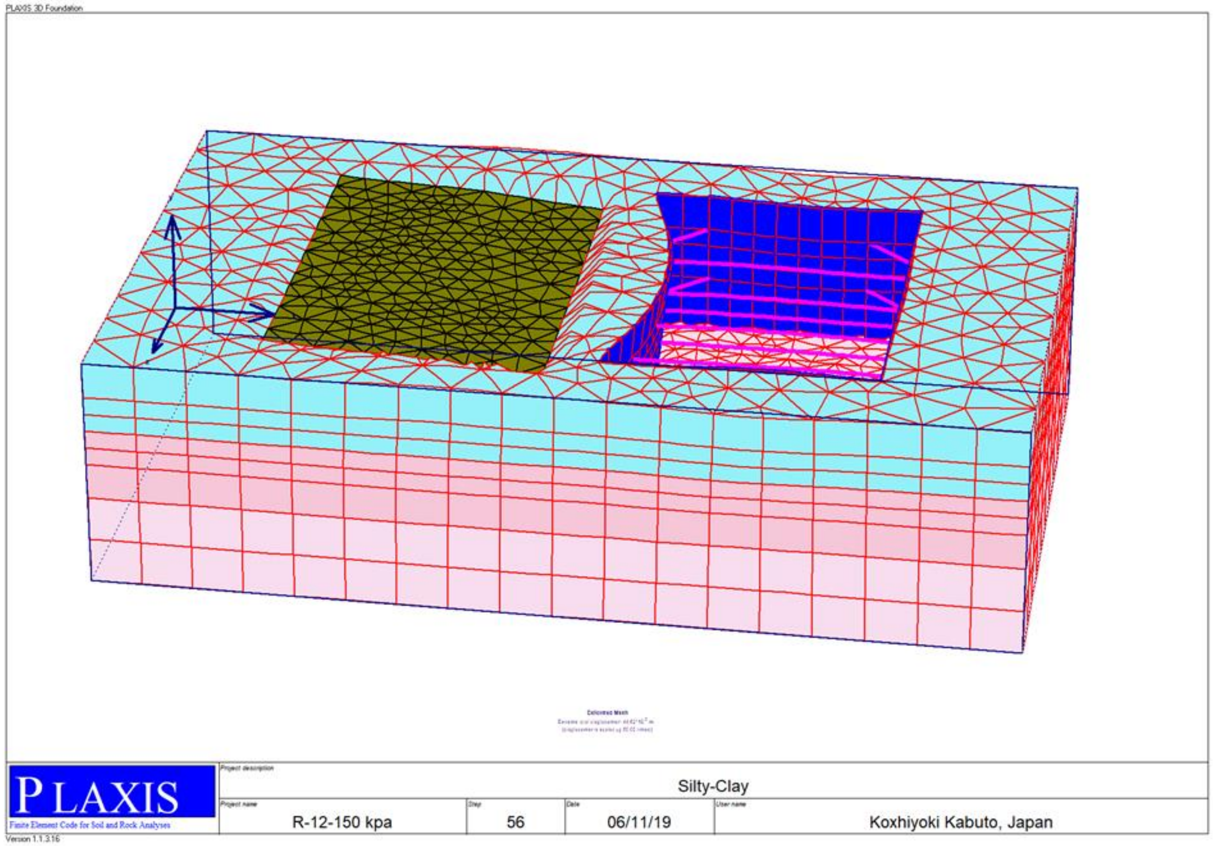

Figure 3.3: deformed mesh showing maximum displacement in the ground for 8m excavation height.

2. **Definition of output terms**

Walls

Output data for walls comprises deformations and forces. From the Deformation sub-menu, the user may select the absolute (vectorial) displacements |u|, the individual displacement components, u_x, u_y and u_z as well as the corresponding incremental displacements. From the Force sub-menu, the options Axial force N1, Axial force N2, shear force Q12, shear force Q13, shear force Q23, Bending moment M11, Bending moment M22 and Torsional moment M12 are available. The numbers behind the particular forces refer to the wall's local system of axes (1, 2, 3) (Figure 3.4b), which is indicated in any plot of the wall in a work plane. The first direction is the vertical in-plane direction of the wall, the second direction is the horizontal in-plane direction of the wall and the third direction is perpendicular to the wall.

The Bending moment M11 is the bending moment due to bending over the horizontal axis (around the horizontal axis), which is generally the direction where the major bending moments occur (Figure 3.5b). The Bending moment M22 is the bending moment due to bending over the vertical axis (around the vertical axis) (Figure 3.5c).

The Torsion moment M12 is the moment according to transverse shear forces (Figure 3.5a).

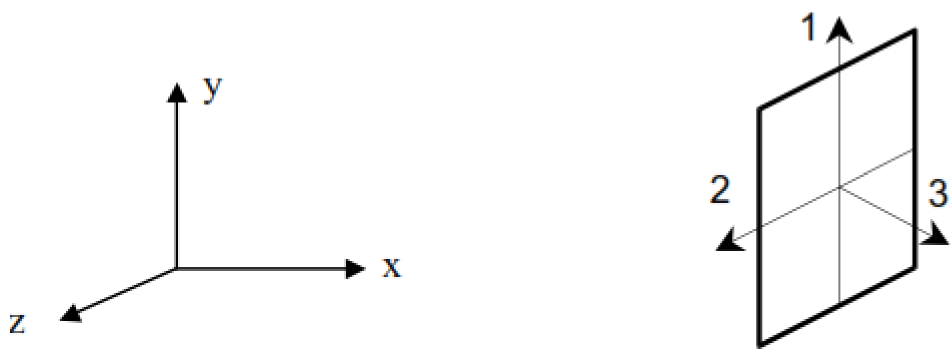

a. Soil model and orientation of the axis   b. local wall directions

Figure 3.4: Orientation of the axis

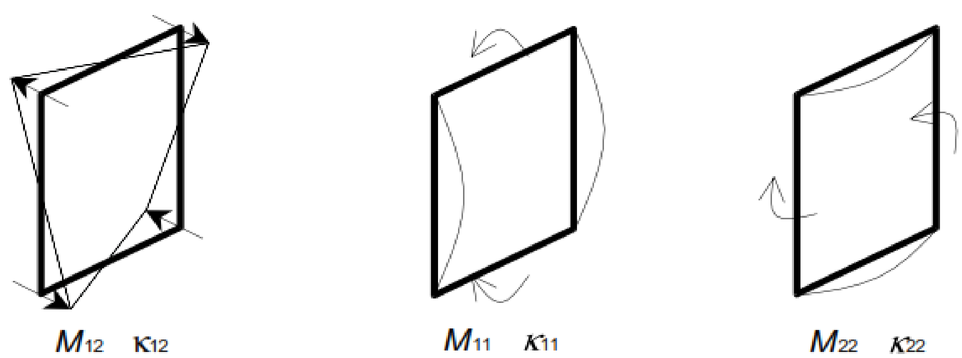

a. Torsion moment M_{12} b. Bending moment M_{11} c. Bending moment M_{22}

Figure 3.5: Bending moment directions of the tangent pile wall

3.3: Summary of Parameters for Base Model

Table 3.2: Wall, Strut and Adjacent Surface Load Parameters for Base Model

Parameters	Unit	1	2	3	4
Wall parameters					
Adapted pile diameter (d)	m	0.65	0.85	1.05	1.25
Equivalent wall thickness(de)	m	0.3	0.6	0.9	1.2
Strut horizontal spacing					
Strut spacing	m	3	4	5	
Adjacent surface load					
Adjacent surface load	kPa	150	200	250	

Table 3.3: Soil Parameters for Base Model from SPT correlation.

Parameters	Unit	Layer 01	Layer 02	Layer 03	Layer 04
Model*		HS	HS	HS	HS
Bulk unit weight (saturated)	γsat (kN/m^3)	18.00	18.50	19.00	20.50
Poisson's ratio	ν (-)	0.2	0.2	0.2	0.2
Secant modulus at 50%**	E_{50}^{ref} (kN/m^2)	6,170	11,200	17,800	47,030
Oedometer modulus	E_{oed}^{ref} (kN/m^2)	6,170	11,200	17,800	47,030
Unloading reference Young's modulus	E_{ur}^{ref} (kN/m^2)	18,510	33,600	53,400	141,090
Cohesion	C (kN/m^2)	12.96	16.83	19.38	33.53
Friction	Φ (^{0})	17.96	21.83	21.76	24.51
Coefficient of lateral earth pressure***	K_o^{nc}(-)	0.692	0.628	0.629	0.585

The secant modulus was found from literatures according to the consistency to the consistency of the soil that was given in the report. Since no data was available for the secant modulus, the secant modulus was taken to approximately equal with the elastic modulus ranges listed in Table 3.3. The oedometer modulus was taken the same as the secant modulus and the unloading modulus was taken as the default value in PLAXIS, which was three times the secant modulus.

Chapter 4: Results and Discussion

4.1: Analysis and Parametric Study

There are a number of parameters to be considered if one is interested in conducting comprehensive parametric study. However, as reported by earlier investigators e.g. (Chavda Jetish, 2014), some of the variables have little effect in the performance of deep excavation supported by pile wall. In this paper, variables that have practical importance and reported to have significant influence in the performance of deep excavations were discussed.

In this section, 84 runs are analyzed using PLAXIS 3-D Foundation software and representative parametric study are presented. The parametric study conducted included a number of alternative arrangements of variables under consideration. The parametric study conducted included the effect of adjacent surface load, pile diameter (equivalent thickness) and strut horizontal spacing. The results of all parametric studies are shown in appendix C. When one of the above parameters is varied, the rest are kept constant. The issue of heave is not addressed in this parametric study, as PLAXIS does not include this parameter in the calculation. Accordingly, the effect of varying a parameter for excavation depth of 8, 11 and 14m with their construction phases is manifested by obtaining the variation in the quantities of maximum horizontal displacement of the tangent pile wall, ground settlement behind the tangent pile wall and bending moment in the tangent pile wall.

4.2: Validation of Finite Element Analysis Results

As no instrumentation was used on site to monitor for wall deflections, therefore, the FEA results cannot be validated from field measurements but it is assumed that the actual deflections on ground were much lesser than as predicted by 3D FEA in Plaxis.

In order to validate the point that the support system used for deep excavation, excavation in Bole was conservative keeping in view the ground conditions (i.e. presence of silty clay) and the built up around it (i.e. single / double story structures and roads). The results are validated with the help of existing case studies of braced excavations worldwide that are reported extensively in literature.

For this purpose, some 25 case histories of braced excavations have been collected from technical papers, which are in appendix C.

The maximum depth of excavation and the horizontal deformation obtained from finite element analysis with allowable load of 150kPa and equivalent thickness of 0.3m is used for validation. The data points from well-reported existing braced wall case histories have been shown in Figure 4.1. Figure 4.1*a* relates the maximum depth of excavation with maximum measured horizontal deformations for 25 braced excavations case histories. In this study, deformation is 48.12mm. Deformations as high as 223.5mm have been measured in field for 11m deep excavation (NGI, 1962). Wall displacements for Tokyo Subway stations was observed to be 176.5mm (Miyoshi, 1977), for HRD-4, Chicago 172.6mm (Finno et. al. 1989), for Far-East Enterprise Center Taiwan 124.5mm (Hsieh, P. G., and Ou, C. Y., 1998), for TNEC Excavation, Taipei 106.4mm (Ou et. al.1993). Figure 4.1*b* gives the plot between depth of excavation and maximum lateral deformation normalized with depth of excavation. In this study, Uxmax/He is 0.34%. (Kung et al., 2007) analyzed 33 case histories of braced excavations (obtained from Taipei, Singapore, Oslo, Tokyo and Chicago) where they studied that maximum lateral deformation fall in the range of 0.20%-0.60%He. The data from few case histories suggested that this range could be as high as 2.03%, for example, in Oslo Subway excavation case; maximum measured lateral wall deflections were 221.1mm for 11m deep excavation (NGI, 1962). Similarly, for HRD-4, Chicago the ratio is 1.42 (Finno et. al. 1989), for Tokyo Subway the ratio is 1.04 (Miyoshi, 1977). Hence based on findings from Figure 4.1 it can be stated that the calculated deformations from 3D FEA fall within very much acceptable range while keeping in view the soil strength and adjacent infrastructure and hence the design is very much Conservative.

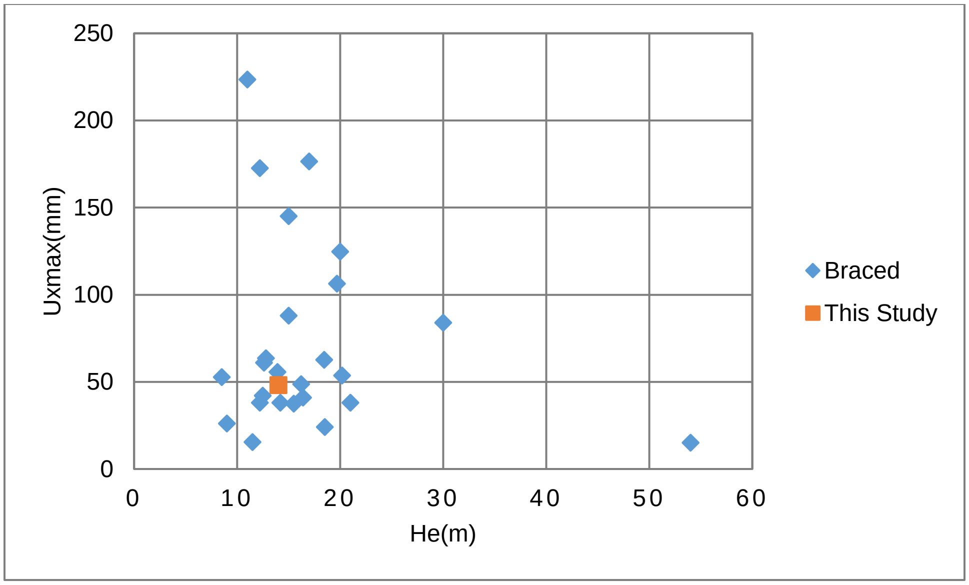

a) Wall displacements

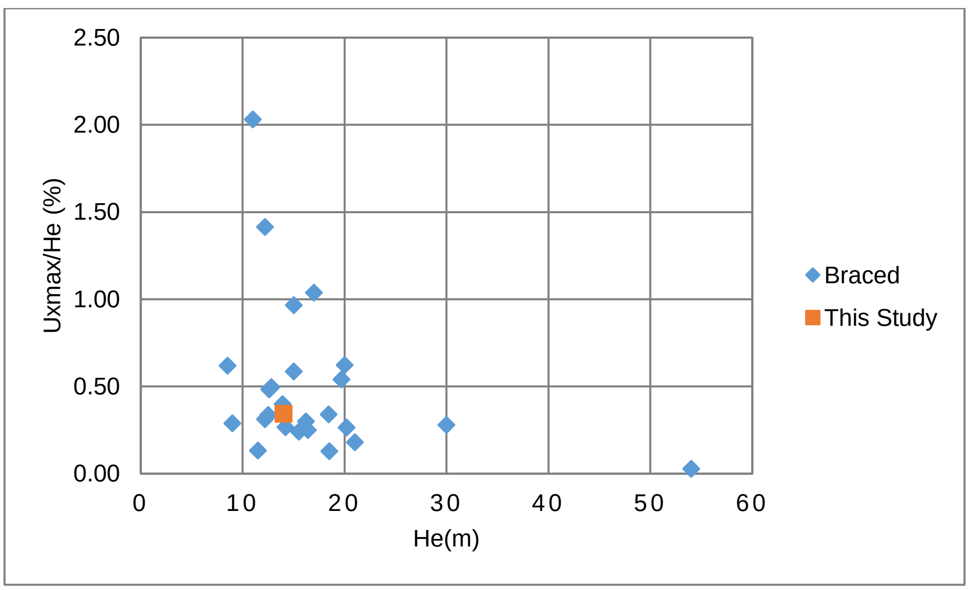

b) Normalized wall displacements

Figure 4.1: Data points from existing braced excavation case histories

4.3: Comparison of Mohr-Coulomb and Hardening soil model results

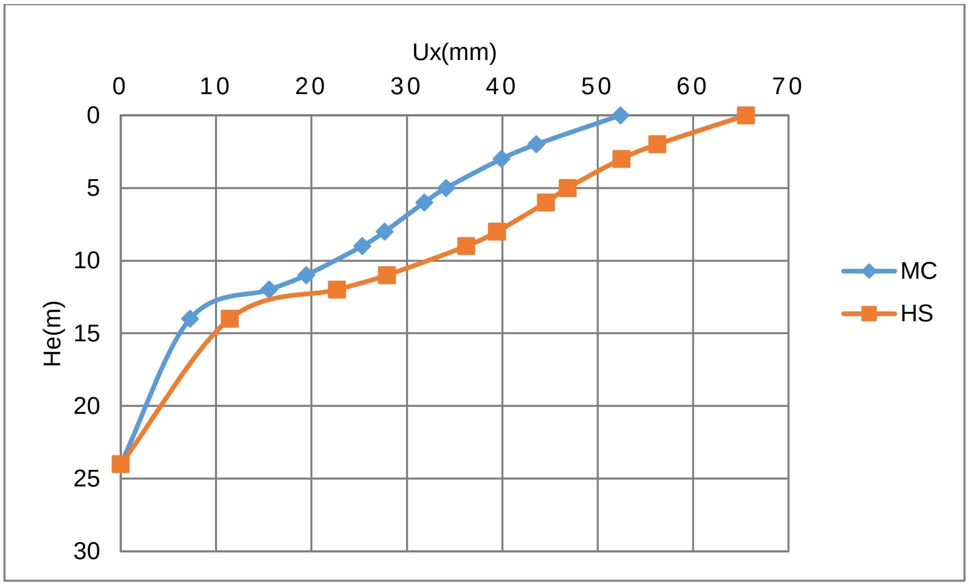

a) Horizontal deformation

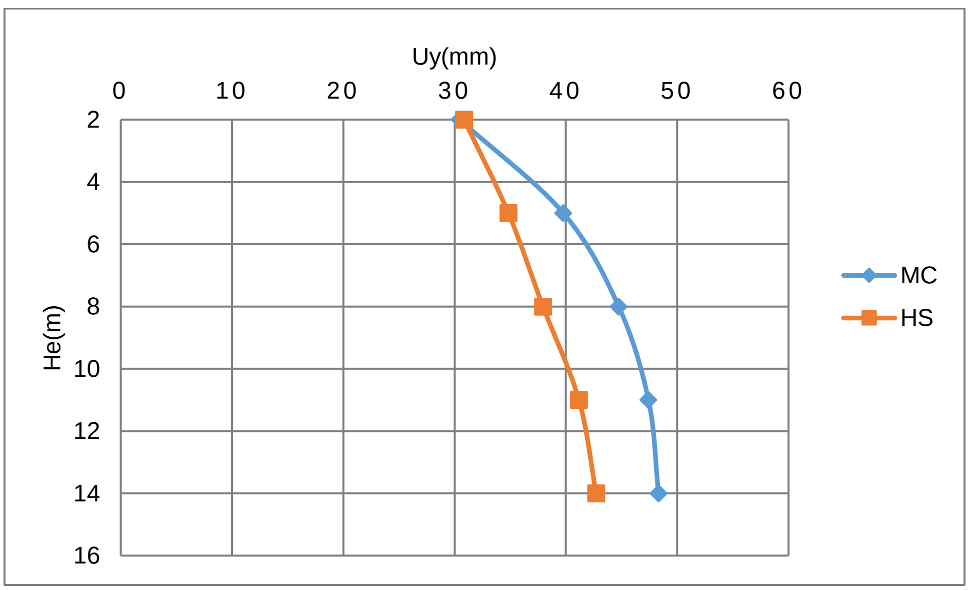

b) Vertical settlement

Figure 4.2: Comparison of Mohr-Coulomb and Hardening soil model deformations

The horizontal deformation and settlement plot for the analysis is shown in Figure 4.2*a* and 4.2*b*.

Compared to HS model, the MC model has small wall deformation. This is due to the model uses constant stiffness and lack of distinction between initial loading and unloading/loading of materials in the soil. In HS model, the strains (elastic and plastic) are calculated based on the hardness of surface tension and this hardness is different for initial loading and unloading/loading. MC model over-predicts ground surface settlement, which is unrealistic due large heave. Thus MC model serve many limitations for excavation related problems as mentioned below and therefore HS model is used for further analysis in case study.

i. Unrealistic surface heave near edge of wall
ii. Under prediction of surface settlements in primary influence zone
iii. Over prediction of surface settlements in secondary influence zone
iv. Over predictions of wall movements in lower portions of wall.

4.4: Parametric Analysis, Results and Discussion

4.4.1: Effect of Change in Adjacent Surface Load

In this section, the amount of adjacent surface load is increased from 150 to 200 and 250kPa. These loads are located at 3.5m from the edge of excavation and the maximum horizontal displacement of the tangent pile wall, the maximum ground surface settlement behind the tangent pile wall and the maximum bending moment induced in the tangent pile wall are presented and discussed. For analysis the soil, pile and the strut parameters listed from table 3.2 and 3.3 are used.

For all the analysis conducted in this section of parametric study, the following quantities or features are kept constant.

- Equivalent thickness of wall (de = 0.3m)
- Strut horizontal spacing 4m.

Figures 4.3 to 4.7 show the effect of change in the adjacent surface load due to deep excavations.

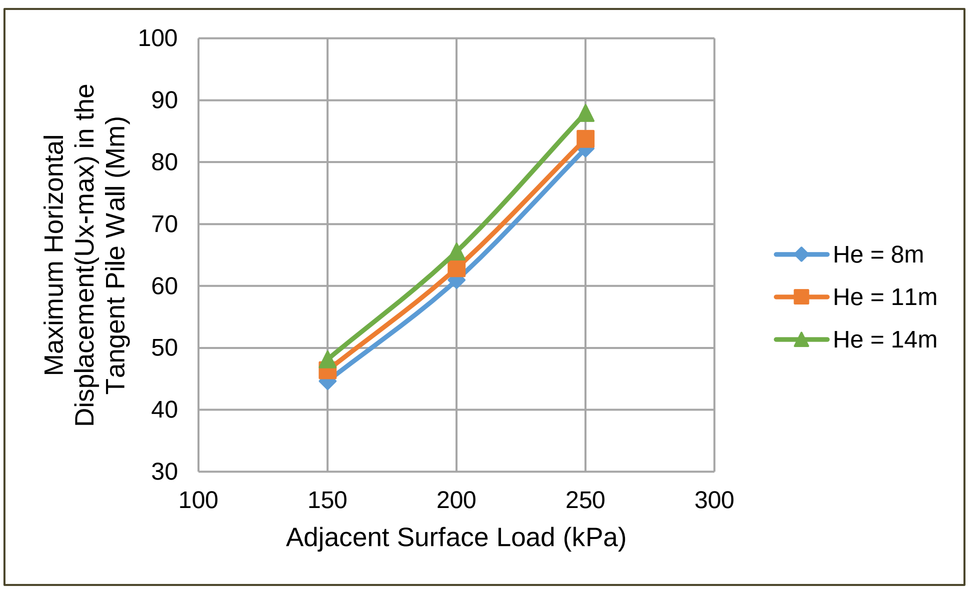

Figure 4.3: Maximum Horizontal Displacement Ux-max of Tangent Pile Wall with Adjacent Surface Load.

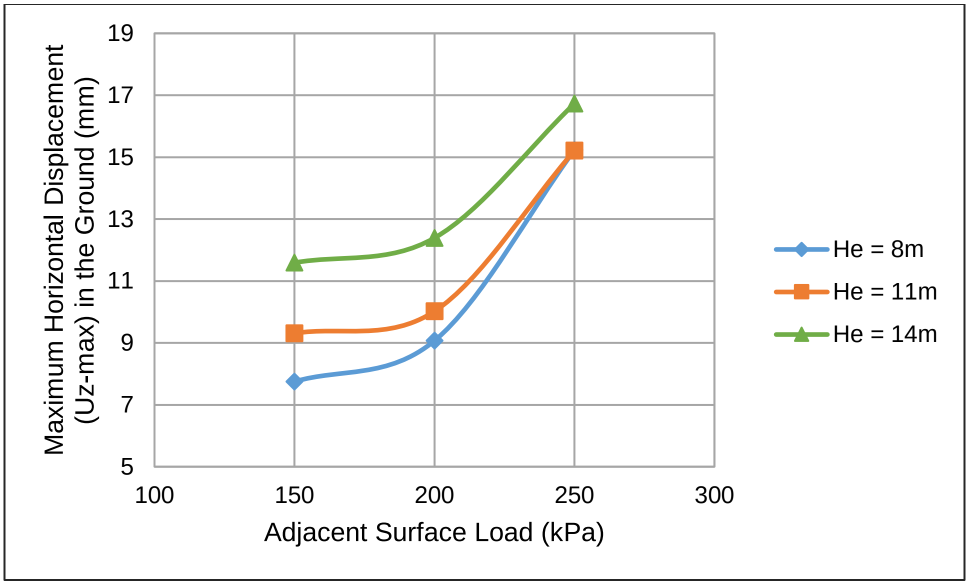

Figure 4.4: Maximum Horizontal Displacement Uz-max with Adjacent Surface Load.

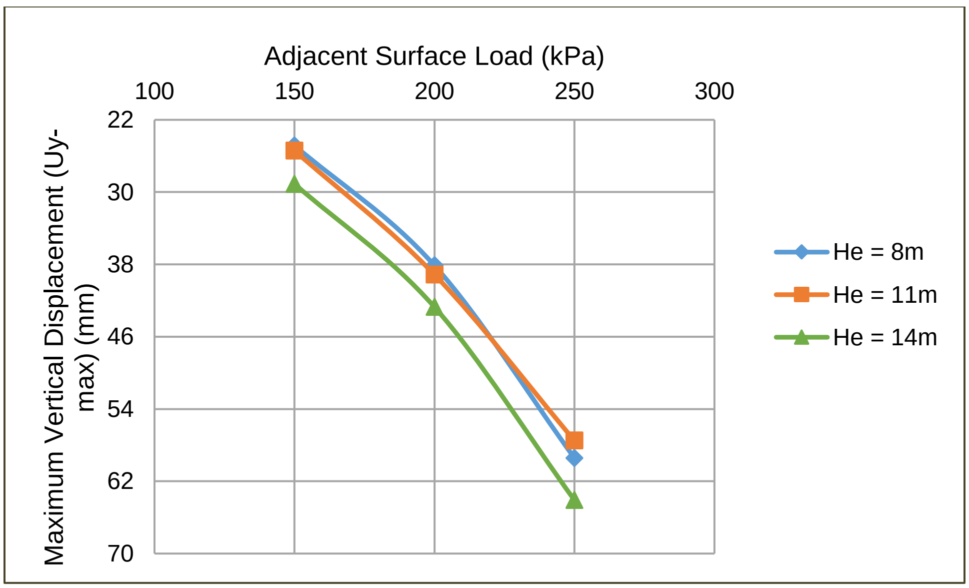

Figure 4.5: Maximum Vertical Settlement Uy-Max in the Ground with Adjacent Surface Load.

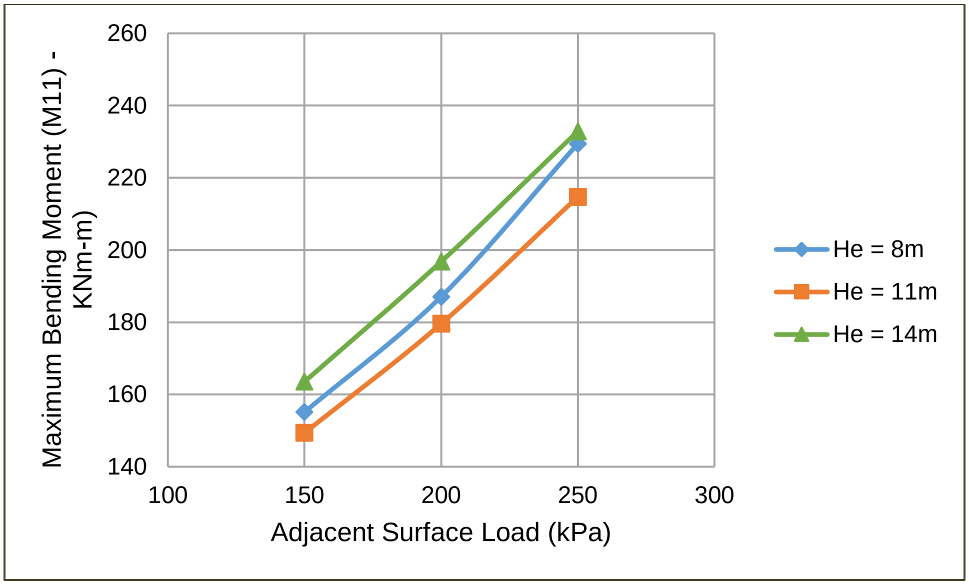

Figure 4.6: Maximum Bending Moment M11 With Adjacent Surface Load.

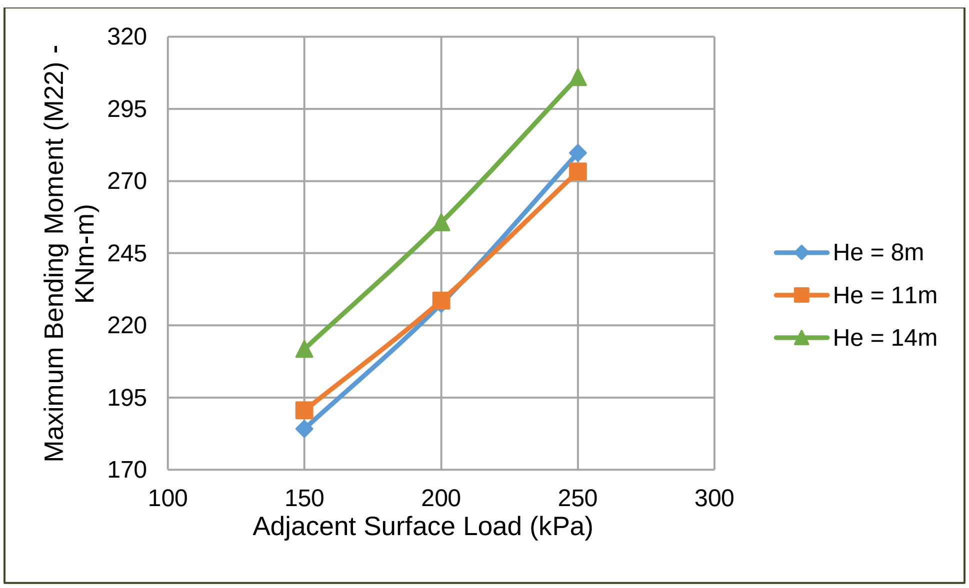

Figure 4.7: Maximum Bending Moment M22 with Adjacent Surface Load.

As observed from Figures 4.3- 4.7, there is a difference of around 40 and 35mm in the horizontal and vertical displacements between the lowest and highest load values respectively. Around 27% increase in the Ux-maximum horizontal displacement when the load is increased from 150 to 200 and from 200 to 250kPa in all excavation depth. There is an increase of 15 and 40%, 7 and 34%, 6 and 26% in Uz- maximum horizontal displacement in excavation height of 8, 11 and 14m respectively as load increased. The Uz-max graph show sharp slope after 200kPa load since the allowable bearing capacity of the soil is in between 100 and 200kPa.

Around 36% increase was observed in vertical displacement on the same load increment in excavation depth of 8m. In excavation depth of 11m, the displacement is increased by 35 and 32%. Moreover, in excavation height of 14m increased by 33% for the same condition.

The maximum bending moment in the tangent pile-wall in the 1-1, direction increased by 17 and 18 % as the surface load increase from 150 to 200 and from 200 to 250kPa in excavation height of 8m. In addition, increased by 17 and 16%, 17 and 15% in excavation depth of 11 and 14m respectively. In the excavation height of 8m, 19 and 17% increase in the bending moment in the direction 2-2. Also, 17 and 16% in depth of 11 and 14m.

As perceived in Figure 4.6, moment induced in the excavation height of 8m is greater than excavation height of 11m. This is due to the greater value of coefficient of lateral earth pressure than 11m excavation height from soil strata, which increases the lateral load on the pile wall. Large soil movement was observed due to the stress of adjacent surface load that induce bending moments and deflections.

The results are less than what is found by (Birhanu, 2016) on red clay soil of Addis Ababa by using PLAXIS 3D Foundation. This due to number of strut level in supporting secant pile wall the author used.

4.4.2: Effect of Change in Tangent Pile-Wall Thickness (Equivalent Diameter)

In this part of the analysis, the paper concentrates on how change in stiffness of tangent pile wall affects the performance of deep excavation. The output from this analysis is presented below.

Table 3.2 gives the range of values for the thickness of tangent pile wall used in the parametric study. Since the young's modulus of the tangent pile wall was kept unchanged for all the analyses, a change in thickness of the tangent pile-wall represents a change in both the bending stiffness and the axial stiffness of the tangent pile wall.

For all the analyses conducted in this section of parametric study, the following quantities or features are kept constant.

- Strut horizontal spacing 4m.

- Adjacent surface load of 200kPa

Figures 4.8 - 4.12 show the effect of change in thickness of the tangent pile wall on the maximum horizontal displacement of the tangent pile wall, maximum ground settlement behind the tangent pile wall and the maximum bending moment induced in the tangent pile wall due to deep excavations.

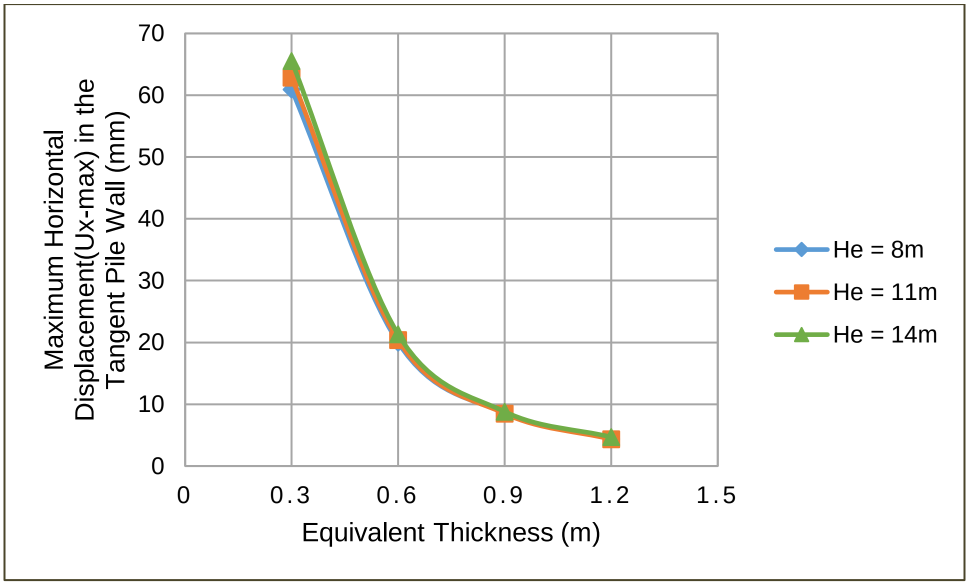

Figure 4.8: Maximum Horizontal Displacement (Ux-Max) of the Tangent Pile Wall with Tangent Pile- Wall Thickness

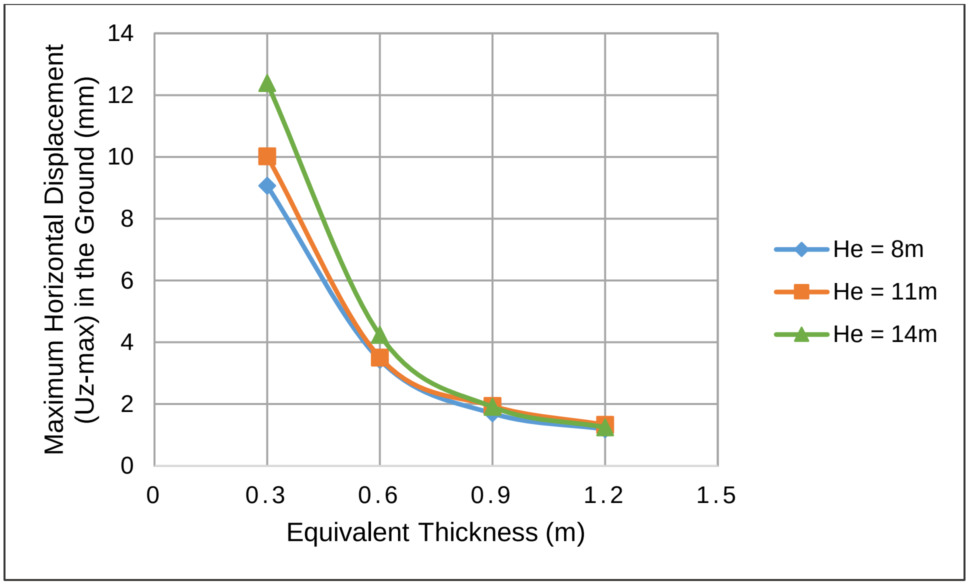

Figure 4.9: Maximum Horizontal Displacement (Uz-Max) with Tangent Pile- Wall Thickness.

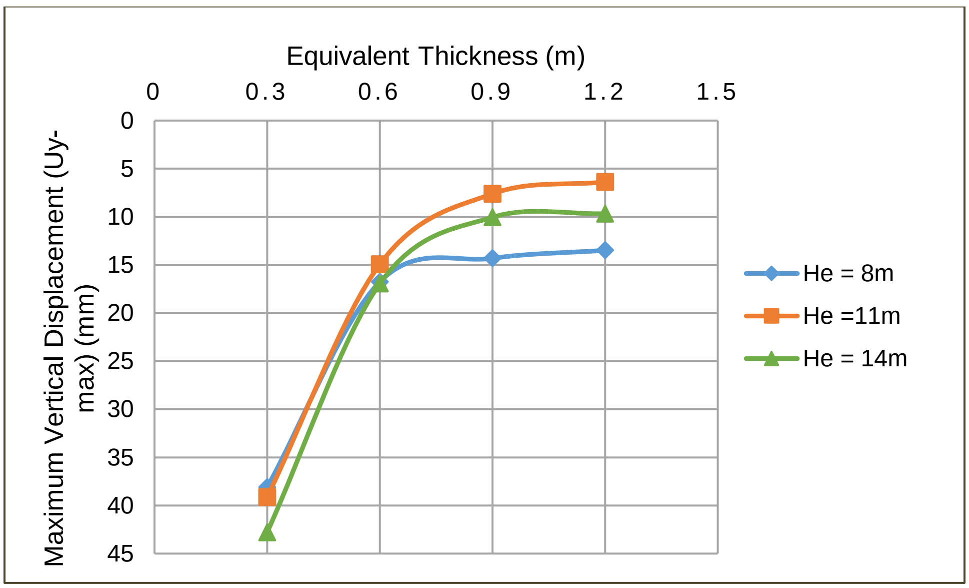

Figure 4.10: Maximum Vertical Settlement (Uy-Max) in the Ground with Tangent Pile-Wall Thickness.

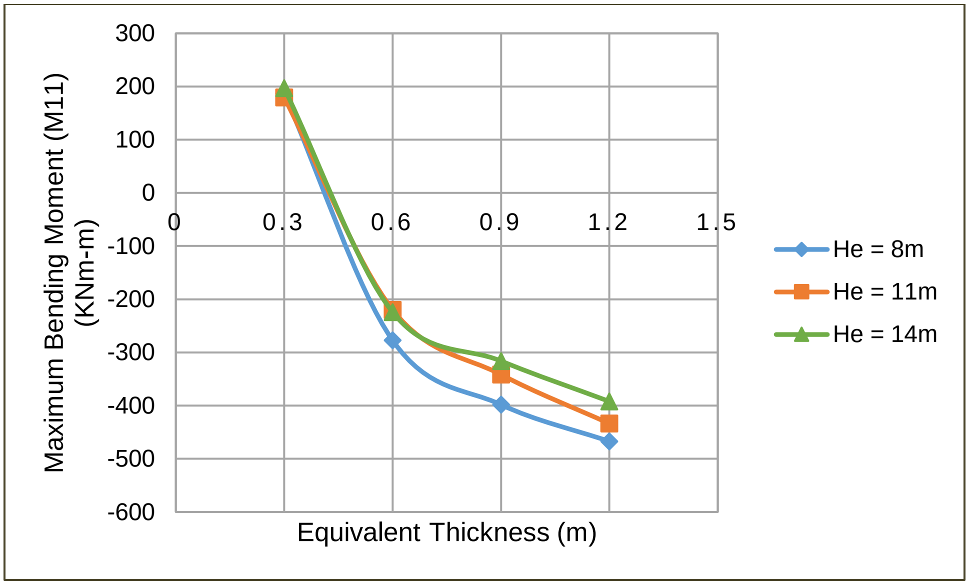

Figure 4.11: Maximum Bending Moment (M11) in the Tangent Pile Wall with Thickness of Tangent Pile Wall

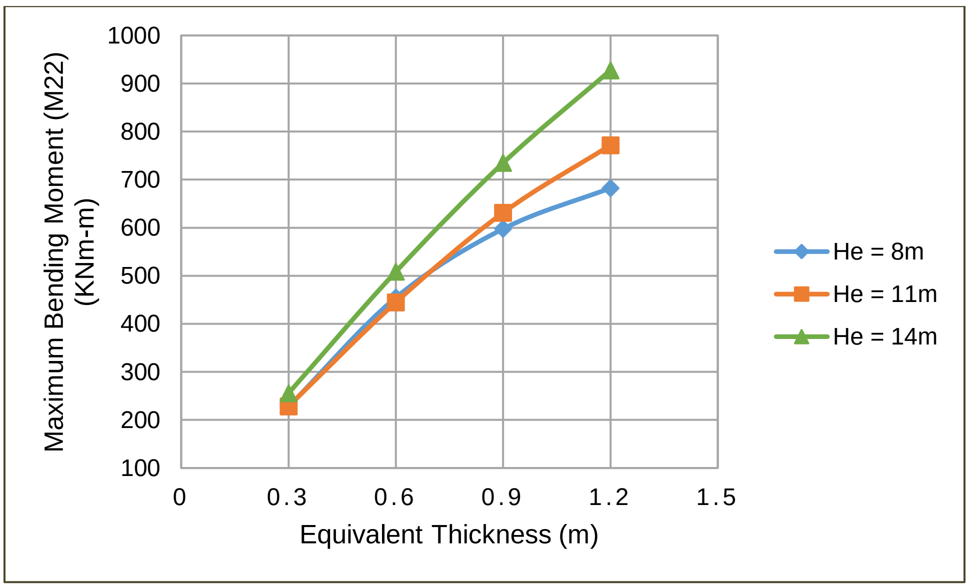

Figure 4.12: Maximum Bending Moment (M22) in the Tangent Pile Wall with Thickness of the Tangent Pile Wall

From the Figures 4.8 – 4.9, the horizontal displacement Ux-max decreased by 67, 57 and 49% when wall thickness is increased from 0.3 – 0.6m, 0.6 – 0.9m and 0.9 – 1.2m in excavation depth of 8m. Similarly decreased by 62, 50 and 30% in the Uz-max. For excavation height of 11 and 14m, the horizontal displacement Ux-max decreased by 68, 59 and 49% when the stiffness is increased. The

Uz-max is decreased by 65, 45 and 31% and 66, 55 and 35% in the excavation height of 11 and 14m respectively. The horizontal displacement graphs show sharp slope when the thickness is increased from 0.3 – 0.6m and smooth after 0.6m. This is due to the stiffness of the pile wall. In the thickness of 0.3 – 0.6m the pile wall is less stiff and the displacement is high. The variation in the displacement is small in last intervals due to high stiffness of the pile wall that comes from their cross-section.

The maximum vertical displacement in the ground decrease by 56, 15 and 6% when the stiffness of tangent pile wall is increased in excavation depth of 8m. In addition, decreased by 62, 49 and 16% in excavation height of 11m and 60, 41 and 4% in the 14m depth. Similarly, the stiffness also affects the ground surface settlement and the variation in the settlement is small after 0.6m.

The maximum bending moment in the tangent pile-wall in the 1-1, direction increased by 33, 30 and 15% increase as the wall thickness increase from 0.3 – 0.6m, 0.6 – 0.9m and 0.9 – 1.2m in excavation height of 8m respectively. In addition, increased by 18, 36 and 21% and 12, 29 and 19% in excavation depth of 11 and 14m respectively. In the excavation height of 8m, 50, 24 and 12% increase in the bending moment in the direction 2-2. The in depth of 11 and 14m the moment is increased by 50, 31 and 21%. The bending moment M11 change in sign after 0.3m thickness. Because in the first thickness the pile wall is less stiff and flexible due to this the moment is in tension but as the stiffness increase the soil behind the wall will be compressed the resulted moment also in compression (negative moment).

In contrast to displacements, bending moments are increased as the wall stiffness increased. This because a thicker wall make the soil behind it more compact and hence giving it small chance for large movements i.e. due to increase in structural stiffness. These results are in agreement with the findings of (Birhanu, 2016) on red clay soil of Addis Ababa and states "thick secant pile walls resist large soil movements and wall movements because of their stiffness that comes from their cross section."

4.4.3: Effect of Change in Strut Horizontal Spacing

In this part of analysis, the effect of change in strut horizontal spacing on the performance of deep excavation is considered.

For all the analyses conducted in this section of parametric study, the following quantities or features were kept constant.

- Equivalent thickness of wall (de = 0.3m)
- Adjacent surface load of 200kPa

Figures 4.13- 4.17 show the effect of change in the strut horizontal spacing on the maximum horizontal displacement in the tangent pile-wall, maximum ground settlement behind the pile wall and the maximum bending moment induced in the pile-wall due to deep excavations.

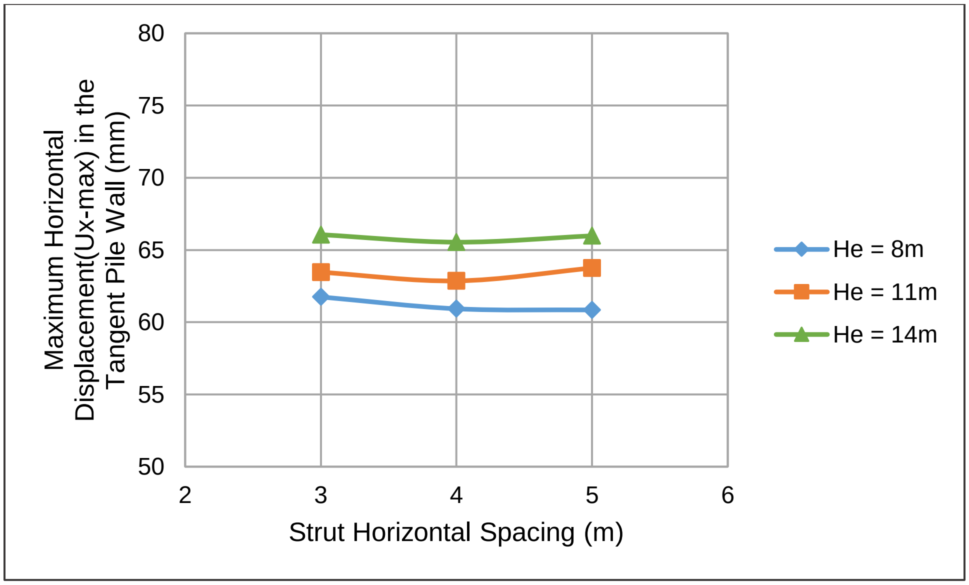

Figure 4.13: Maximum Horizontal Displacement (Ux-max) of the Tangent Pile Wall with Strut Horizontal Spacing.

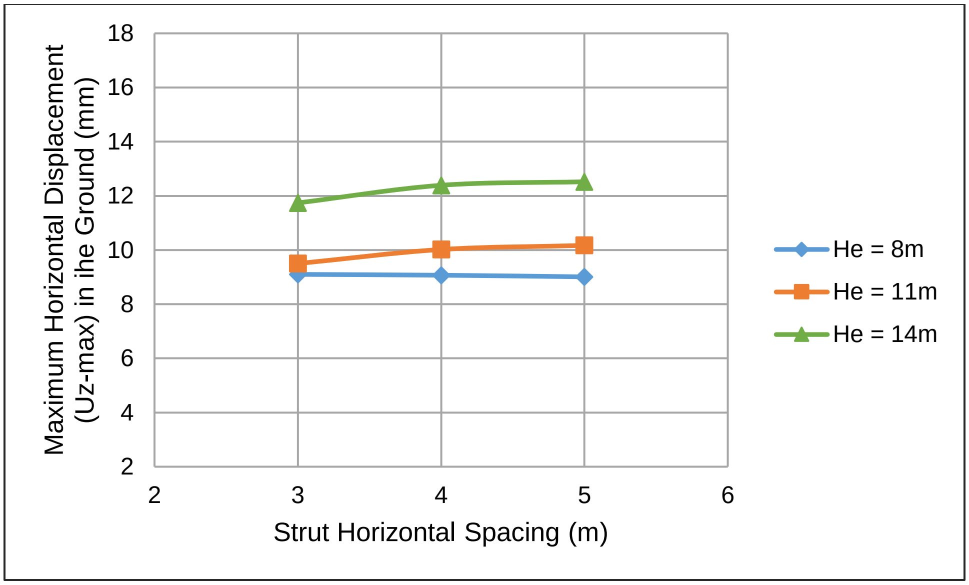

Figure 4.14: Maximum Horizontal Displacement (Uz-Max) with Strut Horizontal Spacing

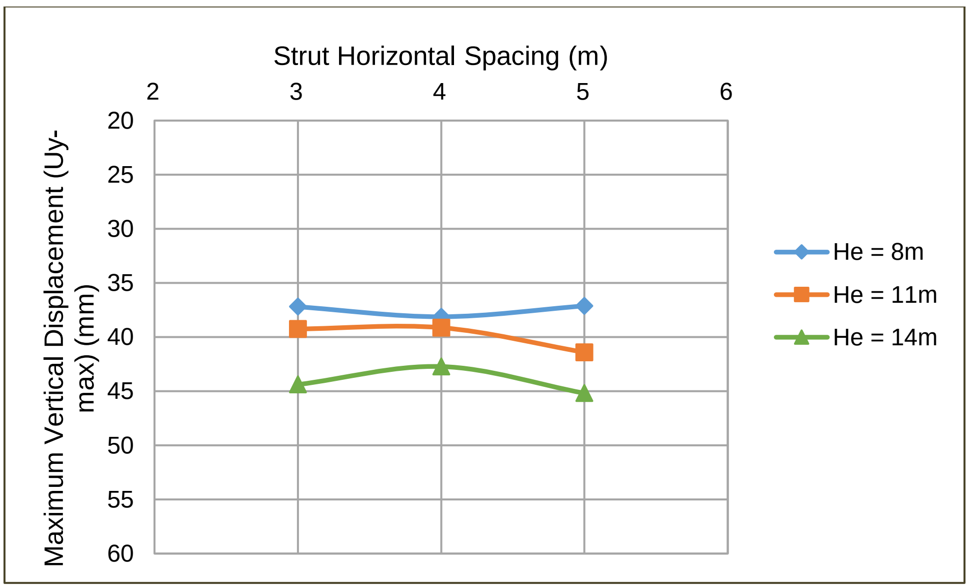

Figure 4.15: Maximum Vertical Settlement (Uy-Max) in the Ground with Strut Horizontal Spacing.

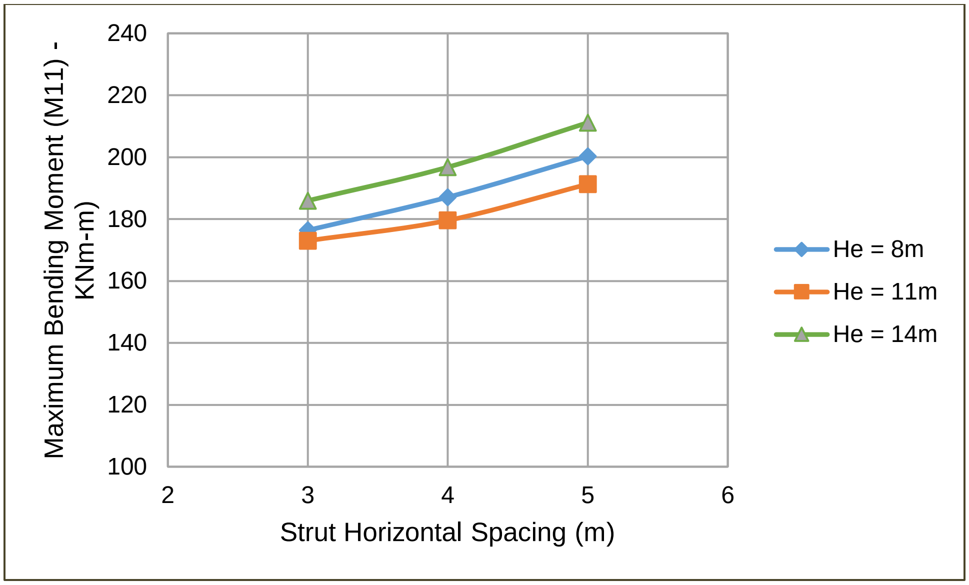

Figure 4.16: Maximum Bending Moment (M11) in the Tangent Pile Wall with Strut Horizontal Spacing.

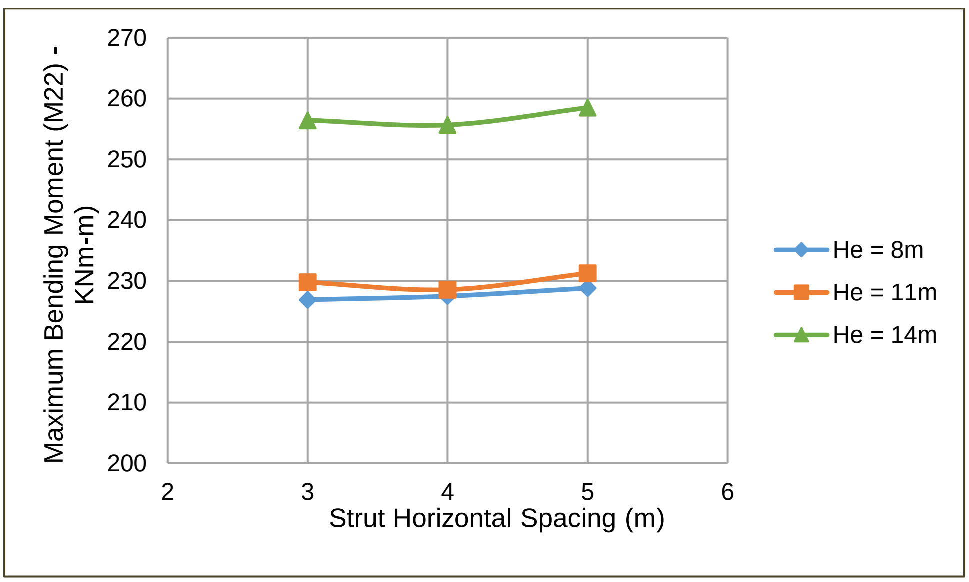

Figure 4.17: Maximum Bending Moment (M22) in the Tangent Pile Wall with Strut Horizontal Spacing.

Figures 4.13 - 4.17 show the influence of the strut horizontal spacing on the lateral wall movements for deep excavations. As expected, the more space between supports the more lateral deformations in the retaining wall. However, as can be seen in the Figures 4.13 and 4.14, the variation in the strut horizontal spacing does not have a significant effect in the lateral wall deformations of the tangent pile wall. In addition, there is no significant variation in ground settlement. The bending moment induced in the pile wall in 1-1 direction increased by 5.5% and 7 % when strut horizontal spacing is increased from 3m to 4m and 4m to 5m respectively as seen from the figures.

This result agrees with the findings previously presented by (Clough, G. W., and O'Rourke, T. D., 1990) and (L. Sebastian Bryson & and David G. Zapata-Medina, 2012), who stated that "for stiff clays where basal stability is not an issue, support spacing have small influence on the lateral movements."

4.4.4: Comparison between Cases: Vertical (Uy) and Horizontal (Ux) Displacements

Case1: Effect of Change in Adjacent Surface Load

This is the case when the load is increased from 150 to 200 and 250kPa. Both these deformation values were normalized with respect to height of excavation He.

The figure below shows the Maximum vertical and horizontal displacements.

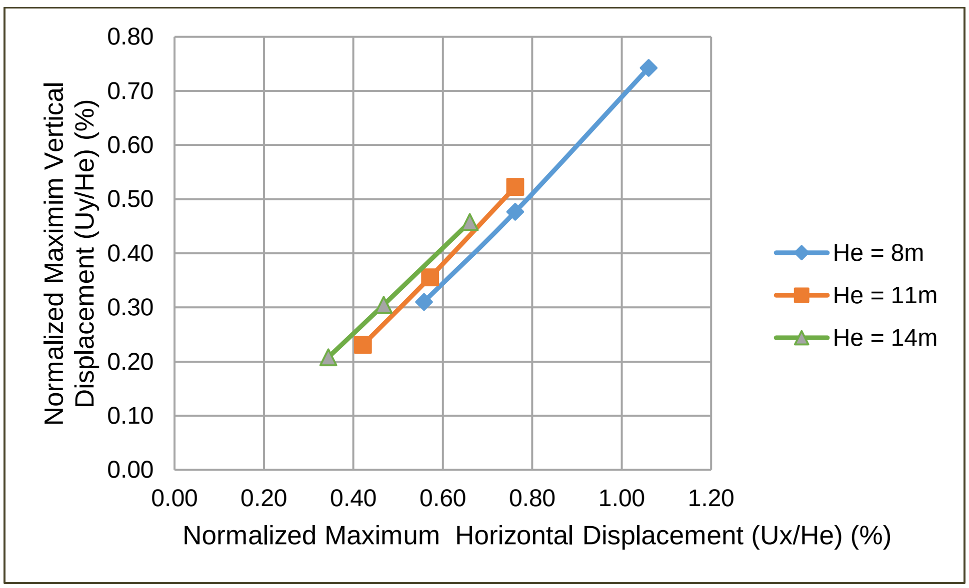

Figure 4.18: Relationship between Maximum Ground Settlement and Maximum Lateral Wall Deflection.

From Figure 4.18, the ratio of normalized maximum ground surface settlement Uy-max/He lie in a range of 0.31 to 0.74% for height of excavation 8m. The ratio of maximum surface settlement to maximum lateral displacement falls in the range of 0.56 to 0.7, with an average value of 0.63

($Uymax = 0.63Uxmax$). For height of excavation of 11m the ratio, lie in range of 0.23 to 0.52%. The ratio of maximum surface settlement to maximum lateral displacement falls in the range of 0.55 to 0.68, with an average value of 0.62($Uymax = 0.62Uxmax$). In addition, for height of excavation 14m, the ratio lies in the range of 0.21 to 0.46%. The maximum surface settlement to maximum lateral displacement ratio falls in ranges of 0.6 to 0.7, with an average value of 0.65 ($Uymax = 0.65Uxmax$). These suggested ranges of Uymax agree well with the findings of (Ou et al., 1993) and (Hsieh, P. G., and Ou, C. Y., 1998).

Case2: Effect of Change in Tangent Pile-Wall Thickness

This is the case when the equivalent thickness of pile changes from 0.3m to 0.6, 0.9 and 1.2m. Both these deformation values were normalized with respect to height of excavation He.

The figure below shows the Maximum vertical and horizontal displacements.

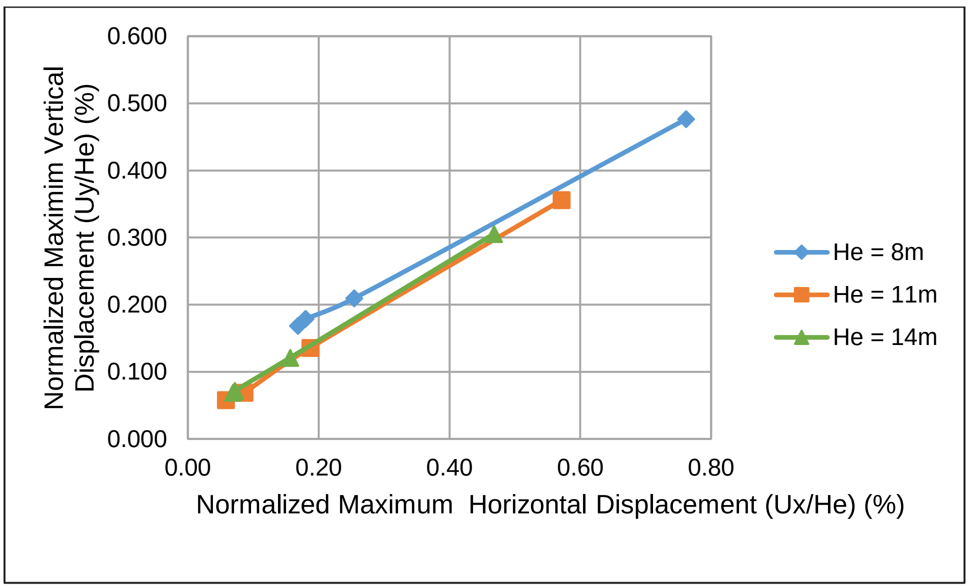

Figure 4.19: Relationship between Maximum Ground Settlement and Maximum Lateral Wall Deflection

In the Figure 4.19, the ratio of normalized maximum ground surface settlement Uy-max/He lie in a range of 0.2 to 0.48% for height of excavation 8m. The ratio of maximum surface settlement to maximum lateral displacement falls in the range of 0.63 to 0.99, with an average value of 0.81 ($Uymax = 0.81Uxmax$). For height of excavation of 11m the ratio, lie in range of 0.1 to 0.4%. The ratio of maximum surface settlement to maximum lateral displacement falls in the range of

0.62 to 0.97, with an average value of 0.80 ($Uymax = 0.80Uxmax$). In addition, for height of excavation 14m, the ratio lies in the range of 0.1 to 0.3%. The maximum surface settlement to maximum lateral displacement ratio falls in ranges of 0.65 to 0.98, with an average value of 0.82 ($Uymax = 0.82Uxmax$). These suggested ranges of Uy-max agree well with the findings (Ou et al., 1993)and (Hsieh, P. G., and Ou, C. Y., 1998).

Case 3: Strut Horizontal Spacing

The displacements are normalized with respect to height of excavation (He) and the spacing axis is normalized with respect to the spacing specified for model (SHS)1=4m.

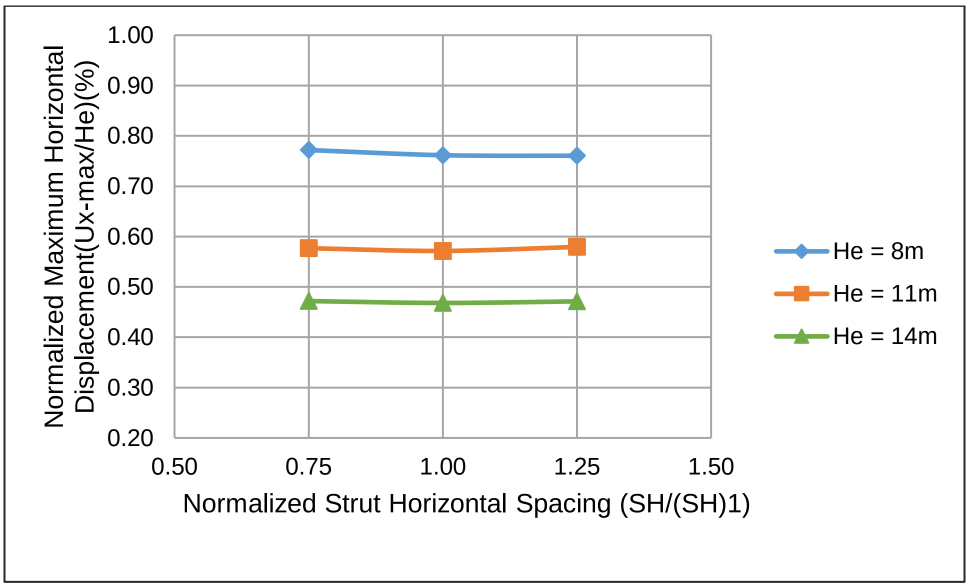

Figure 4.20: Normalized Maximum Horizontal Displacement Vs. Horizontal Spacing.

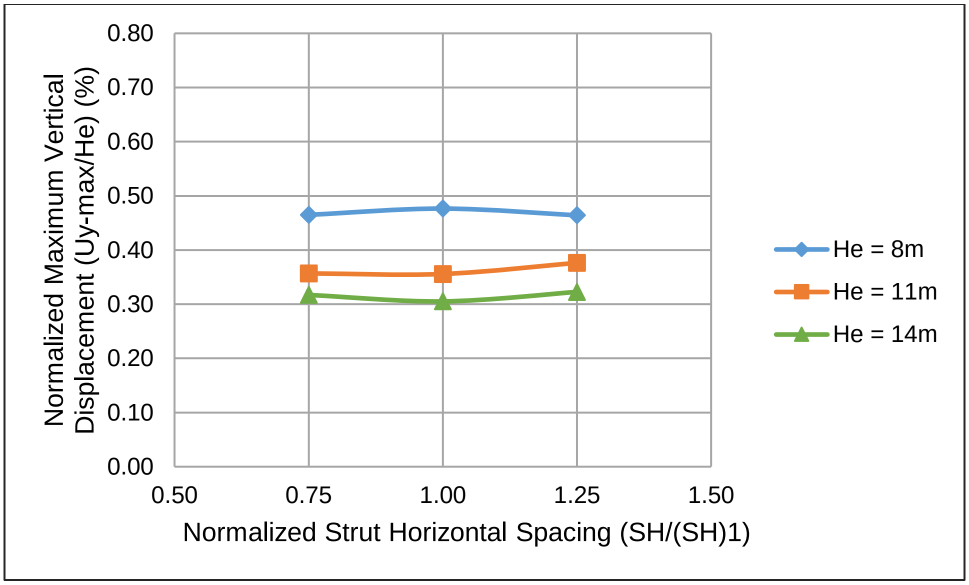

Figure 4.21: Normalized Maximum Vertical Displacement Vs. Horizontal Spacing.

From the Figuers 4.20 - 4.21 it is observed that for 8m height of excavation the horizontal displacement ratio is 0.77 and 0.76% for SH/(SH)1 0.75 and 1.25 respectively. The vertical displacement ratio is 0.47 and 0.46% for the same strut spacing ratio. The maximum surface settlement to maximum lateral displacement ratio falls in ranges of 0.60 to 0.605, with an average value of 0.60 ($Uymax = 0.60Uxmax$). In 11 and 14m heigth of excavation for the strut spacing ratio the horizontal displacement ratio is 0.577 and 0.580%, and 0.472 and 0.471% respectively. And the vertical displacement ratio is 0.357 and 0.376%, and 0.317 and 0.323% respectively.The ratio of maximum surface settlement to maximum lateral displacement falls in the range of 0.62 to 0.65, with an average value of 0.635($Uymax = 0.635Uxmax$) for excavation height 11m. Moreover, for 14m height excavation the ratio of maximum surface settlement to maximum lateral displacement falls in the range of 0.67 to 0.69, with an average value of 0.68($Uymax = 0.68Uxmax$).

The results show that, there is no significant in change the displacements when the horizontal spacing is increased from 3 to 4 and 5m.The results agree well with the findings of (L. Sebastian Bryson & and David G. Zapata-Medina, 2012).

Chapter 5: Conclusions and Recommendations

5.1: Conclusions

This study was concerned with the analysis of tangent pile-wall as deep excavation support system using PLAXIS 3D Foundation that is based on finite element analysis.

Different excavation levels with different equivalent pile-wall thickness strut horizontal spacing and different adjacent surface loads at 3.5m from excavation edge were involved in this study. The retaining system used was tangent pile-wall in all cases. Hardening soil model was used to model the soil. The following conclusions have been made from the research.

1. The displacements and bending moments induced in the pile wall increases as the magnitude of the adjacent surface load increases. The normalized figures could be used as a reference to the vertical and horizontal displacement with careful consideration of relating cases.

1.1. The maximum horizontal displacement is increased by 27% in all depth and there is an increase of 15 and 40%, 7 and 34%, 6 and 26% in Uz- maximum horizontal displacement in excavation height of 8, 11 and 14m respectively as load increased.

1.2. The vertical displacement behind the pile wall increased by 36% as load is increased from 150 to 200 and 250kPa in depth of excavation 8m. The ratio of *Uy-max/Ux-max* falls in the range of 0.56 to 0.7.

1.3. In excavation depth of 11m, 35 and 32% increase in the vertical displacement when the load is increased. The ratio of *Uy-max/Ux-max* falls in the range of 0.55 to 0.68.

1.4. For the excavation height of 14m, the vertical displacement increased by 33% when load is increased from 150 to 250kPa. The ratio of *Uy-max/Ux-max* falls in the range of 0.6 to 0.7.

1.5. The bending moment in the tangent pile-wall in direction the 1-1 is increased by 17 and 18 %, 17 and 16%, and 17 and 15% when the load is increased from 150 to 200 and from 200 to 250kPa in excavation depth of 8, 11 and 14m respectively. In addition, the maximum bending moment in the direction 2-2 is increased.

2. The maximum bending moment in the tangent pile wall increased but the horizontal displacement of the tangent pile wall and vertical displacement in the ground decreased

when the thickness of tangent pile wall is increased due to increase in structural stiffness. The maximum surface settlement is with an average value of $0.81(Uymax = 0.81Uxmax)$, $0.80(Uymax = 0.80Uxmax)$ and $0.82(Uymax = 0.82Uxmax)$ for excavation height of 8, 11 and 14m respectively.

3. As the horizontal spacing between strut increases, the displacements and bending moments induced in the pile-wall increases i.e. the more space between supports the more lateral deformations in the retaining wall. The strut spacing is increased from 3 to 4m and 4 to 5m.

3.1. The ratio of *Uy-max/Ux-max* falls in ranges of (0.6- 0.605), (0.62-0.65) and (0.67-0.69) for excavation height of 8, 11 and 14m respectively. However, the trend in the result shows that the variation in the strut horizontal spacing does not have a significant effect in the lateral wall deformations of the tangent pile wall. In addition, there is no significant variation in ground settlement behind the pile wall.

3.2. The bending moment induced in the pile wall in 1-1 direction increases by 5.5 and 7 % when strut horizontal spacing is increased from 3m to 4m and 4m to 5m respectively.

5.2: Recommendations

For soils with low stiffness values, the support system to retain an excavation must be stiff and with an adequate number of strut levels or tiebacks as they would result in large deformations on adjacent grounds.

Monitoring of adjacent structure is recommended as the excavations affect areas the nearby in turn affecting the foundation and the building.

Before beginning an excavation near adjacent structures, it is advised to document the existing condition of adjacent properties prior to construction in order to help observe the new changes due to new excavations and resolve claims.

For a better understanding, field measurements using inclinometers and other deformation measuring instruments can be used and make a comparison between computational methods and the measured results. Excavations must be instrumented and data be made available to research institutions to develop indigenous database on deep excavation.

This study could be better extended to other types of support systems and see the different effects thereby. It could also be extended to the effects of dewatering, the effect of strut vertical spacing, soil modulus and coefficient of lateral earth pressure.

References

Addis Geosystems Plc. (2016). *Geotechnical Investigation Report for 2B+SB+G+18 Mixed Use Building.* Addis Ababa, Bole area.

Birhanu, M. (2016). *Investigation of Effects of Excavations on Adjacent Foundations using Finite Element Modeling.* Msc thesis , Addis Ababa Institute of technology, Civil and Environmental Engineering, Addis Ababa.

Caquot, A. and Kerisel, J. (1948). Tables for the Calculation of Passive Pressure, Active Pressure, and Bearing Capacity of Foundations. In Gauthier-Villars. Paris, France. .

Chai J., Shen S., Ding W., Zhu H., Carter J. (2014). Numerical investigation of the failure of a building in Shanghai. *Computers and Geotechnics Journal, Vlo. 55,* pp. 482-493.

Chavda Jetish, D. A. (2014, september 30). Parametric Study On Pile Wall Used As Retention System For Deep Excavation. *Internal Journal Of Soil Mechanics and Foundations-IJSMF, ; ., Volume 1*(Issue 2).

Clough, G. W., and O'Rourke, T. D. (1990). Construction induced movements of in situ walls. *Proc., Design and Performance of Earth Retaining Structure, Geotechnical Special Publication No. 25, ASCE, New York, 439–470.*

Deep excavation manual. (1996). London: Thomas Telford.

Ergun, M. (2008). Deep excavations. *Electronic Journal of Geotechnical Engineering*.

FHWA. (1999). *Ground Anchors and Anchored System.* Technical Manual, US Department of Transportation Federal Highway Administration, Washington.

Finno, R. J., Blackburn, J. T., and Roboski, J. F. (2007). Three-Dimensional Effects for Supported Excavations in Clay. *Journal of Geotechnical and Geoenvironmental Engineering, ASCE, Vol. 133(1),* pp. 30-36.

G.Look, B. (2007). *Hand book of geotechnical investigation and design.* UK, London: Taylor and Francis .

H. Popa, A. Marcu & L. Batali. (2009). Numerical modelling and experimental measurements for a retaining wall of a deep excavation in Bucharest. *Geotechnical Aspects of Underground Construction in Soft Ground – Ng, Huang & Liu (eds) © 2009 Taylor & Francis Group, London, ISBN 978-0-415-48475-6*.

Hara A, Ohata T, Niwa M. (1971). *Shear modulus and shear strenght of cohesive soils.*

Hoe N.H. (2007). *Numerical Modeling of Diaphragm Wall in Kuala Lumpur Limestone Formation.* MSc Thesis, Universiti Teknologi Malaysia, Civil Engineering, Kuala Lumpur.

Hsieh, P. G., and Ou, C. Y. (1998). Shape of ground surface settlement profiles caused by excavation. *Can. Geotech. J., 35(6), 1004–1017.* .

Korff M. & Mair R.J. (2013). Ground displacements related to deep excavation in Amsterdam. *Proceedings of the 18th International Conference on Soil Mechanics and Geotechnical Engineering.*, (pp. 2779-2782). Paris.

Kulhawy FH and Mayne Paw. (1990). *Manual on estimating soil properties for foundation design.* Electric Power Research Institute , California, USA.

Kung, T. C., Juang, H., Hsiao, C. L., and Hashash, Y. M. (2007). A Simplified model for wall deflection and ground-surface settlement caused by braced excavation in clays. *J. Geotech. Geoenviron.* .

L. Sebastian Bryson, M., & and David G. Zapata-Medina, S. (2012, september). Method for Estimating System Stiffness for Excavation Support Walls. *J. Geotech. Geoenviron. Eng., 138*(9).

Lin, D. G., Phien-wej, N., and Chung, T. C. (2003). Quantitative evaluation of corner effect on deformation behavior of multi-strutted deep excavation in Bangkok subsoil. *Journal of the Southeast Asian Geotechnical Society, 34*(1), 41-57.

Michael Carter and Stephen P.Bentley. (1991). *Correlations of soil properties.*

Ministry of Works and Urban Development. (1995). *Ethiopian Building Code Standard.* Addis Ababa.

Moormann, C. (2004). Analysis of wall and ground movements due to deep excavations in soft soil based on a new worldwide database.

NGI, N. G. (1962). Measurements at a strutted excavation, Oslo subway, Vaterland. *echnical Rep. 6, NGI, Oslo, Norway.*

Ou, C. Y., Hsien, P. G., and Chiou, D. C. (1993). "Characteristics of Ground Surface Settlement during Excavation.". *Canadian Geotechnical Journal, Vol. 30*(5), pp. 758–767.

Ou, C. Y. (2006). *Deep Excavation: Theory and Practice*. Taylor & Francis/Balkema, The Netherlands. .

Peck, R. B. (1969). Deep excavation and tunneling in soft ground. *Proc., 7th Int. Conf. on Soil Mechanics and Foundation Engineering, Mexico City, International Society for Soil Mechanics and Foundation Engineering, 225–290.*

R.B.J. Brinkgreve & W. Broere. (2004). *PLAXIS 3DFOUNDATION version 1.* Delft University of Technology . Netherland: A.A. Balkema Publishers, a member of Swets & Zeitlinger Publishers.

Ramadan E.H., R. M. (2013). Analysis of Piles Supporting Excavation Adjacent to Existing Buildings. *Proceedings of the 18th International Conference on Soil Mechanics and Geotechnical Engineering.* Paris.

Schweiger, H. (2009). 3D finite element analysis of a deep excavation and comparison with in situ measurements. *Computational Geotechnics Group, Institute for Soil Mechanics and Foundation Engineering, Graz University of Technology, Austria*.

Sorensen KK and Okkels N. (2013). Correlation between drained shear strength and plasticity index of undisturbed overconsolidated clays. *Proceedings of the 18th international conference on soil mechanics and geotechnical engineering.* Paris.

Venkata Ramasubbarao GODAVARTHI, D. M. (2011). Contiguous Pile Wall as a Deep Excavation Supporting System. *Leonardo Electronic Journal of Practices and Technologies*, 144-160.

Wong, I., Poh, T., & Chuah, H. (1996). Analysis of case histories from construction of the Central Expressway in Singapore. *Canadian Geotechnical Journal*, *33*(5), 732-746.

Zhou, T. (2015). *3D FEM analysis for sequential excavation.* Master Thesis, Delft University of Technology.

Appendix A: Hardening Soil Model (Isotropic hardening)

In contrast to an elastic perfectly plastic model, the yield surface of a hardening plasticity model is not fixed in principal stress space, but it can expand due to plastic straining. Distinction can be made between two main types of hardening, namely shear hardening and compression hardening. Shear hardening is used to model irreversible strains due to primary deviatoric loading. Compression hardening is used to model irreversible plastic strains due to primary compression in oedometer loading and isotropic loading. Both types of hardening are contained in the present model**.**

The Hardening-Soil model is an advanced model for simulating the behavior of different types of soil, both soft soils and stiff soils. When subjected to primary deviatoric loading, soil shows a decreasing stiffness and simultaneously irreversible plastic strains develop. The Hardening-Soil model, however, supersedes the hyperbolic model by far. First, by using the theory of plasticity rather than the theory of elasticity, second, by including soil dilatancy and third by introducing a yield cap. Some basic characteristics of the model are:

- Stress dependent stiffness according to a power law. Input parameter m
- Plastic straining due to primary deviatoric loading. Input parameter E_{50}^{ref}
- Plastic straining due to primary compression. Input parameter E_{oed}^{ref}
- Elastic unloading / reloading. Input parameters E_{ur}^{ref} , νur
- Failure according to the Mohr-Coulomb model. Parameters c, ϕ and ψ

A basic feature of the present Hardening-Soil model is the stress dependency of soil stiffness. For oedometer conditions of stress and strain, the model implies for example:

$$E_{oed=}\ E_{oed}^{ref}\left({}^{\sigma}/_{p^{ref}}\right)^{m}$$

In the special case of soft soils it is realistic to use m = 1. In such situations there is also a simple relationship between the modified compression index λ *, as used in the PLAXIS Soft Soil Creep model and the oedometer loading modulus.

$$E_{oed}^{ref} = \left(p^{ref} / _{\lambda^*} \right) \qquad \lambda^* = \frac{\lambda}{(1 + e_o)}$$

Where p^{ref} is a reference pressure. Here it is considered that a tangent oedometer modulus at a particular reference pressure pref. Hence, the primary loading stiffness relates to the modified compression index λ* or to the standard Cam-Clay compression index λ. Similarly, the unloading-reloading modulus relates to the modified swelling index κ* or to the standard Cam-Clay swelling index κ. There is the approximate relationship:

$$E_{ur}^{ref} = \frac{3p^{ref}(1-2v_{ur})}{k^*} \qquad k^* = \frac{k}{(1+e_o)}$$

Again, this relationship applies in combination with the input value m = 1.

A.1: Hyperbolic relationship for standard drained triaxial test

A basic idea for the formulation of the Hardening-Soil model is the hyperbolic relationship between the vertical strain, ε1, and the deviatoric stress, *q*, in primary triaxial loading. Here standard drained triaxial tests tend to yield curves that can be described by:

$$-\varepsilon_1 = \frac{1}{2E_{50}} \frac{q}{1-{}^{q}/_{q_a}} \qquad \text{For: } q < q_f \text{ .... Equation (A. 1)}$$

Where q_a is the asymptotic value of the shear strength.

This relationship is portrayed in Figure A.1 .The parameter E_{50} is the confining stress dependent stiffness modulus for primary loading and is given by the equation

$$\mathrm{E}_{50} = \mathrm{E}_{50}^{\mathrm{ref}} \left(\frac{\mathrm{c}\cot\varphi - \sigma_3'}{\mathrm{c}\cot\varphi + \mathrm{p}^{\mathrm{ref}}} \right)^{\mathrm{m}} \text{ ....Equation (A. 2)}$$

Where E_{50}^{ref} , is a reference stiffness modulus corresponding to the reference confining pressure. p^{ref}. In PLAXIS, a default setting p^{ref} = 100 stress units is used. The actual stiffness depends on the minor principal stress, σ_3', which is the confining pressure in a triaxial test. Please note that σ'_3 is negative for compression. The amount of stress dependency is given by the power m. In order to simulate a logarithmic stress dependency, as observed for soft clays, the power should be taken equal to 1.0. It is suggested that values of m around 0.5 for Norwegian sands and silts.

The ultimate deviatoric stress, q_f, and the quantity q_a in Eq.(A.1) are defined as:

$$q_f = (c\ cot\varphi - \sigma'_3)\ \frac{2sin\varphi}{1-sin\varphi} \quad \text{And} \quad q_a = \frac{q_f}{R_f} \text{ ....Equation (A. 3)}$$

Again, it is remarked that σ'_3 is usually negative. The above relationship for q_f is derived from the Mohr-Coulomb failure criterion, which involves the strength parameters c and ϕ. As soon as $q = q_f$, the failure criterion is satisfied and perfectly plastic yielding occurs as described by the Mohr-Coulomb model. The ratio between q_f and q_a is given by the failure ratio R_f, which should obviously be smaller than 1. In PLAXIS, $R_f = 0.9$ is chosen as a suitable default setting. For

Unloading and reloading stress paths, another stress-dependent stiffness modulus is used:

$$E_{ur} = E_{ur}^{ref} \left(\frac{c\ cot\varphi - \sigma'_3}{c\ cot\varphi + p^{ref}}\right)^m \text{ .... Equation (A. 4)}$$

Where E_{ur}^{ref} is the reference Young's modulus for unloading and reloading, corresponding to the reference pressure p^{ref}. In many practical cases, it is appropriate to set E_{ur}^{ref} equal to 3 $E_{50}^{ref;}$ this is the default setting used in PLAXIS.

A.1.1: Approximation of hyperbola by the hardening-soil model.

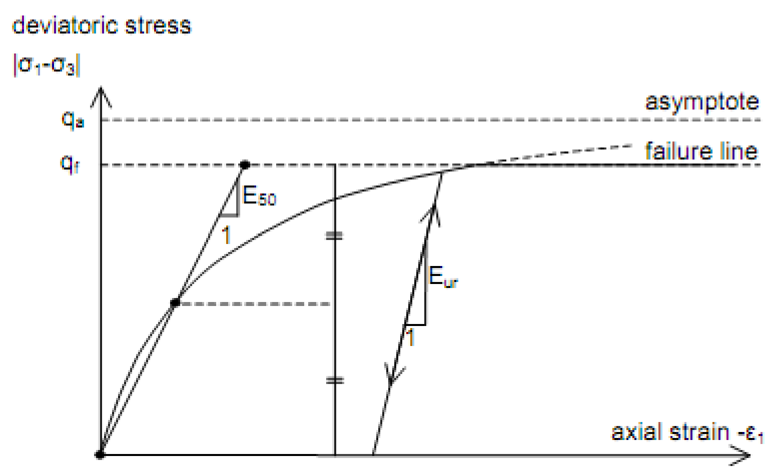

Figure A. 1: Hyperbolic Stress-Strain Relation in Primary Loading For a Standard Drained Triaxial Test (R.B.J. Brinkgreve & W. Broere, 2004)

Moreover, it is assumed that $q < q_f$, as also indicated in Figure A.1. It should also be realized that compressive stress and strain are considered positive. When considering the corresponding plastic strains. This stems from a yield function of the form:

$$f = \bar{f} - \gamma^p \text{..........Equation (A. 5)}$$

Where f is a function of stress and γ p is a function of plastic strains:

$$\bar{f} = \frac{1}{E_{50}} \frac{q}{1-{}^{q}/_{q_a}} - \frac{2q}{E_{ur}} \qquad \gamma^p = -\left(2\varepsilon_1^p - \varepsilon_v^p\right) \approx -2\varepsilon_1^p \text{ ....Equation (A. 6)}$$

With q, q_a, E_{50} *and* E_{ur} as defined by equation (A.2) to (A.4) whilst the superscript p is used to denote plastic strains. For hard soils, plastic volume changes (ε^p_v) tend to be relatively small and this leads to the approximation $\gamma^p \approx -2\varepsilon_1^p$. The above definition of the strain hardening parameter γ^p will be referred to later. An essential feature of the above definitions for f is that it matches the well-known hyperbolic law. For checking this statement, one has to consider primary loading, as this implies the yield condition f = 0. For primary loading, it thus yields $\gamma^p = f$ and it follows from Eq. (A.6) that:

$$-\varepsilon_1^p \approx \frac{1}{2}\bar{f} = \frac{1}{2E_{50}} \frac{q}{1-{}^{q}/_{q_a}} - \frac{q}{E_{ur}} \text{..........Equation (A. 7)}$$

In addition to the plastic strains, the model accounts for elastic strains. Plastic strains develop in primary loading alone, but elastic strains develop in both primary loading and unloading/ reloading. For drained triaxial test stress paths with $\sigma_2' = \sigma_3'$ = constant, the equations:

$$-\varepsilon_1^e = \frac{q}{E_{ur}} \qquad -\varepsilon_2^e - \varepsilon_3^e = -\nu_{ur}\frac{q}{E_{ur}} \text{ ....Equation (A. 8)}$$

Where $\nu_{ur}$is the unloading / reloading Poisson's ratio. Here it should be realized that restriction is made to strains that develop during deviatoric loading, whilst the strains that develop during the very first stage of the test are not considered. For the first stage of isotropic compression (with consolidation) the, Hardening-Soil model predicts, fully elastic volume changes according to Hooke's law, but these strains are not included in Eq. (A.8). For the deviatoric loading stage of the triaxial test the axial strain is the sum of an elastic component given by Eq. (A.8) and a plastic component according to Eq. (A.7) Hence, it follows that:

$$-\varepsilon_1 = -\varepsilon_1^e - \varepsilon_1^p \approx \frac{1}{2E_{50}} \frac{q}{1-{}^{q}/_{q_a}}$$ ……………………………….Equation (A. 9)

This relationship holds exactly in absence of plastic volume strains, i.e. when $\varepsilon^p_v = 0$. In reality, plastic volumetric strains will never be precisely equal to zero, but for hard soils, plastic volume changes tend to be small when compared with the axial strain, so that the approximation in Eq. (A.9) will generally be accurate. It is thus made clear that the present Hardening-Soil model yields a hyperbolic stress-strain curve under triaxial testing conditions. For a given constant value of the hardening parameter, γ^p, the yield condition $f = 0$, can be visualized in p'-q-plane by means of a yield locus. When plotting such yield loci, one has to use Eq. (A.6) as well as Eqs. (A.2) and (A.4) for E_{50} and E_{ur} respectively. Because of the latter expressions, the shape of the yield loci depends on the exponent m. For $m = 1$, straight lines are obtained, but slightly curved yield loci correspond to lower values of the exponent. Figure A.2 shows the shape of successive yield loci for $m = 0.5$, being typical for hard soils.

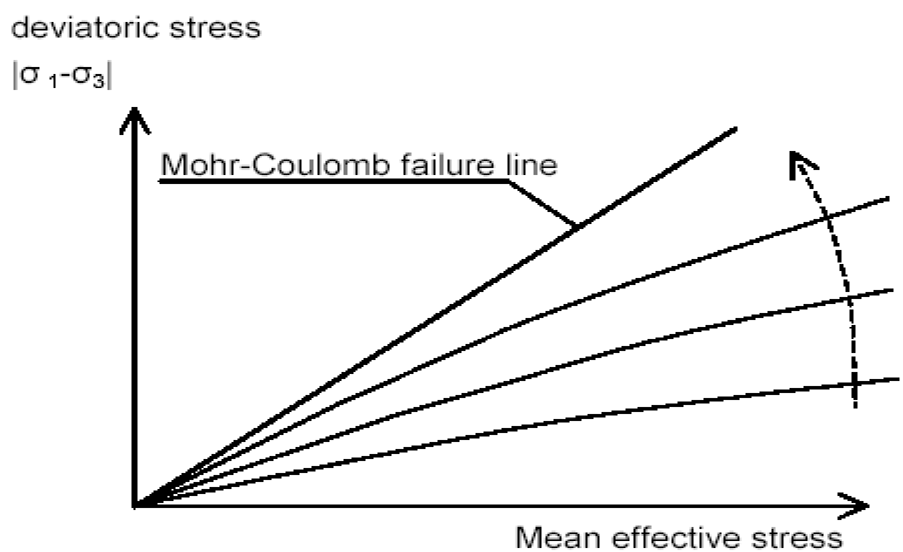

Figure A. 2: Successive Yield Loci for Various Constant Values of the Hardening Parameter (R.B.J. Brinkgreve & W. Broere, 2004)

A.2: Parameters of the Hardening-Soil Model

Some parameters of the present hardening model coincide with those of the non-hardening Mohr Coulomb model.

Failure parameters as in Mohr-Coulomb model:

- c : (Effective) cohesion [kN/m2]
- φ :(Effective) angle of internal friction [°]
- ψ : Angle of dilatancy [°]

Basic parameters for soil stiffness:

- E_{50}^{ref} : Secant stiffness in standard drained triaxial test [kN/m2]
- E_{eod}^{ref} : Tangent stiffness for primary oedometer loading [kN/m2]
- m : Power for stress-level dependency of stiffness [-]

Advanced parameters (it is advised to use the default setting):

- E_{ur}^{ref} :Unloading / reloading stiffness (default $E_{ur}^{ref} = 3\ E_{50}^{ref}$) [kN/m2]
- v_{ur} :Poisson's ratio for unloading-reloading (default vur = 0.2) [-]
- P^{ref} :Reference stress for stiffness (default $P^{ref} = 100$ stress units)[kN/m2]
- Ko^{nc} :K_o-value for normal consolidation (default $Ko^{nc} = 1\text{-}\sin\varphi$) [-]
- R^f : Failure ration q_f / q_a (default $R_f = 0.9$ (see figure 4.1) [-]
- $\delta tension$:Tensile strength (default *$\delta tension$ = 0 stress units)* [kN/m2]
- $c_{\ increment}$: As in Mohr-Coulumb model (default $c_{\ increment} = 0$) [kN/m2]

Stiffness Moduli E_{50}^{ref} & E_{eod}^{ref} Power (M)

The advantage of the Hardening-Soil model over the Mohr-Coulomb model is not only the use of a hyperbolic stress-strain curve instead of a bi-linear curve, but also the control of stress level dependency. When using the Mohr-Coulomb model, the user has to select a fixed value of Young's modulus whereas for real soils this stiffness depends on the stress level. It is therefore necessary to estimate the stress levels within the soil and use these to obtain suitable values of stiffness. With the Hardening-Soil model, however, this cumbersome selection of input parameters is not required. Instead, a stiffness modulus E_{50}^{ref} is defined for a reference minor principal stress of $-\sigma'_3 = p'^{ref}$. As a default value, the program uses $p^{ref} = 100$ stress units.

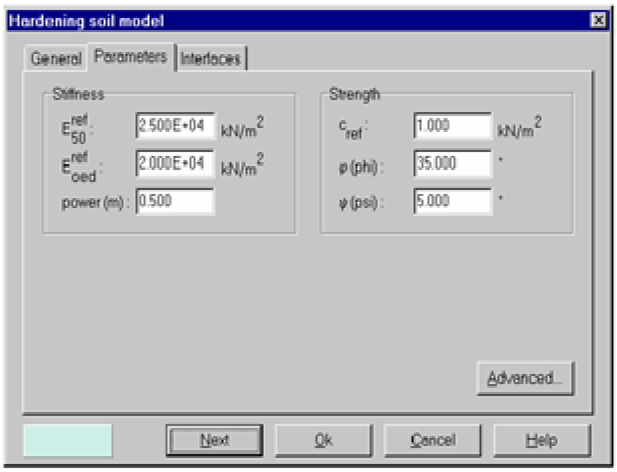

Figure A. 3: Basic Parameters for the Hardening-Soil Model (R.B.J. Brinkgreve & W. Broere, 2004).

Within Hooke's theory of elasticity conversion between E and G goes by the equation

$E = 2\ (1+\nu)\ G$. As E_{ur} is a real elastic stiffness, one may thus write $E_{ur} = 2\ (1+\ \nu)\ G_{ur}$, where G_{ur} is an elastic shear modulus. PLAXIS allows for the input of E_{ur} and ν_{ur} but not for a direct input of G_{ur}. In contrast to E_{ur}, the secant modulus E_{50} is not used within a concept of elasticity. Therefore, there is no simple conversion from E_{50} to G_{50}. In contrast to elasticity-based models, the elastoplastic Hardening-Soil model does not involve a fixed relationship between the (drained) triaxial stiffness E_{50} and the oedometer stiffness E_{oed} for one-dimensional compression. Instead, these stiffnesses can be inputted independently. Having defined E_{50} by Eq. (A.2), it is now important to define the oedometer stiffness. Here we use the equation:

$$E_{oed} = E_{oed}^{ref}\left(\frac{c\ cot\varphi - \sigma_1'}{c\ cot\varphi + p^{ref}}\right)^m \quad \text{...Equation (A. 10)}$$

Where E_{oed} is a tangent stiffness modulus as indicated in Figure (A.4). Hence, $E^{ref}{}_{oed}$ is a tangent stiffness at a vertical stress of .$\sigma'_1 = pref$ (R.B.J. Brinkgreve & W. Broere, 2004).

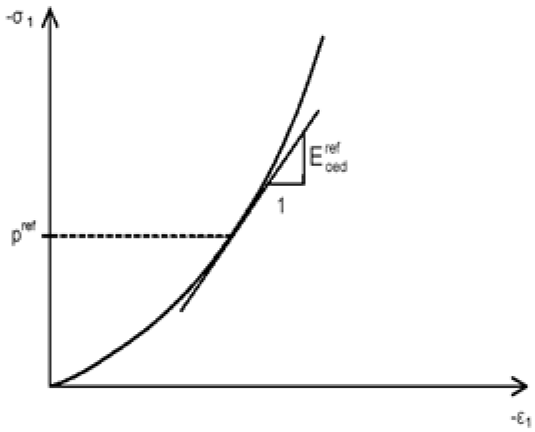

Figure A. 4: Definition of E_{ref} in Oedometer Test Results (R.B.J. Brinkgreve & W. Broere, 2004)

Appendix B: PLAXIS Input Parameters

SHEET 1 of 2

BH No: -3

ADDIS GEOSYSTEMS PLC.

Tittle: BOREHOLE LOG SHEET

PROJECT: 2B+SB+G+M+18 Mixed Use Building
LOCATION : Addis Ababa /Bole Area
CLIENT : Ato Fitsum G/Medhin
DATE STARTED:21/04/2016
DATE COMPLETED :25/04/2016

BORING TYPE : Rotary coring
GROUND WATER LEVEL : Nil
BH COORDINATES : N-994785, E-476608
BH ELEVATION : 2202m
INCLINATION : Vertical. TOTAL BH DEPTH 28m

Depth (cm)	Hole Diameter (mm)	Sample Record	SPT/DPT N_value	Legend	Strata Description	Run Length Depth (m)	TCR (%)	RQD (%)	Remark
					Made Ground	0.4	100		
0						0.5	100		
1						2	100		
2						2.35	100		
		UD				2.75	100		
						3.2	100		
3			8						
					Firm to stiff, light gray, silty CLAY	4.25	100		
4						4.6	100		
		UD				5	100		
5						5.45	100		
			14						
						6	100		
6						6.35	100		
		UD							
						7	100		
7						7.45	100		
	89		13			7.65	100		
8						9	100		
9						9.45	100		
			23						
						10	100		
10		UD				10.35	100		
					Stiff to hard, light brownish to reddish brown, sandy silty CLAY/ sandy clayey SILT with thin layer of IGINIMBRITE rock at the depth of (7.65-8.40m)	11.4	100		
11									
						11.85	100		
			21			12.2	100		
12						12.55	100		
		UD							
						13.15	100		
13						13.6	100		
			56						
14						15.3	100		

P.o. Box 27067 code 1000 Addis Ababa, Ethiopia
ADDIS GEOSYSTEMS PLC

BH BOREHOLE
(Nc) CONE PENETRATION TEST
SPT STANDARD PENETRATION TEST
N BLOWS/30cm
W WATER SAMPLE
NGL NATURAL GROUND LEVEL
RQD ROCK QUALITY DESIGNATION
TCR TOTAL CORE RECOVERY
▼ STATIC GROUND WATER LEVEL

DS DISTURBED SOIL SAMPLE
UD UNDISTURBED SOIL SAMPLE
RK ROCK SAMPLE
R REFUSAL

LOGGED BY : Biruk Wolde Date:09/05/2016
DRAWN BY: Hanan Yassin Date:09/05/2016
APPROVED BY : Dr.Addis A.Zeleke Date:09/05/2016

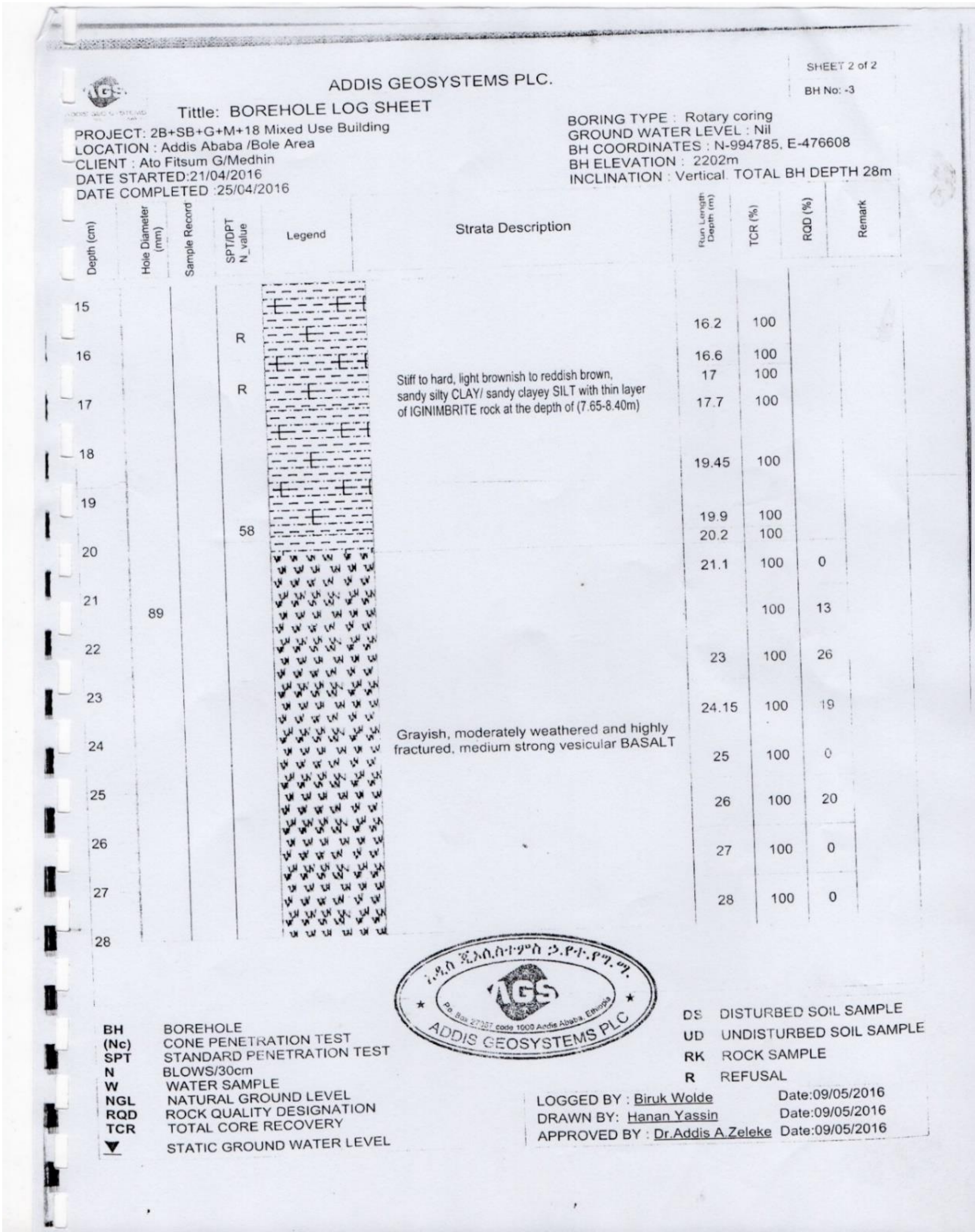

SHEET 2 of 2
BH No: -3

ADDIS GEOSYSTEMS PLC.

Tittle: BOREHOLE LOG SHEET

PROJECT: 2B+SB+G+M+18 Mixed Use Building
LOCATION : Addis Ababa /Bole Area
CLIENT : Ato Fitsum G/Medhin
DATE STARTED:21/04/2016
DATE COMPLETED :25/04/2016

BORING TYPE : Rotary coring
GROUND WATER LEVEL : Nil
BH COORDINATES : N-994785, E-476608
BH ELEVATION : 2202m
INCLINATION : Vertical. TOTAL BH DEPTH 28m

Depth (cm)	Hole Diameter (mm)	Sample Record	SPT/DPT N_value	Legend	Strata Description	Run Length Depth (m)	TCR (%)	RQD (%)	Remark
15					Stiff to hard, light brownish to reddish brown, sandy silty CLAY/ sandy clayey SILT with thin layer of IGINIMBRITE rock at the depth of (7.65-8.40m)	16.2	100		
16			R			16.6	100		
			R			17	100		
17						17.7	100		
18						19.45	100		
19			58			19.9	100		
						20.2	100		
20					Grayish, moderately weathered and highly fractured, medium strong vesicular BASALT	21.1	100	0	
21	89						100	13	
22						23	100	26	
23						24.15	100	19	
24						25	100	0	
25						26	100	20	
26						27	100	0	
27						28	100	0	
28									

ADDIS GEOSYSTEMS PLC

BH BOREHOLE
(Nc) CONE PENETRATION TEST
SPT STANDARD PENETRATION TEST
N BLOWS/30cm
W WATER SAMPLE
NGL NATURAL GROUND LEVEL
RQD ROCK QUALITY DESIGNATION
TCR TOTAL CORE RECOVERY
▼ STATIC GROUND WATER LEVEL

DS DISTURBED SOIL SAMPLE
UD UNDISTURBED SOIL SAMPLE
RK ROCK SAMPLE
R REFUSAL

LOGGED BY : Biruk Wolde Date:09/05/2016
DRAWN BY: Hanan Yassin Date:09/05/2016
APPROVED BY : Dr.Addis A.Zeleke Date:09/05/2016

Figure B. 1: Representative Borehole Log Sheet (Addis Geosystems Plc., 2016)

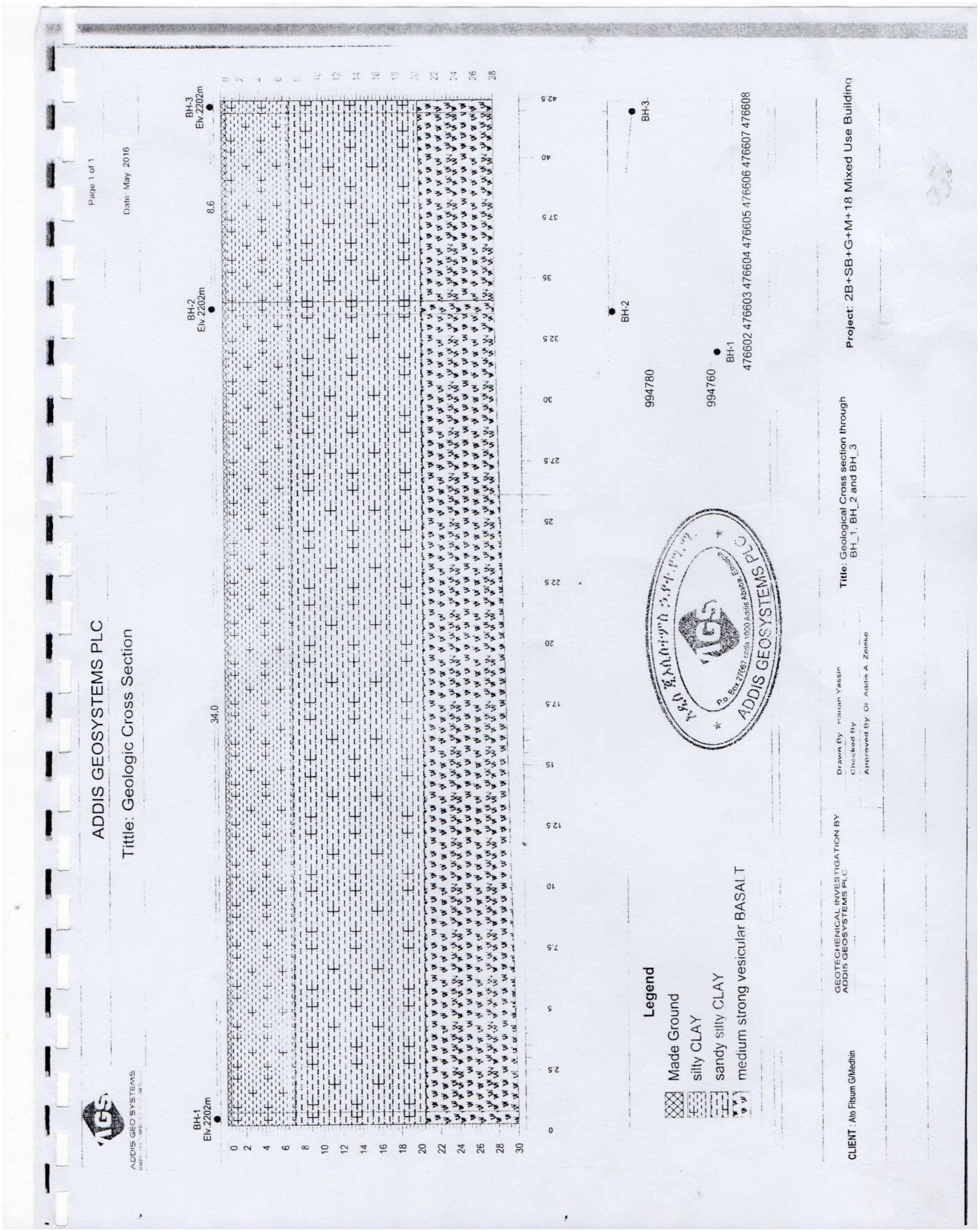

Figure B. 2: Geologic Cross-Section (Addis Geosystems Plc., 2016)

Table B.1: Effective strength of cohesive soils (G.Look, 2007)

Effective Cohesion (kPa)	Friction angle (degrees)
5-10	10-20
10-20	15-25
20-50	20-30
50-100	25-30

Table.B.1**:** Typical values for bulk and saturated unit weights (Michael Carter and Stephen P.Bentley, 1991).

Type of material		Bulk unit weight (kN/m^3)		Saturated unit weight (kN/m^3)	
		loose	dense	loose	dense
Granular soils	gravel	16.0	18.0	20.0	21.0
	Well graded sand and gravel	19.0	21.0	21.5	23.0
	Coarse or medium sand	16.5	18.5	20.0	21.5
	Well graded sand	18.0	21.0	20.5	22.5
	Fine or silty sand	17.0	19.0	20.0	21.5
	Rock fill	15.0	17.5	19.5	21.0
	Brick hardcore	13.0	17.5	16.5	19.0
	Slag fill	12.0	15.0	18.0	20.0
	Ash fill	6.5	10.0	13.0	15.0
Cohesive soils	Peat (high variability)	12.0		12.0	
	Organic clay	15.0		15.0	
	Soft clay	17.0		17.0	
	Firm clay	18.0		18.0	
	Stiff clay	19.0		19.0	
	Hard clay	20.0		20.0	
	Stiff or hard glacial clay	21.0		21.0	

Table B.2: Elastic parameters of various soils (G.Look, 2007)

Type	Strength of soil	Elastic modulus, E, (MPa)	
		Short term	Long term
Gravel	Loose	25-50	
	Medium	50-100	
	Dense	100-200	
Medium to coarse sand	Very loose	<5	
	Loose	3-10	
	Medium dense	8-30	
	Dense	25-50	
	Very dense	40-100	
Fine sand	Loose	5-10	
	Medium	10-25	
	Dense	25-50	
Silt	Soft	<10	<8
	Stiff	10-20	8-15
	Hard	>20	>15
Clay	Very soft	<3	<2
	Soft	2-7	1-5
	Firm	5-12	4-8
	Stiff	10-25	7-20
	Very stiff	20-50	15-35
	Hard	40-80	30-60

Table B.3: Soil properties obtained from borehole log.

Depth of N count	SPT N30 (uncorrected)	consistency	Bulk, $\gamma (kN/m^3)$	N70 (corrected)	N60 (approximated)	ϕ(deg)	Cu (kPa)	Eu (MPa)
1	8	Med.stiff	18.00	7	8	17.96	129.6	8.8
2								
3								
4								
5	14	Stiff	18.50	10	12	22.35	173.5	15.4
6								
7	13	Stiff	18.50	9	11	21.30	163.0	14.3
8								
9	23	Very stiff	19.00	13	15	20.13	203.8	25.3
10								
11								
12	21	Very stiff	19.00	11	13	23.38	183.8	23.1
13								
14	56	Hard	20.50	28	33	25.32	359.5	61.6
15								
16								
17								
18								
19								
20	58	Hard	20.50	23	27	23.71	311.2	63.8

B.1: Lateral Earth Pressure

Incorrect implementation of design earth pressure may lead to uneconomical or even unsafe designs. Traditionally, apparent earth pressure diagrams are used for designing excavation support systems. These diagrams are semi-empirical approaches back calculated from field measurements of strut loads, which do not represent the actual earth pressure or its distribution with depth. Therefore, apparent earth pressure diagrams are only appropriate for sizing the struts. The use of these diagrams yield support systems that are adequate about preventing structural failure, but may result in excessive wall deformations and ground movements. In this study (Caquot, A. and Kerisel, J., 1948) were assumed and they included the friction factor, δ, between the retaining wall and the soil and assumed an elliptical curved failure surface which is recognized to be very close to the actual failure surface. (Caquot, A. and Kerisel, J., 1948) Coefficients for the active and passive conditions, are presented in Appendix B respectively

Strut loads were determined by tributary area methods from apparent earth pressure diagrams proposed by (FHWA, 1999)

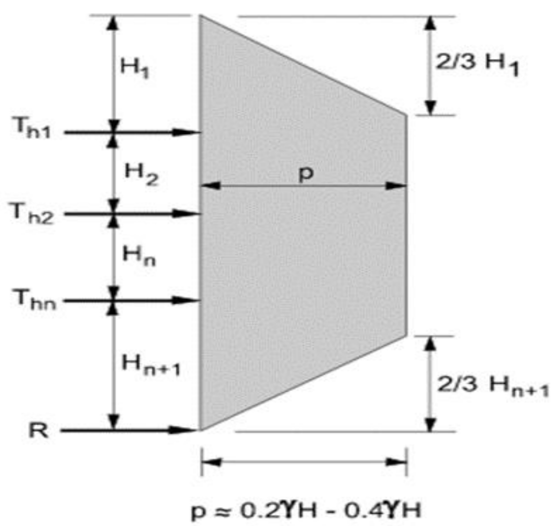

Figure B. 3 : Recommended Earth Pressure Diagram for Stiff to Hard Clays: Walls with Multiple Levels of Ground Anchors (FHWA, 1999)

$\mathrm{Pe} = 0.2 * \gamma * \mathrm{H}$ to $0.4 * \gamma * \mathrm{H}$……………………………………………………equation (0.1)

For this thesis the average ($0.3\gamma\mathrm{H}$) was taken

Where:

Hn+1= Distance from the base of excavation to the lowermost ground anchor.

Th1=Horizontal load in strut over length H1+H2/2

Th2= Horizontal load in strut over length H2/+Hn/2

Thn= Horizontal load in strut over length Hn/2+Hn+1/2

R=Reaction force to be resisted by subgrade over length Hn+1/2.

P=Maximum ordinate of diagram.

ϒ= Unit weight of soil.

H= Depth of excavation.

H1= Distance from ground surface to upper most strut.

The horizontal spacing of strut in this study taken as 3, 4 and 5m randomly in the parametric study.

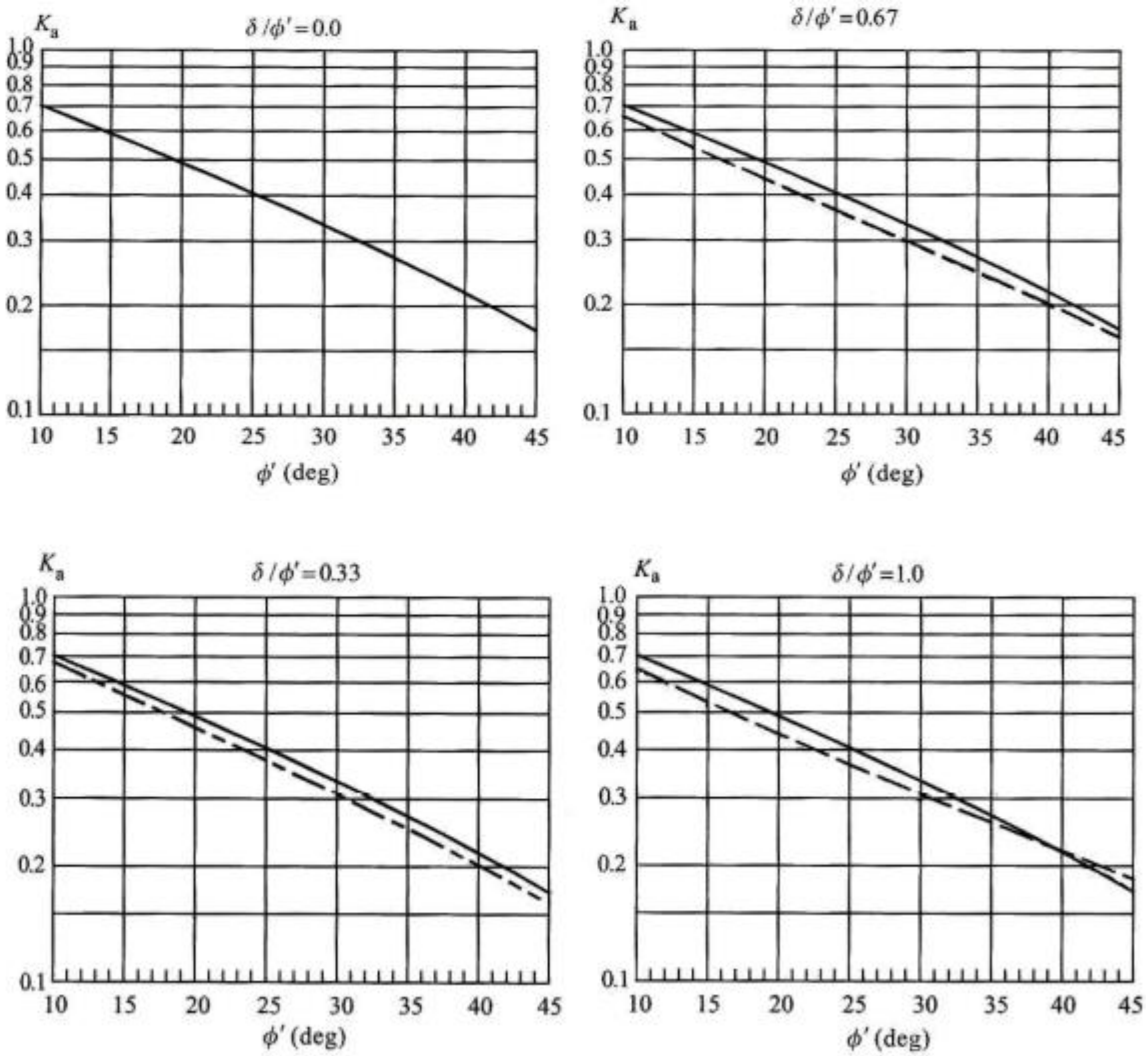

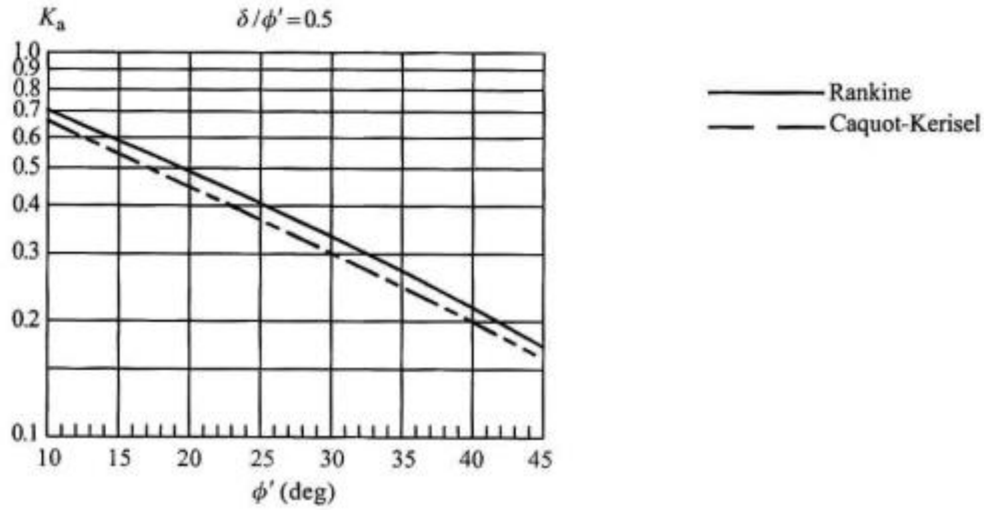

Figure B. 4 - Coefficients of Caquot-Kerisel Active Earth Pressure. Horizontal Component Ka.H = Kacosδ Adapted From (Ou, 2006).

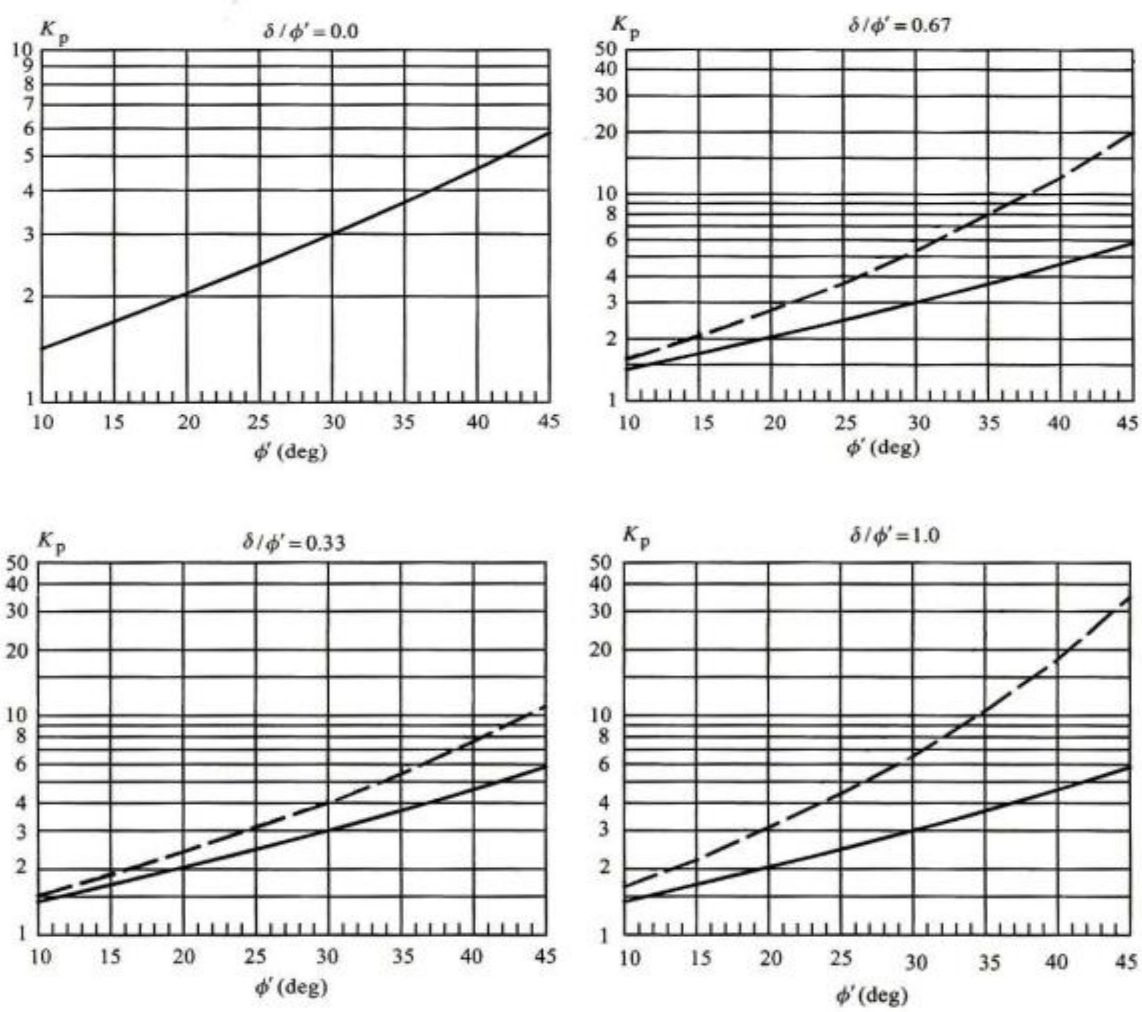

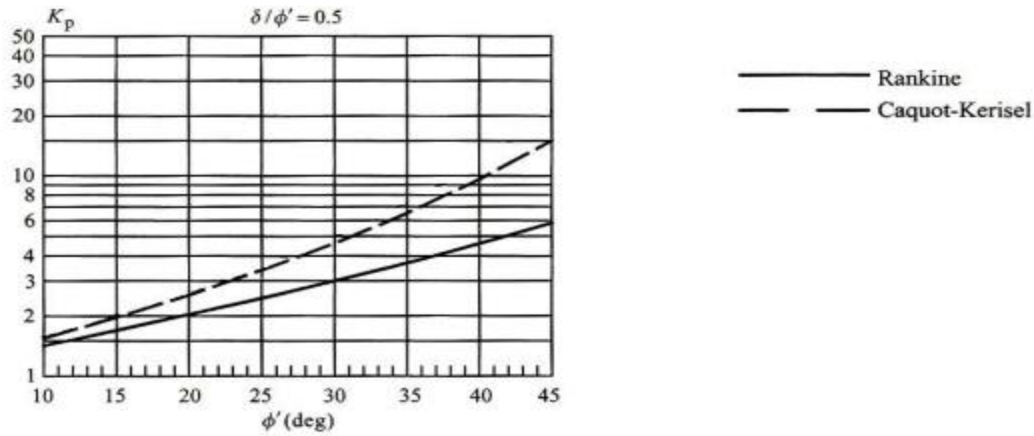

Figure B. 5 - Coefficients of Caquot-Kerisel Passive Earth Pressure. Horizontal Component Kp.H = Kpcosδ Adapted From (Ou, 2006).

Table B.4: Wall Parameters for Base Model

Name of parameters	d1	d2	d3	Unit
Adapted pile diameter (d)	0.65	0.85	1.05	m
Equivalent wall thickness(de)	0.3	0.6	0.9	m
Unit weight of concrete(γ_c)	24	24	24	kN/m^3
Modulus of elasticity of concrete(Ec)	3*10^7	3*10^7	3*10^7	kPa
Poisson's ratio(*v*)	0.15	0.15	0.15	-

Table B.5: Strut (Wailing Beam) Parameters

Parameters	Name	Strut	Wailing	Unit
Material model	-	Linear	Linear	-
Cross section area	A	0.027	0.02	m^2
Volumetric weight	γ	78.5	78.5	kN/m^3
Young’s modulus	E	$2.1*10^8$	$2.1*10^8$	kN/m^2
Moment of Inertia	I_2	$1.37*10^{-3}$	$5.77*10^{-4}$	m^4
Moment of Inertia	I_3	$1.31*10^{-4}$	$1.08*10^{-4}$	m^4
Moment of Inertia	I_{23}	0	0	m^4
Poisson's ratio	V	0.1	0	-

Table 0.6: Excavation and Embedment Depth for the Base Model

Parameters	Unit	He		
Depth of excavation	m	8	11	14
Depth of embedment	m	5	7	10

Appendix C: PLAXIS Output

C.1: Extreme Displacements and Bending Moments.

Run-11 = thickness 0.3m and strut horizontal spacing 3m.

Run-12 = thickness 0.3m and strut horizontal spacing 4m.

Run-13 = thickness 0.3m and strut horizontal spacing 5m.

Run-24 = thickness 0.6m and strut horizontal spacing 3m.

Run-25 = thickness 0.6m and strut horizontal spacing 4m.

Run-26 = thickness 0.6m and strut horizontal spacing 5m.

Run-37 = thickness 0.9m and strut horizontal spacing 3m.

Run-38 = thickness 0.9m and strut horizontal spacing 4m.

Run-39 = thickness 0.9m and strut horizontal spacing 5m.

Run-42 = thickness 1.2m and strut horizontal spacing 4m.

Table C. 1: PLAXIS Output For Excavation Height of 8m with Adjacent Load 150kpa

He= 8m, load =150kPa						
Run	Total displacement (mm)	Ux (mm)	Uy (mm)	Uz-wall (mm)	M11 (kN-m/m)	M22 (kN-m/m)
Run-11	44.77	44.77	24.07	-7.3	143.95	182.39
Run-12	44.62	44.62	24.84	-7.75	155.11	184.18
Run-13	44.69	44.69	24.95	-7.9	166.96	185.25
Run-24	15.69	15.69	14.43	-2.02	-212.32	373.83
Run-25	15.64	15.64	14.48	-2.1	-215.17	375.58
Run-26	15.71	15.71	14.54	-2.13	-225.23	377.71
Run-37	12.73	6.67	12.72	-0.7767	-306.94	493.28
Run-38	12.02	5.41	12.02	0.79119	-257.39	428.14
Run-39	12.75	6.69	12.75	-0.73475	-324.38	498.47

Table C. 2: PLAXIS Output For Excavation Height of 8m with Adjacent Load 200kpa

He= 8m, load =200kPa						
Run	Total displacement (mm)	Ux (mm)	Uy (mm)	Uz-wall (mm)	M11 (kN-m/m)	M22 (kN-m/m)
Run-11	61.75	61.75	37.2	-7.94	176.39	226.9
Run-12	60.93	60.93	38.12	-8.38	187.07	227.49
Run-13	60.85	60.85	37.12	-8.46	200.29	228.81
Run-24	20.09	20.09	16.68	-2.38	-273.16	452.82
Run-25	20.36	19.97	16.76	-2.28	-277.24	454.54
Run-26	20	20	16.83	2.24	-289.72	457.46
Run-37	14.35	8.58	14.28	-1.1	-393.61	594.88
Run-38	14.39	8.57	14.31	-1.07	-398.19	597.62
Run-39	14.41	8.62	14.34	1.07	-413.01	600.9
Run-42	13.48	4.4	13.48	-0.550	-467.22	682.54

Table C. 3: PLAXIS Output For Excavation Height of 8m with Adjacent Load 250kpa

He= 8m, load =250kPa						
Run	Total displacement (mm)	Ux (mm)	Uy (mm)	Uz-wall (mm)	M11 (kN-m/m)	M22 (kN-m/m)
Run-11	81.44	81.39	56.6	-8.58	222.17	276.67
Run-12	84.84	82.16	59.43	-9.05	229.41	279.71
Run-13	82.12	82.12	57.22	-9.18	246.97	283.47
Run-24	24.69	24.69	19.17	-3.13	-345.03	538.23
Run-25	24.97	24.61	19.25	-3.05	-348.63	541.8
Run-26	25.35	24.75	19.34	-3.03	-362.73	545.57
Run-37	16.31	10.42	16.12	-1.46	-488.48	692.03
Run-38	16.34	10.23	16.16	-1.4	-494.81	691.01
Run-39	16.4	10.3	16.21	-1.4	-512.56	694.85

Table C. 4: PLAXIS Output For Excavation Height of 11m with Adjacent Load 150kpa

He= 11m, load =150kPa						
Run	Total displacement (mm)	Ux (mm)	Uy (mm)	Uz-wall (mm)	M11 (kN-m/m)	M22 (kN-m/m)
Run-11	46.62	46.62	25.38	-8.82	140.88	191.34
Run-12	46.36	46.36	25.41	-9.31	149.35	190.52
Run-13	46.61	46.61	25.96	-9.51	160.37	191.43
Run-24	16.04	16.04	10.91	-2.76	170.83	369.86
Run-25	15.99	15.99	11.16	2.87	-175.9	370.69
Run-26	16.05	16.05	11.52	2.93	191.78	374.28
Run-37	6.66	6.66	6.09	-1.15	-256.1	517.18
Run-38	7.1	6.65	6.12	-1.17	-268.18	523.26
Run-39	6.66	6.66	6.18	-1.17	-279	527.91

Table C. 5: PLAXIS Output For Excavation Height of 11m with Adjacent Load 200kpa

He= 11m, load =200kPa						
Run	Total displacement (mm)	Ux (mm)	Uy (mm)	Uz-wall (mm)	M11 (kN-m/m)	M22 (kN-m/m)
Run-11	63.46	63.46	39.25	-9.48	172.99	229.78
Run-12	62.86	62.86	39.13	-10.02	179.57	228.55
Run-13	63.75	63.75	41.41	-10.17	191.28	231.26
Run-24	20.51	20.51	15.62	-2.84	-209.73	443.9
Run-25	20.59	20.37	14.94	-2.95	-219.76	444.76
Run-26	20.94	20.39	15.62	2.99	-231.85	447.68
Run-37	8.91	8.54	8.08	-1.12	-329.33	627
Run-38	9.55	8.49	7.61	-1.14	-341.61	631.28
Run-39	9.63	8.34	7.87	1.14	-356.95	634.95
Run-42	6.39	4.34	6.38	-0.533	-433.79	771.72

Table C. 6: PLAXIS Output For Excavation Height of 11m with Adjacent Load 250kpa

He= 11m, load =250kPa						
Run	Total displacement (mm)	Ux (mm)	Uy (mm)	Uz-wall (mm)	M11 (kN-m/m)	M22 (kN-m/m)
Run-11	84.55	84.4	59.06	-10.17	213.22	273.84
Run-12	83.83	83.71	57.5	-10.72	214.71	273.27
Run-13	86.6	84.85	61.17	10.79	227.85	274.96
Run-24	26.84	25.57	19.95	-3.28	-255.68	524.55
Run-25	24.9	24.9	17.85	-3.12	-267.86	522.96
Run-26	26.22	25.18	19.77	-3.08	-282.3	529.24
Run-37	10.76	10.27	8.66	-1.43	-402.97	731.36
Run-38	10.2	10.19	7.79	-1.38	-417.28	736.88
Run-39	10.61	10.24	8.96	-1.36	-432.29	743.34

Table C. 7: PLAXIS Output For Excavation Height of 14m with Adjacent Load 150kpa

He= 14m, load =150kPa						
Run	Total displacement (mm)	Ux (mm)	Uy (mm)	Uz-wall (mm)	M11 (kN-m/m)	M22 (kN-m/m)
Run-11	48.32	48.32	28.84	-10.92	150.1	211.31
Run-12	48.12	48.12	29.09	-11.59	163.53	211.83
Run-13	48.14	48.14	30.01	-11.78	181.63	213.31
Run-24	16.76	16.76	12.69	-3.93	178.66	425.59
Run-25	16.77	16.71	12.82	-4.1	183.53	426.19
Run-26	16.6	16.6	13.24	-4.15	-198.3	429.64
Run-37	9.3	6.99	9.29	-1.73	-225.49	617.37
Run-38	9.29	7.05	9.29	-1.76	-246.46	621.11
Run-39	9.32	6.94	9.32	-1.76	-282.05	628.4

Table C. 8: PLAXIS Output For Excavation Height of 14m with Adjacent Load 200kpa

He= 14m, load =200kPa						
Run	Total displacement (mm)	Ux (mm)	Uy (mm)	Uz-wall (mm)	M11 (kN-m/m)	M22 (kN-m/m)
Run-11	66.06	66.06	44.39	-11.74	185.95	256.43
Run-12	65.54	65.54	42.72	-12.39	196.78	255.65
Run-13	65.98	65.98	45.19	-12.52	211.17	258.49
Run-24	22.6	21.61	18.25	-4.08	223.6	507.23
Run-25	21.9	21.3	16.95	-4.24	224.17	508.39
Run-26	22.58	21.36	18.59	-4.27	-248.95	512.53
Run-37	10.42	8.89	10	-1.73	-288.67	727.91
Run-38	10.05	8.8	10.05	-1.75	-316.06	734.85
Run-39	10.35	8.81	10.09	-1.74	-355.18	742.9
Run-42	6.98	4.69	9.67	-0.865	-392.12	927.5

Table C. 9: PLAXIS Output For Excavation Height of 14m with Adjacent Load 250kpa

He= 14m, load =250kPa						
Run	Total displacement (mm)	Ux (mm)	Uy (mm)	Uz-wall (mm)	M11 (kN-m/m)	M22 (kN-m/m)
Run-11	91.13	88.26	65.8	-12.56	223.97	304.89
Run-12	92.46	87.93	64.09	-13.27	232.87	305.93
Run-13	94.04	88.76	67.46	-13.35	254.81	310.28
Run-24	28.61	26.94	23.84	-4.18	270.06	593.99
Run-25	28.29	26.52	22.17	-4.34	-265.02	594.7
Run-26	29.06	26.62	24.78	-4.36	-297.78	600.03
Run-37	12.11	10.99	11.03	1.7	-351.49	847.12
Run-38	12.21	10.86	10.92	1.72	-379.79	852.92
Run-39	12.84	10.94	12.03	-1.69	-427.78	865.82

C.2: Tables of Analysis results

Table C. 10: Results from Varying Adjacent Surface Loads.

Run-12 (0.3m , SH =4m)							
	loads (kPa)	Utot (mm)	Ux-max(mm)	Uy-max(mm)	Uz-tot max(mm)	M11(kN-m/m)	M22(kN-m/m)
He = 8m	150	44.62	44.62	24.84	7.75	155.11	184.18
	200	60.93	60.93	38.12	8.38	187.07	227.49
	250	84.84	82.16	59.43	9.05	229.41	279.71
He = 11m	150	46.36	46.36	25.41	9.31	149.35	190.52
	200	62.86	62.86	39.13	10.02	179.57	228.55
	250	83.83	83.71	57.5	10.72	214.71	273.27
He= 14m	150	48.12	48.12	29.09	11.59	163.53	211.83
	200	65.54	65.54	42.72	12.39	196.78	255.65
	250	92.46	87.93	64.09	13.27	232.87	305.93

Table C. 11: Results from Varying Thickness of Tangent Pile Wall.

Run-12,Run-25, Run-38 and Run-42							
	Thickness (m)	Utot (mm)	Ux-max(mm)	Uy-max(mm)	Uz-tot max(mm)	M11(kN-m/m)	M22(kN-m/m)
He=8m	0.3	60.93	60.93	38.12	9.07	187.07	227.49
	0.6	20.36	19.97	16.76	3.43	-277.24	454.54
	0.9	14.39	8.57	14.31	1.7	-398.19	597.62
	1.2	13.48	4.4	13.48	1.19	-467.22	682.54
He=11m	0.3	62.86	62.86	39.13	10.02	179.57	228.55
	0.6	20.59	20.37	14.94	3.51	-219.76	444.76
	0.9	9.55	8.49	7.61	1.94	-341.61	631.28
	1.2	6.39	4.34	6.38	1.33	-433.79	771.72
He=14m	0.3	65.54	65.54	42.79	12.39	196.78	255.65
	0.6	21.9	21.3	16.95	4.24	224.17	508.39
	0.9	10.05	8.8	10.05	1.91	-316.06	734.85
	1.2	6.98	4.69	9.67	1.25	-392.12	927.5

Table C. 12: Results from Varying Strut Horizontal Spacing.

load 200, Run-11, Run-12 and Run-13							
He=8m	SHS (m)	Utot(mm)	Ux-max(mm)	Uy-max(mm)	Uz-tot max(mm)	M11(kN-m/m)	M22(kN-m/m)
	3	61.75	61.75	37.2	7.94	176.39	226.9
	4	60.93	60.93	38.12	8.38	187.07	227.49
	5	60.85	60.85	37.12	8.46	200.29	228.81
He=11m	3	63.46	63.46	39.25	9.48	172.99	229.78
	4	62.86	62.86	39.13	10.02	179.57	228.55
	5	63.75	63.75	41.41	10.17	191.28	231.26
He=14m	3	66.06	66.06	44.39	11.74	185.95	256.43
	4	65.54	65.54	42.72	12.39	196.78	255.65
	5	65.98	65.98	45.19	12.52	211.17	258.49

Table C.13: Well Documented Braced Excavations Case studies

Case No.	***Case name***	***Excavation width,m***	***Excavation depth,He(m)***	***Wall length, H(m)***	***wall thickness,m***	***Max. lateral deflection δh(max),mm***	***δhmax/He, %***	***Max. surface settlement, δv(max),mm***	***δvmax/He, %***	***Reference***
1	TNEC Excavation, Taipei	41	19.7	35	0.9	106.4	0.54	77.18	0.39	Ou et. al. 1993
2	Taiwan Formosa, Taipei	35	18.45	31	0.8	62.73	0.34	43.16	0.23	Ou et. al. 1993
3	Tokyo Subway	30	17	32	0.8	176.56	1.04	152.42	0.90	Miyoshi,1977
4	New Palace Yard Park,London	50	18.5	30	0.9	24.05	0.13	19.53	0.11	Burland and Hancock,1977
5	HRD-4, Chicago	12.2	12.2	19.2	NA	172.64	1.42	255.7	2.10	Finno et al., 1989
6	Oslo Subway, Norway	11	11	16	NA	223.58	2.03	200	1.82	NGI,1962
7	Far East Enterprise Center	70	20	33	0.9	124.75	0.62	77.76	0.39	Hesish and Ou, 1998
8	Bell Common Tunnel London	40	9	21	NA	26.1	0.29	20	0.22	Tedd et al., 1984
9	Neasden Underpass London	20	8.5	13	NA	52.7	0.62	28	0.33	Sills et al., 1977
10	Lurie Medical Research Building, Chicago	68	12.8	19	NA	63.48	0.50	74	0.58	Finno Roboski, 2005
11	Yishan Road station Shanghai	17.4	15.5	28	0.6	37.5	0.24	13.95	0.09	Liu et al., 2005
12	Bangkok MRT station	23	21	27.9	1	38	0.18	26	0.12	Likitlersuang et al., 2013
13	Chichago Subway	22	12.2	18.3	0.9	38.13	0.31	27.43	0.22	Finno et al., 2002
14	Post Office Square Garage,Boston	61	20.2	25.6	0.9	53.61	0.27	45	0.22	Whittle and Hasash, 1993
15	Shahghai Bank Building	80	14.2	31.2	1	38	0.27	22.5	0.16	Dong, 2014

16	North Square Shanghai,Railway station	100	12.5	31.25	0.8	42	0.34	17	0.14	Dong, 2014
17	One-North MRT station, Singapore	60	30	36	1.27	84	0.28	43.5	0.15	Tan, 2010

Table C.14: Other Braced Excavations Case studies

Case No.	***Case name***	***Excavation width,(m)***	***Excavation depth,He(m)***	***Wall length, H(m)***	***wall thickness,m***	***Max. lateral deflection, δh(max),mm***	***δhmax/He, %***	***Max. surface settlement, δv(max),mm***	***δvmax/He, %***	***Reference***
1	Tai Kai	54.1	12.6	22	0.6	61	0.48	30.5	0.24	Kung et al., 2009
2	MRT-2	19	16.4	30	0.8	41	0.25	24.6	0.15	Kung et al., 2009
3	MRT-4	20	16.2	33	1	48.7	0.30	39	0.24	Kung et al., 2009
4	Singapore CE II	NA	15	NA	NA	88	0.59	75	0.50	Wong et al., 1997
5	Singapore CBD	NA	15	NA	NA	145	0.97	100	0.67	Brooms et al., 1986
6	Deep excavation adjacent to the shanghai metro Tunnels	28.8	11.5	21	0.8	15.39	0.13	7	0.06	Hu et al.,2003
7	Tzunching	31.2	13.9	28	0.7	55.6	0.40	NA	NA	Ou et. al. 1993
8	Bagcilar Metro station, Istanbul	31	54	54	1.5	15	0.03	NA	NA	Unpublished data